IMPRS Lecture @ MPS

Magnetospheres – Earth and Outer Planets

12-16 September 2005

Norbert Krupp
Max-Planck-Institut für Sonnensystemforschung
Katlenburg-Lindau, Germany

MPS
Max-Planck-Institut für
Sonnensystemforschung

Outline

Part 1: Planetary Magnetospheres – Overview

Part 2: Magnetosphere of Jupiter

Part 3: Magnetosphere of Saturn

Part 1: Planetary Magnetospheres - Overview

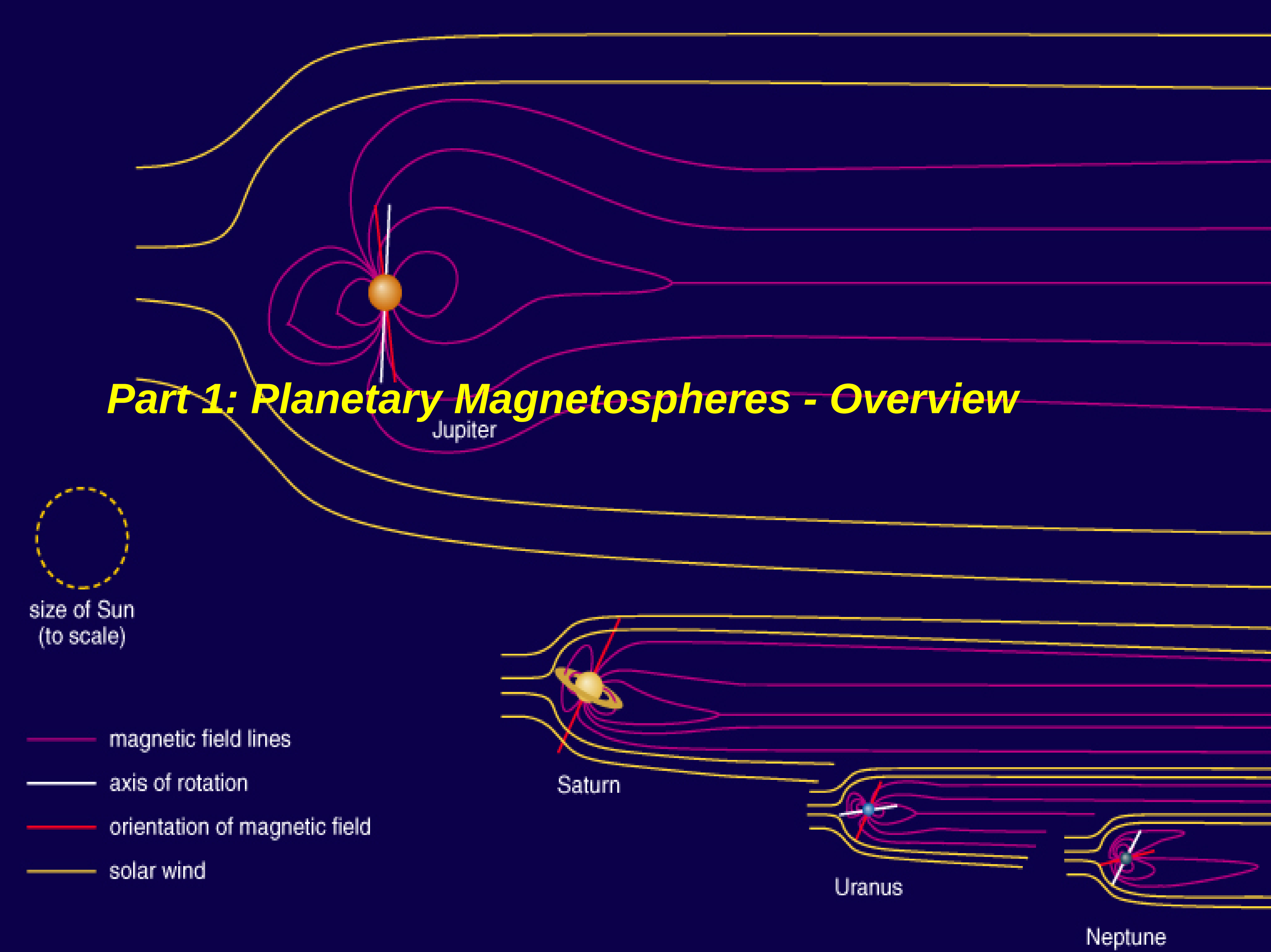

Magnetospheres

Local interstellar Medium (LISM)

Intrinsic

Sun (Heliosphere)

Solar wind

Intrinsic

Mercury
Earth
Jupiter
Saturn
Uranus
Neptune

Induced

Comets
Venus

Mars

Planetary plasma

Intrinsic

Ganymede

Induced

Titan

MPS
Max-Planck-Institut für Sonnensystemforschung

Intrinsic planetary magnetospheres - comparison

small

intermediate

huge

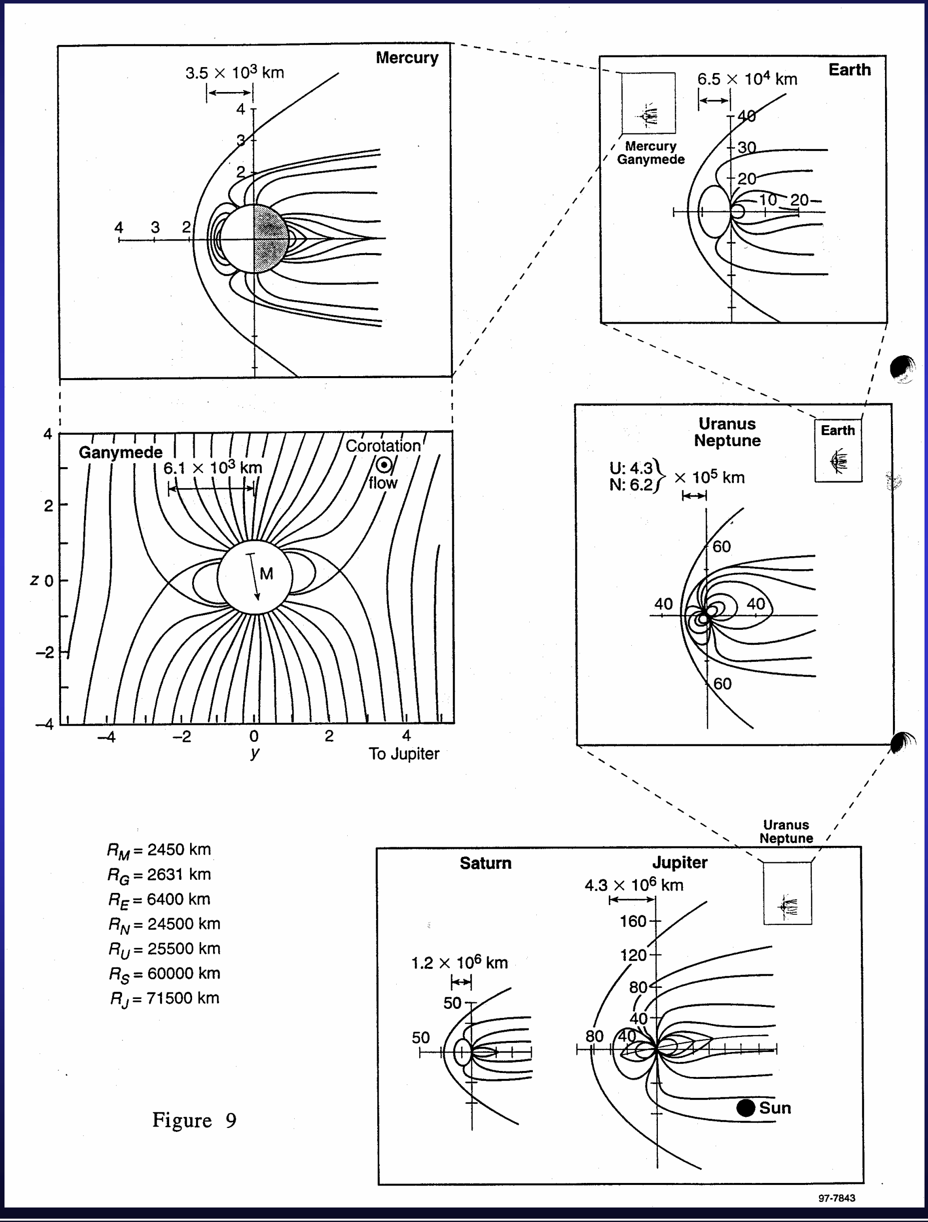

Figure 9

Comparative magnetospheres

MERCURY:
- Small
- Minute timescales
- Solar wind dominated

EARTH:
- Intermediate
- Hour timescales
- Solar wind driven

JUPITER: and other Gas Giants
- Giant
- Timescales - minutes to months?
- Rotationally driven - solar wind triggered?

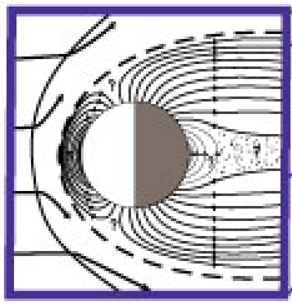

Mariner,
MESSENGER
Bepi Colombo

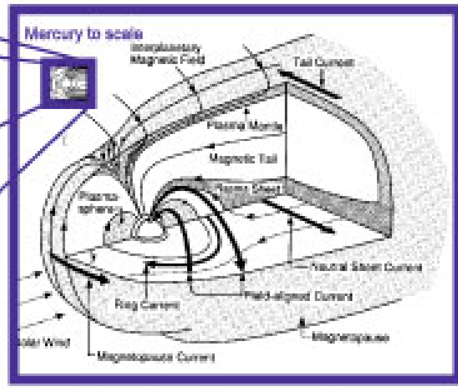

~100 missions since 1957
e.g. Polar, Geotail, FAST,
Sampex , Cluster

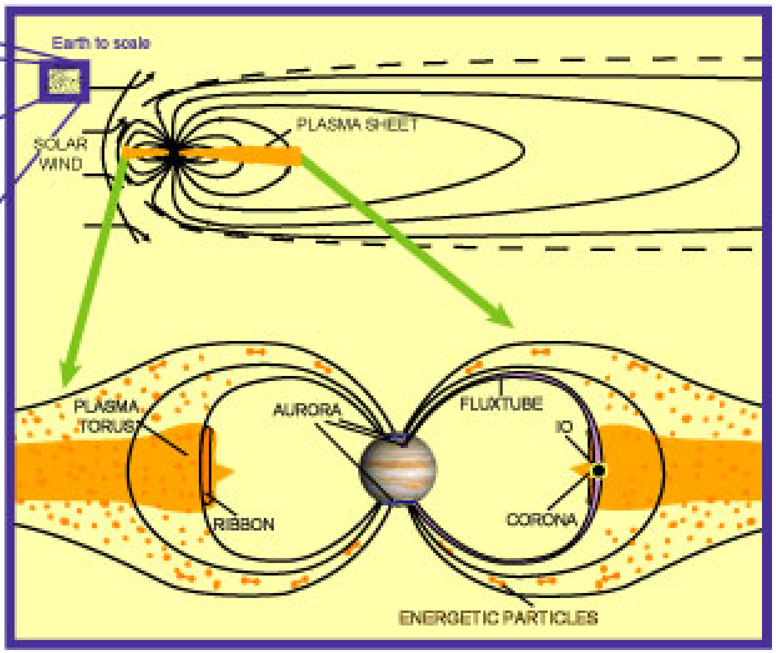

Pioneer, Voyager, Ulysses,
Galileo, Cassini Juno

Testing our understanding of Sun-Earth connections through application to other planetary systems

Orientation of rotation and magnetic axes

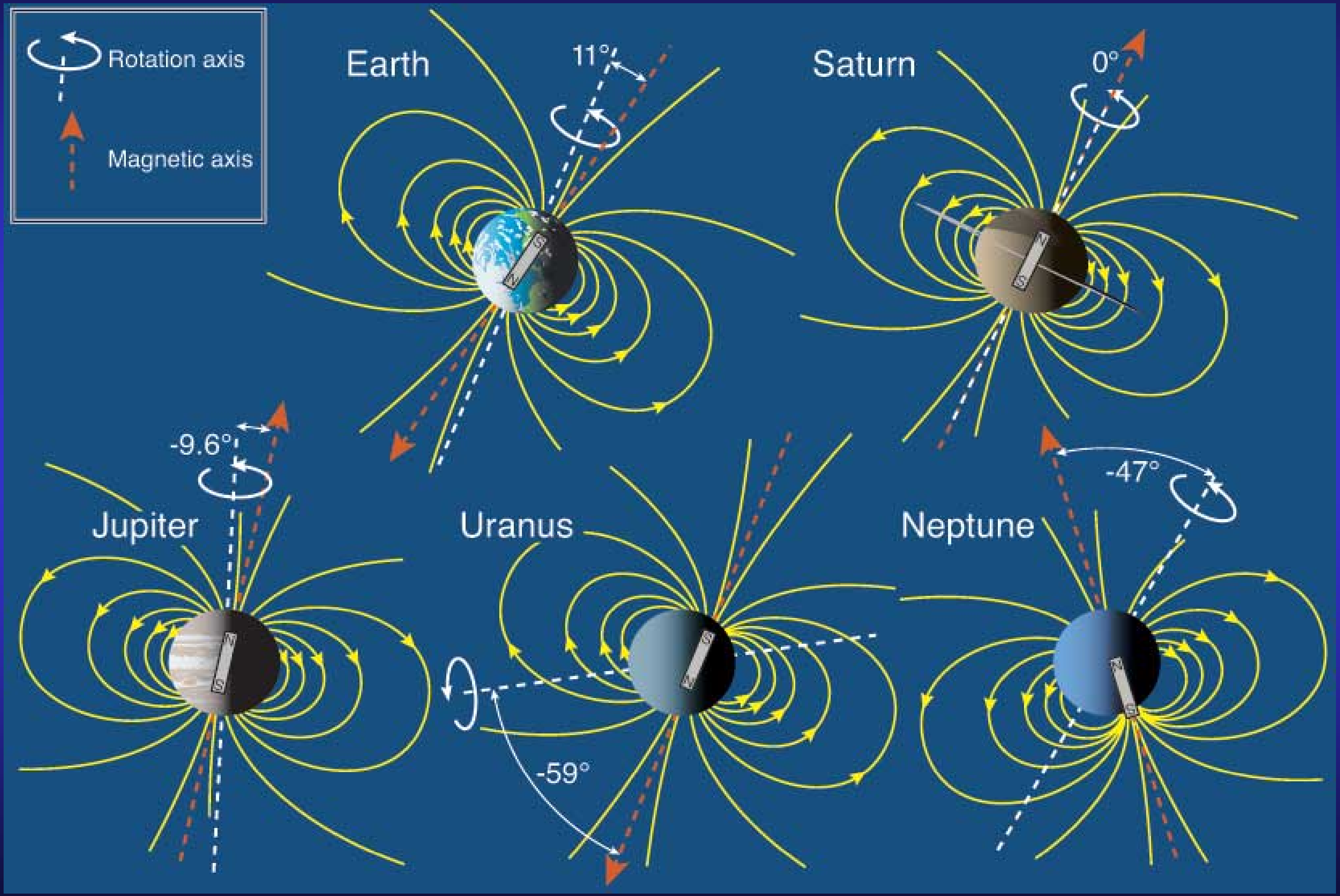

MPS Max-Planck-Institut für Sonnensystemforschung

Solar wind conditions in the vicinity of the magnetospheres

Planet	Magnetic field [nT]	plasma density [cm^{-3}]
Mercury	46 – 21	73 - 33
Earth	8	5
Jupiter	1	0.2
Saturn	0.6	0.06
Uranus	0.3	0.01
Neptune	0.005	0.005

The velocity is almost constant in the inner part of the heliosphere and ranges between 400 and 800 km/s

Max-Planck-Institut für Sonnensystemforschung

Sizes and shape of planetary magnetospheres

$R_M/R_p \sim 1.2\{B_o^2/\rho_{sw} V_{sw}\}^{1/6}$

	Mercury	Earth	Jupiter	Saturn	Uranus	Neptune
B_o	.003	.31	4.28	.22	.23	.14
R_M Calc.	1.4 R_M	10 R_E	42 R_J	19 R_S	25 R_U	24 R_N
R_M Obs.	1.4-1.6 R_M	8-12 R_E	50-100 R_J	16-22 R_S	18 R_U	23-26 R_N

MPS Max-Planck-Institut für Sonnensystemforschung

Plasma sources of planetary magnetospheres

	Mercury	Earth	Jupiter	Saturn	Uranus	Neptune
N_{max} cm^{-3}	~1	1-4000	>3000	~100	~3	~2
Compo sition	H^+ Solar Wind	O^+ H^+ Iono-sphere	O^{n+} S^{n+} H^+ Io	O^+, H_2O^+ H^+, N_2 Rings, icy satellites Titan	H^+ Iono-sphere	H^+ N^+ Triton, Iono-sphere
Source kg/s	?	5	700-1200	~2	~0.02	~0.2

Charge Energy Mass Spectrometer (CHEMS) on Cassini records "fingerprints" of ion composition at Earth, Jupiter, and Saturn

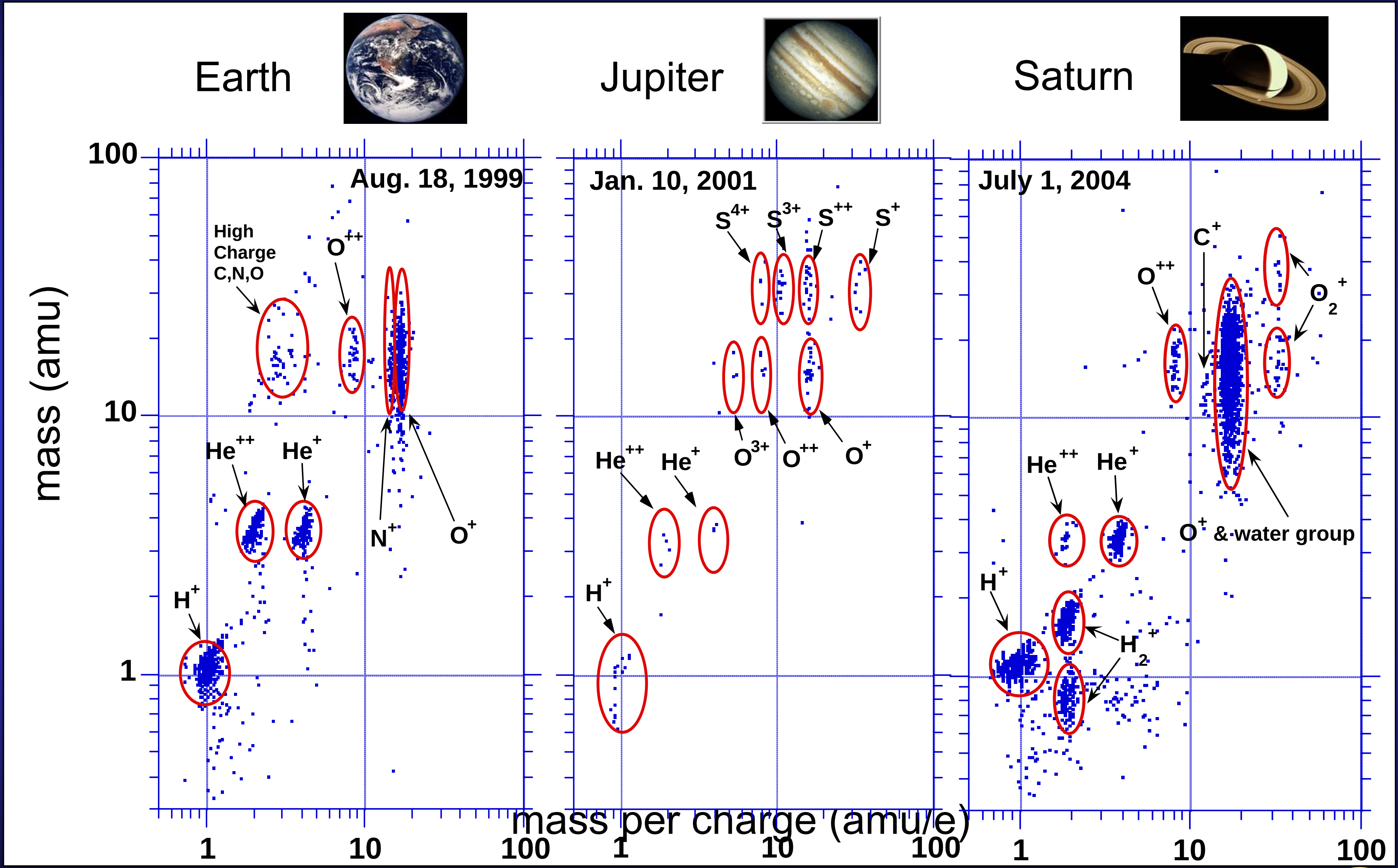

Small magnetospheres

Mercury and Ganymede

Mercury - Magnetic field detected by *Mariner 10* in 1974

Ganymede - Magnetic field detected by *Galileo* in 1996

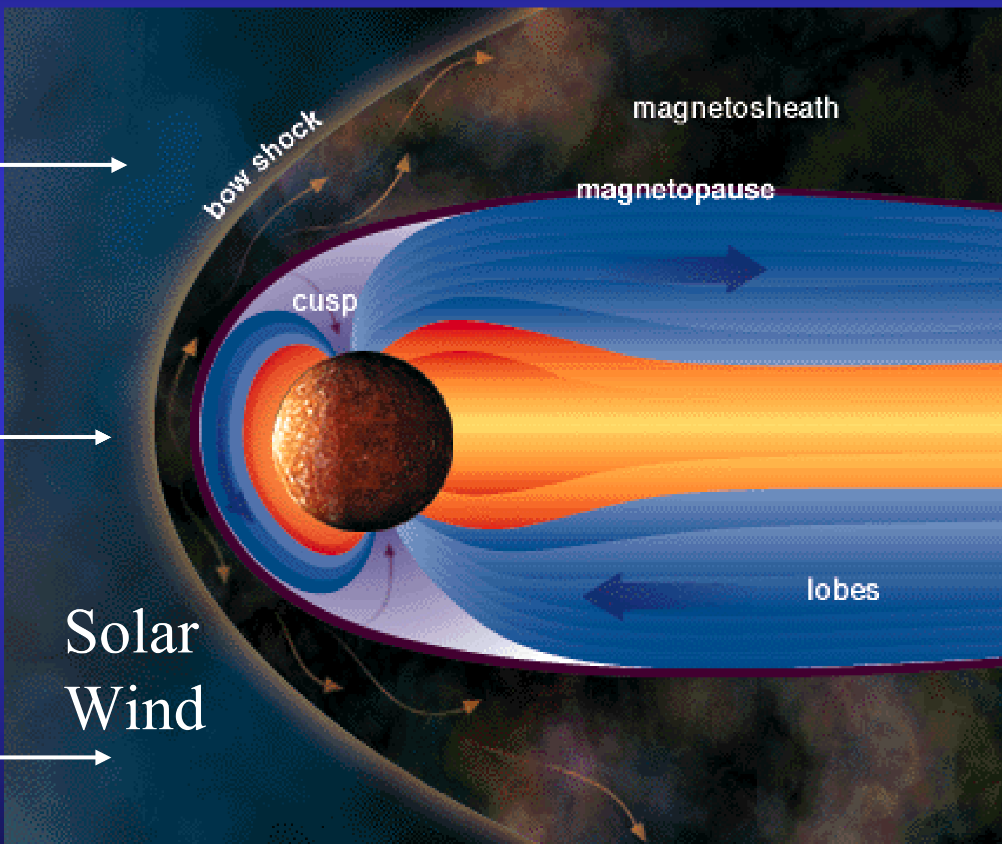

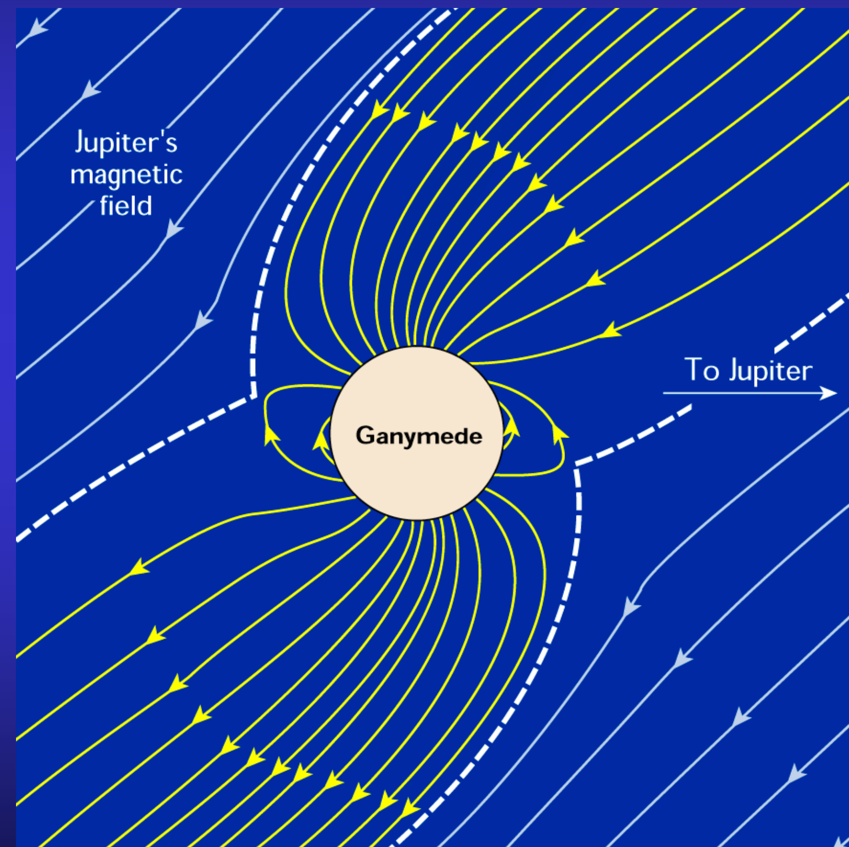

$B_{surface}$ ~ 1/100 Earth

Diameter of Earth

Huge magnetospheres

Giant Planet Magnetospheres

Main differences from Earth:

1. Rotation dominated; driving energy is the fast rotation and not the solar wind
   - plasma is (partly) corotating with the planet
2. Strong plasma sources inside the magnetosphere (satellites or rings)
   - radial outward plasma transport; additional loss mechanisms

Jupiter and Saturn

- Symmetric
- ~Dipolar
- Strong plasma production
- Limited solar wind influence

Uranus and Neptune

- Highly asymmetric,
- Highly non-dipolar
- Complex transport (SW + rotation)
- Multiple plasma sources (ionosphere + solar wind + satellites)

Corotation in planetary magnetospheres

Neutral atmosphere must corotate with the planet
+
Electrical conductivity Σ must be very large (effective atmosphere/ ionosphere coupling)

$$\vec{I} = \overline{\overline{\Sigma}} \cdot \left(\vec{E} + \vec{v}_n \times \vec{B}\right)$$

$$\vec{E} = -\vec{v}_{flow} \times \vec{B}$$

$$\Downarrow$$

$$\vec{I} = \overline{\overline{\Sigma}} \cdot (\vec{v}_n - \vec{v}) \times \vec{B}$$

Σ : height-integrated conductivity
v_n : neutral atmosphere velocity
E : horizontal electric field
I : height-integrated current density
v_{flow} : flow velocity above ionosphere

↓

I is coupled by field-aligned currents to the current system in the magnetosphere with current density j

$$\rho \cdot \frac{d\vec{v}}{dt} + \nabla \cdot \overline{\overline{P}} = \vec{j} \times \vec{B}$$

+

radial stress balance

↓

Corotation of plasma

Earth‘s-like magnetosphere

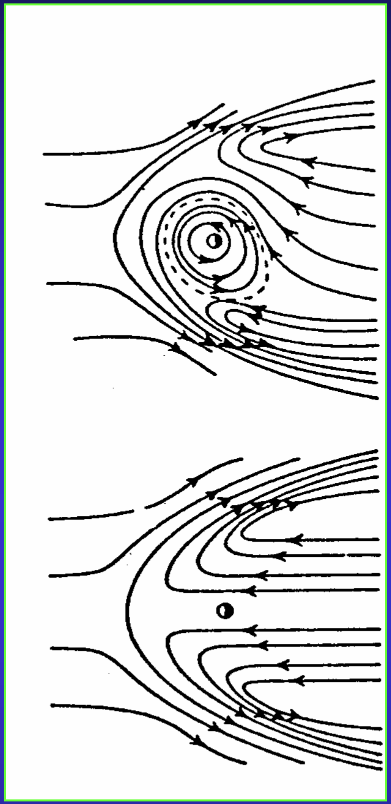

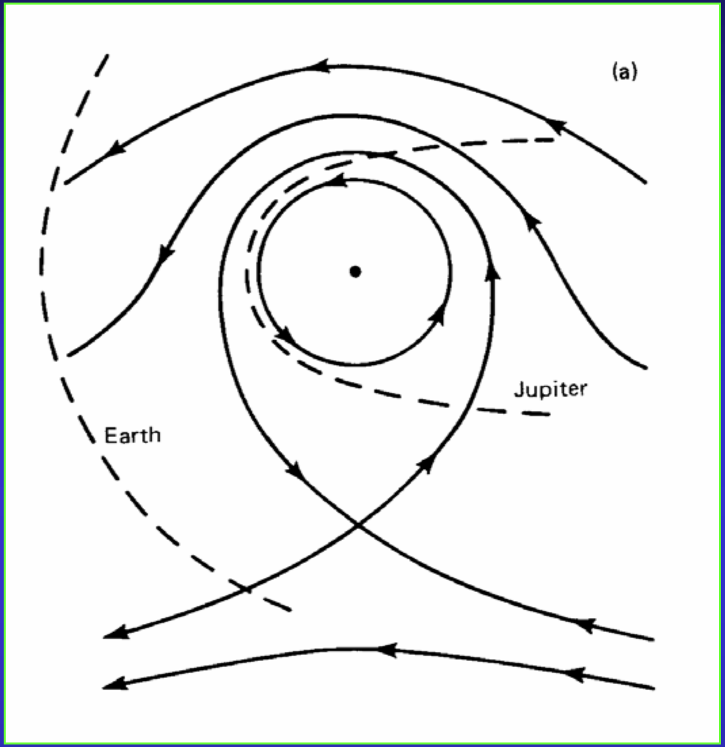

- plasmasphere in the inner magnetosphere with closed flow lines
- if scaled to Jupiter: closed flow lines outside the magnetosphere
  - rotation dominated

Magnetosphere interactions

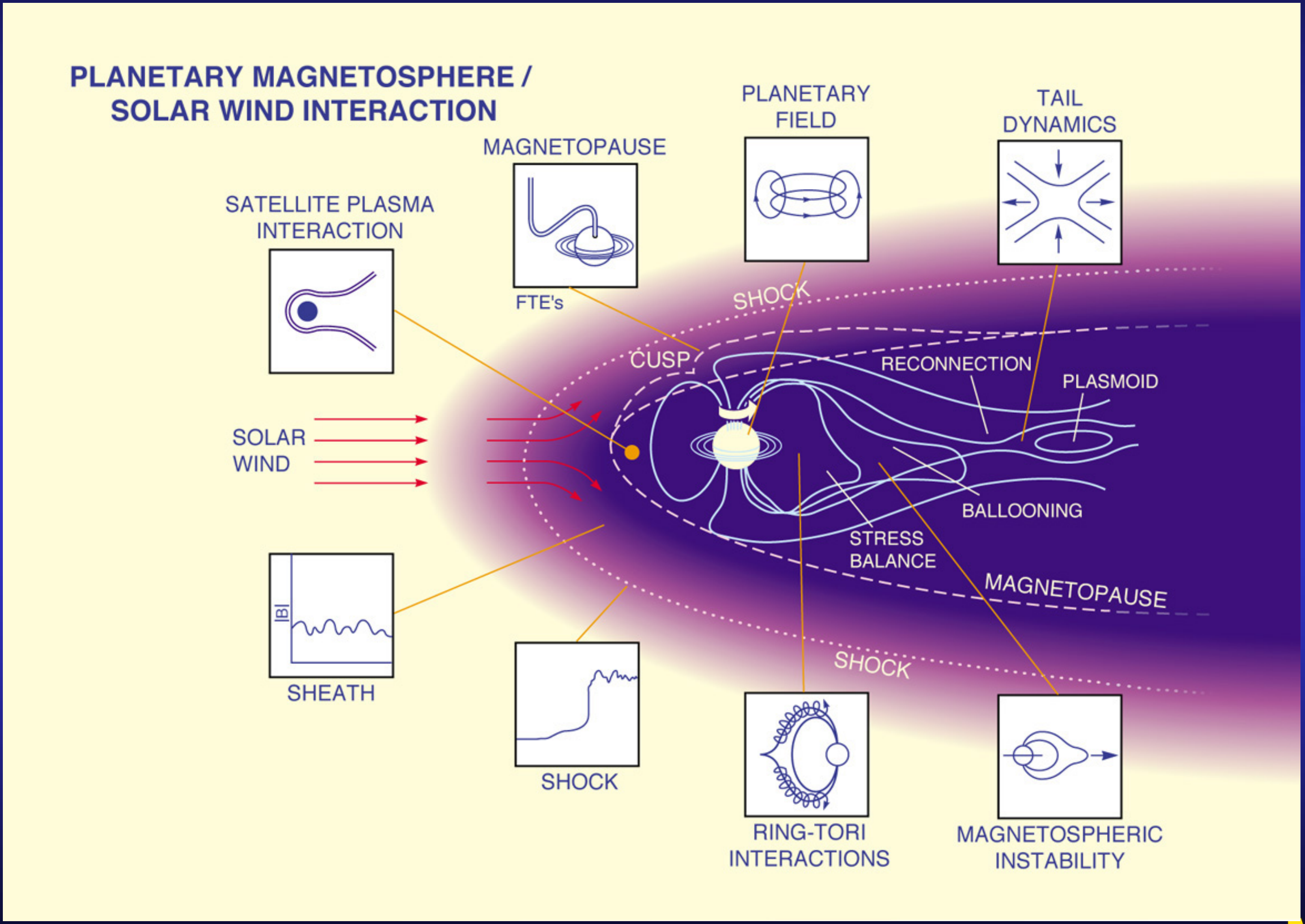

MPS Max-Planck-Institut für Sonnensystemforschung

Magnetospheres of Jupiter and Saturn
Comparison

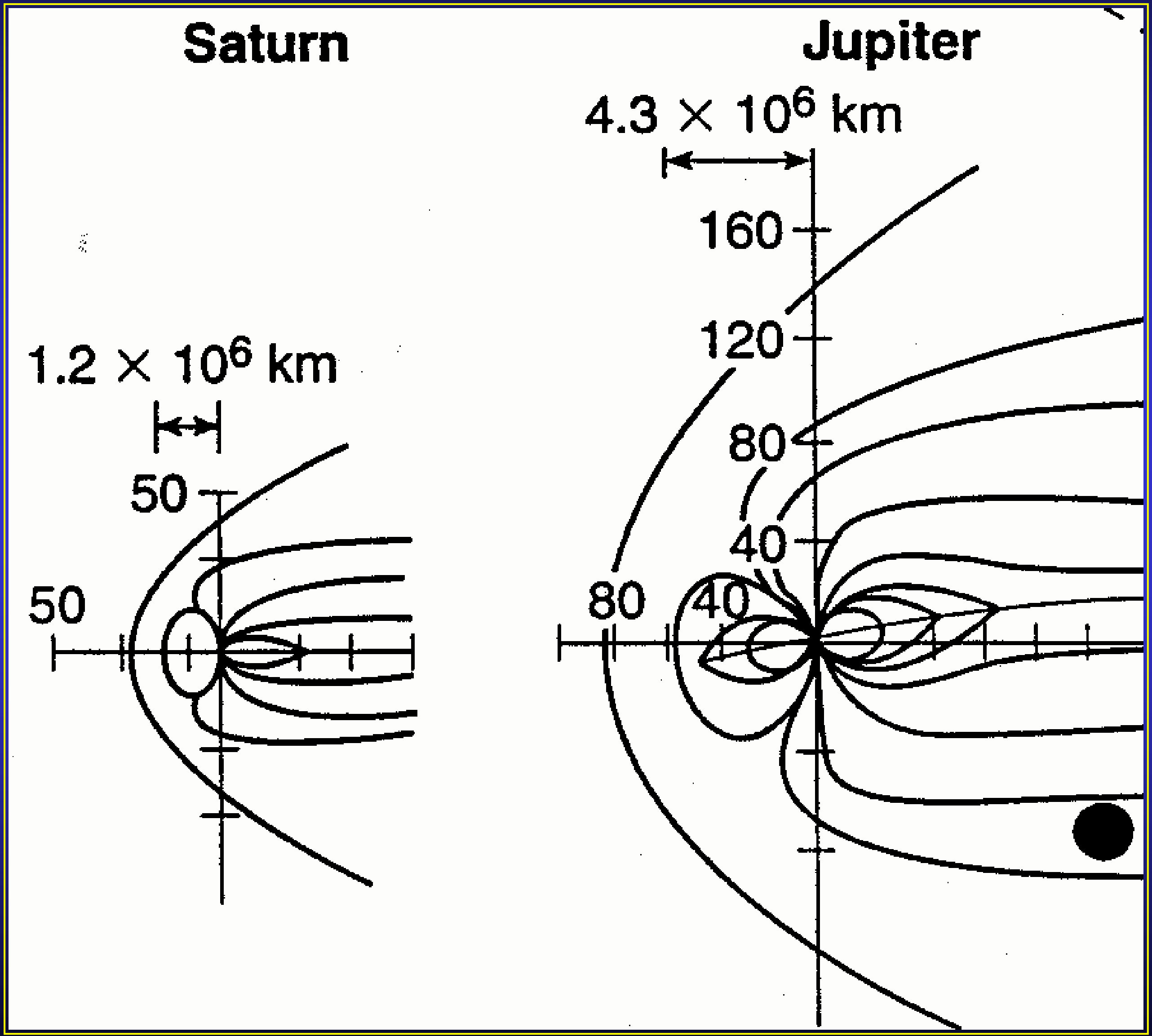

Recently published books about outer planets

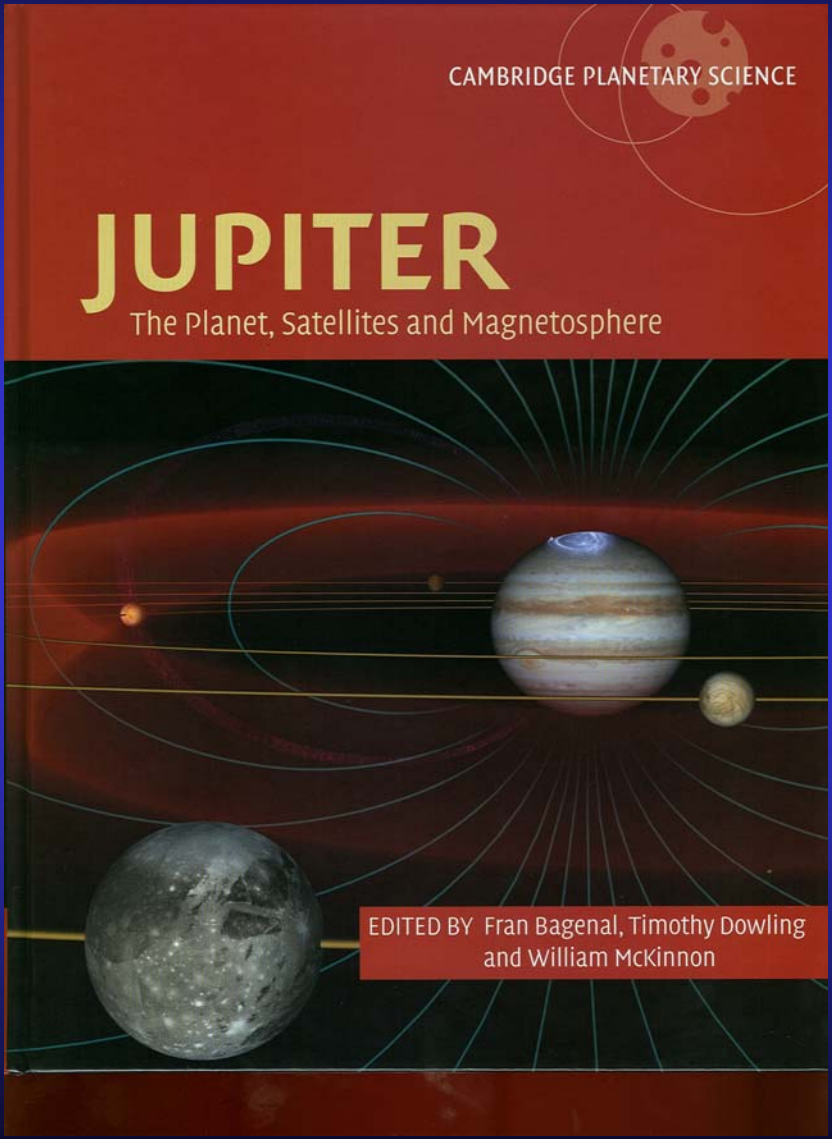

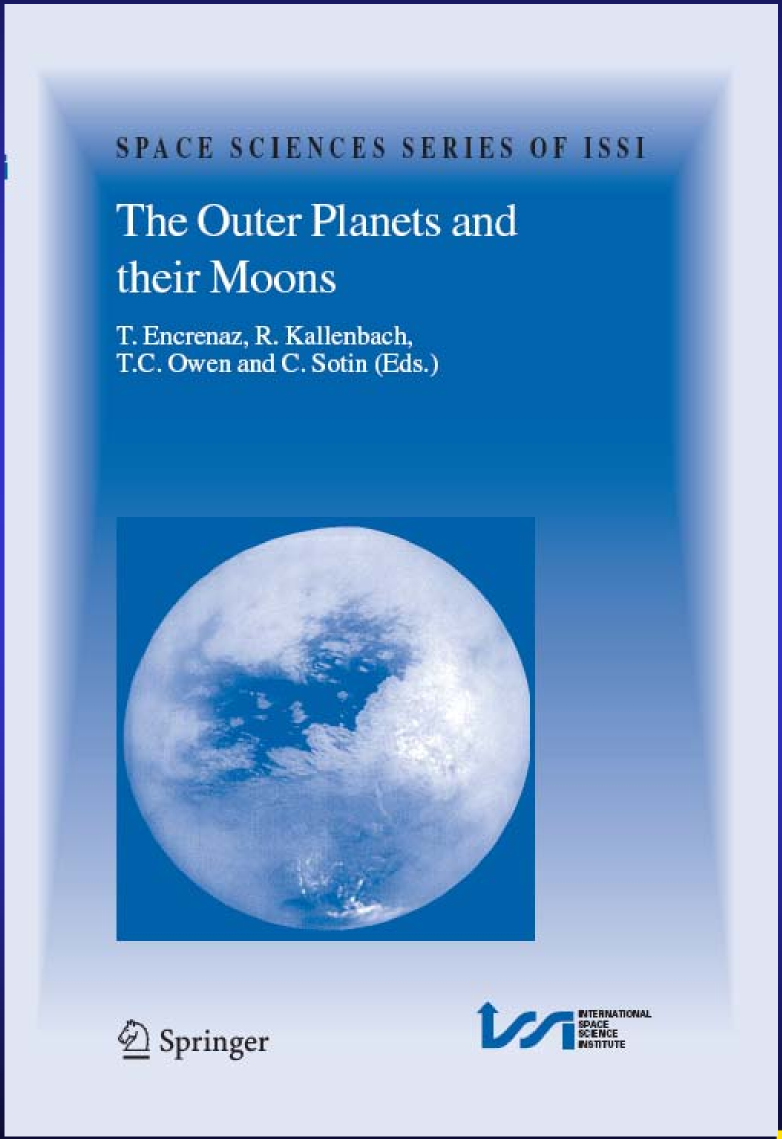

Spacecraft exploration of Jupiter and Saturn

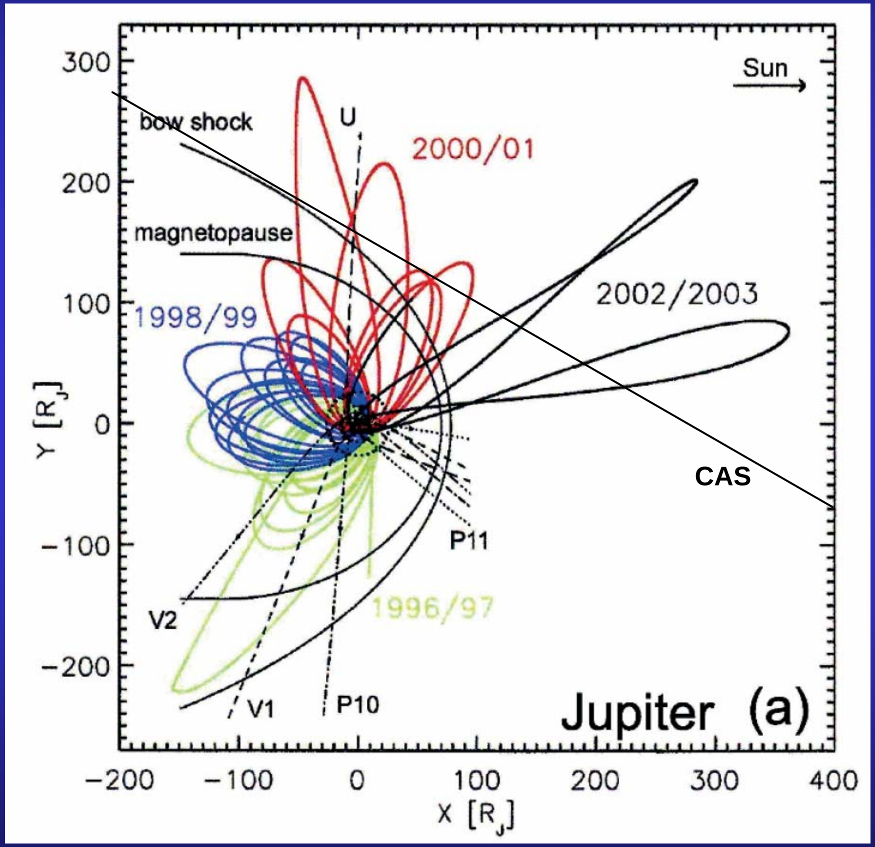

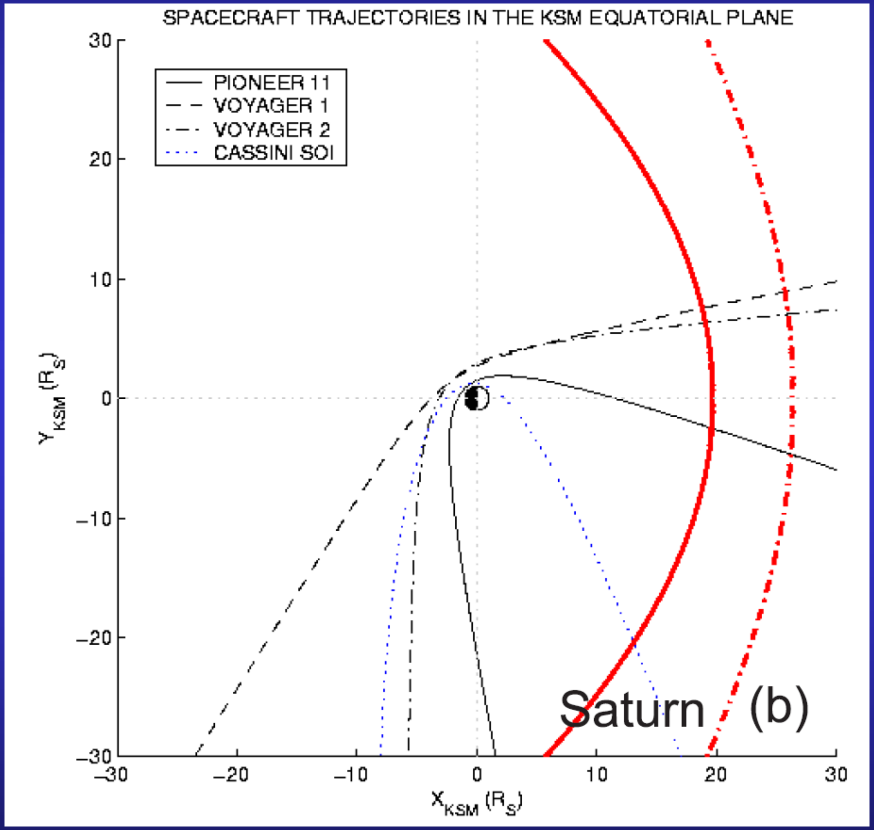

Max-Planck-Institut für Sonnensystemforschung

Spacecraft exploration of Jupiter and Saturn

TABLE I

Measured positions of magnetospheric boundaries at Jupiter and Saturn.

			local time	distance BS (R_p)	standoff BS (R_p)	distance MP (R_p)	standoff MP (R_p)
P 10	1974	Jupiter	1000	108.9	102-130	96.4-50	80-96
		Jupiter	0600	124-189		98-150	
P 11	1974	Jupiter	1000	109.7-79.5	92-100	97-64.5	80-90
		Jupiter	1200	90.8-95		56.6-80	
	1979	Saturn	1000	24-20		17	
		Saturn	1200	49-102		30-40	
VG 1	1979	Jupiter	1000	85.7-55.7	77-103	67.1-46.7	62-85
		Jupiter	0400	199.2-258		158.3-165.4	
	1980	Saturn		26	23	23-24	
		Saturn		78		43-47	
VG 2	1979	Jupiter	1000	98.8-66.5	79-95	71.7-61.9	70-101
		Jupiter	0300	282.3-283.3		169.1-279.4	
	1981	Saturn		32-24	18.5	19	
		Saturn		78-88	50-70		
ULS	1992	Jupiter	1000	113	85-104	110-87	72-104
		Jupiter	1800	109-149		83-124	
GLL	1995	Jupiter	0600	130-214	100-130	120	90
	2000	Jupiter	1750			107-149	84-107
		Jupiter	1920	130-133	82-105	120-150	88-98
	2001	Jupiter	1625	108-125	82-96	102	90
CAS	2001	Jupiter	1900	> 450		204	111
	2004	Saturn	0750 -0800	49.2-40.5		35	
	(SOI)	Saturn	0540				

Cassini trajectory around Saturn

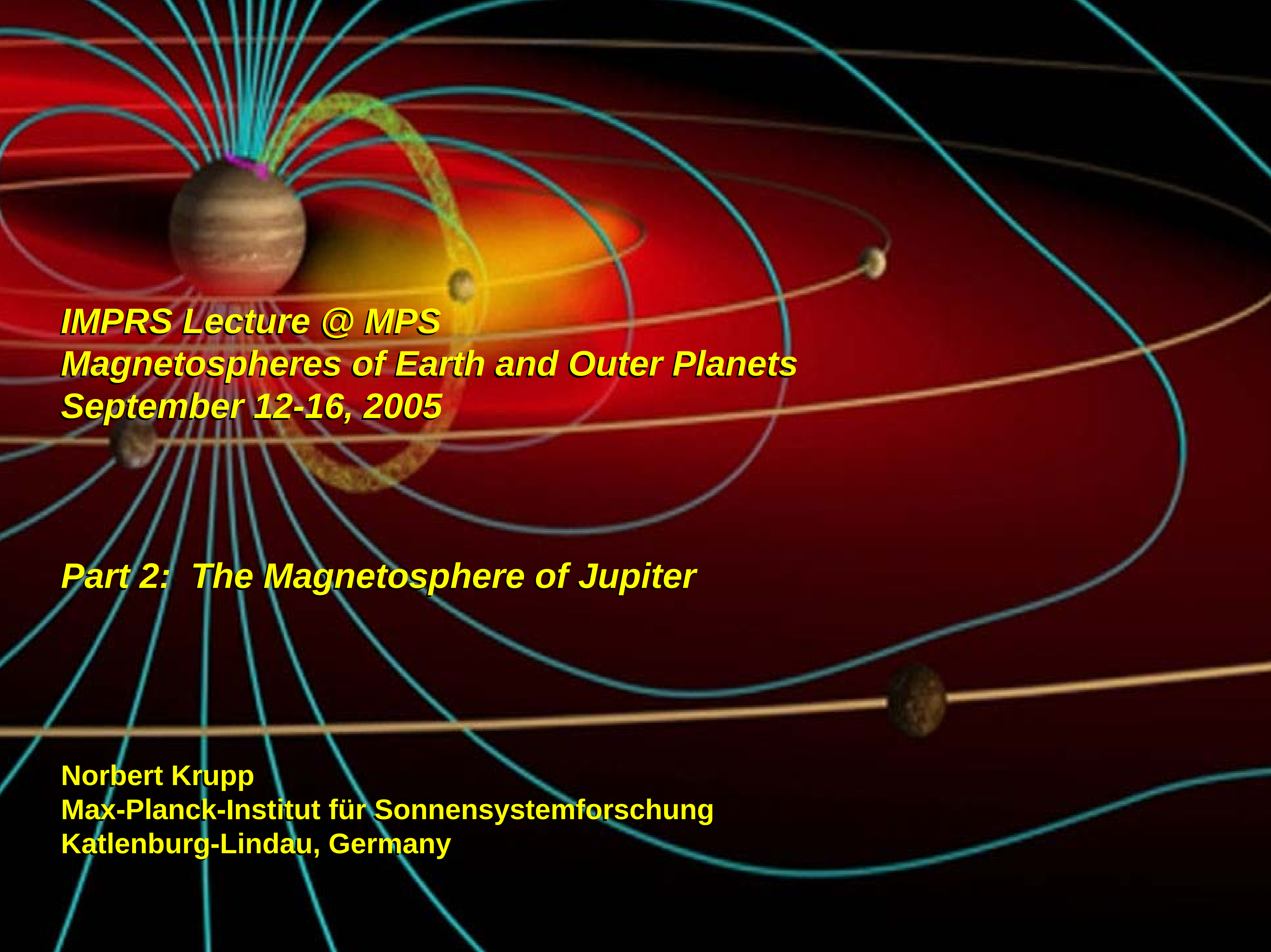

IMPRS Lecture @ MPS
Magnetospheres of Earth and Outer Planets
September 12-16, 2005

Part 2: The Magnetosphere of Jupiter

Norbert Krupp
Max-Planck-Institut für Sonnensystemforschung
Katlenburg-Lindau, Germany

Outline Jupiter

- Global configuration
  - regions
  - the special role of Io
  - particle flow pattern
  - global ion composition
  - neutrals
- Dynamics
  - interchange motion
  - aurora
  - particle injections
  - substorm-like processes (particle bursts)
  - boundary phenomena
- Moon phenomena
  - Ganymede's magnetosphere
  - Io torus
  - Europa torus

Global configuration of the Jovian magnetosphere

regions
the special role of Io
particle flow pattern
global ion composition
neutrals

Jupiter's magnetosphere

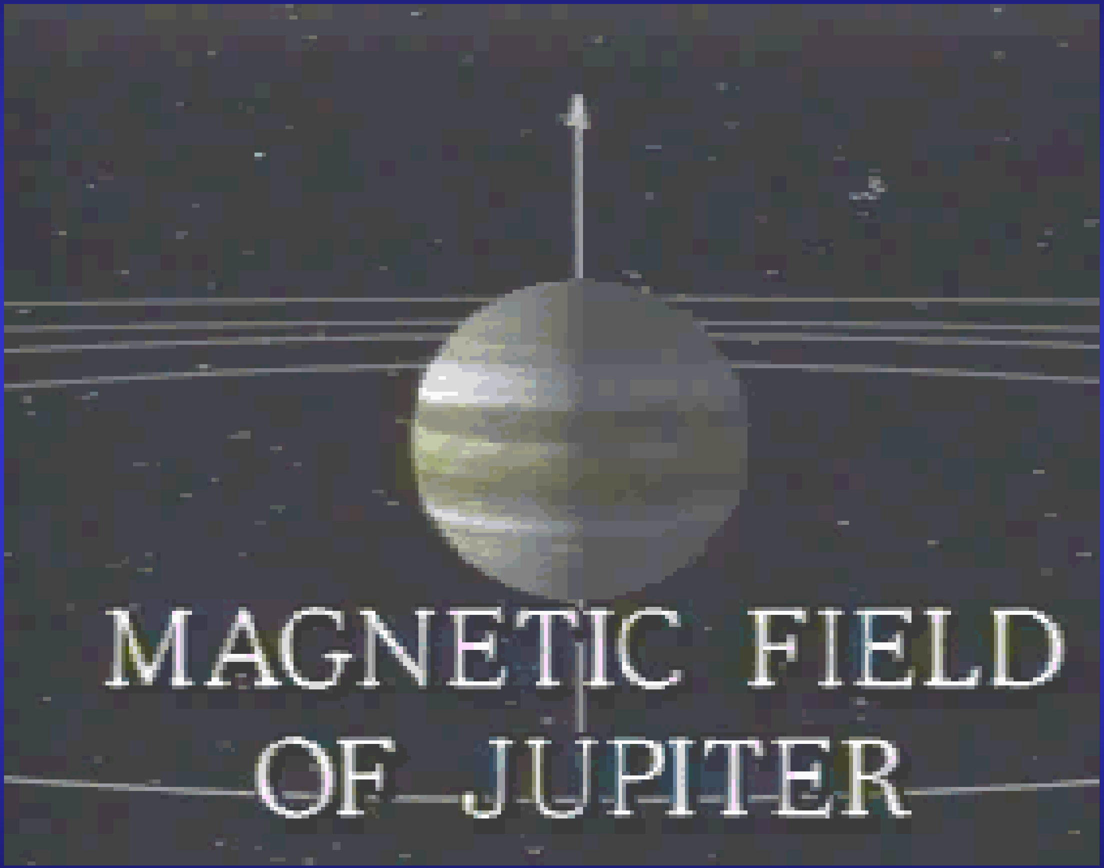

Jupiter's inner radiation belts inside r = 5 RJ

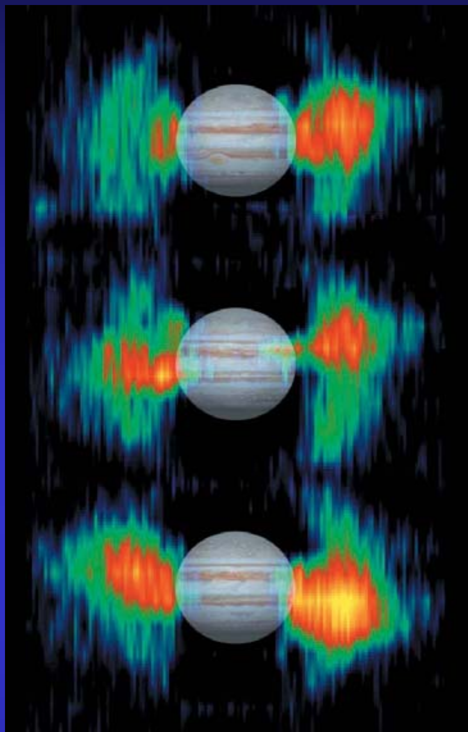

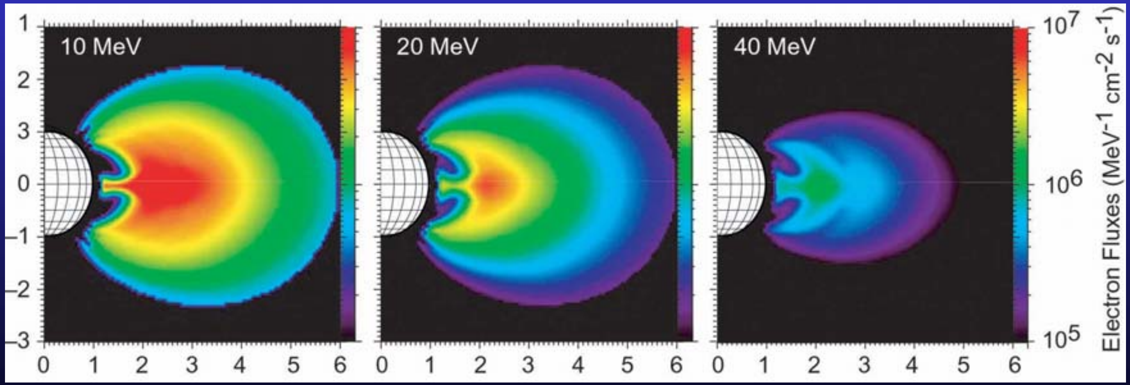

discovered after the detection of bursts in the radio waves Burke and Franklin (1955):

synchrotron emission from trapped particles in radiation belts was used to determine the rotation period

particles in this region interact with the moons (Metis, Adrastea, Amalthea, Thebe);

the Jovian rings

Jupiter's moon Io

source of sulfur and oxygen in Jupiter's magnetosphere

After quantities of lava are removed from below, the crust cracks and tilts, making tall, blocky mountains.

Io's volcanoes and geysers

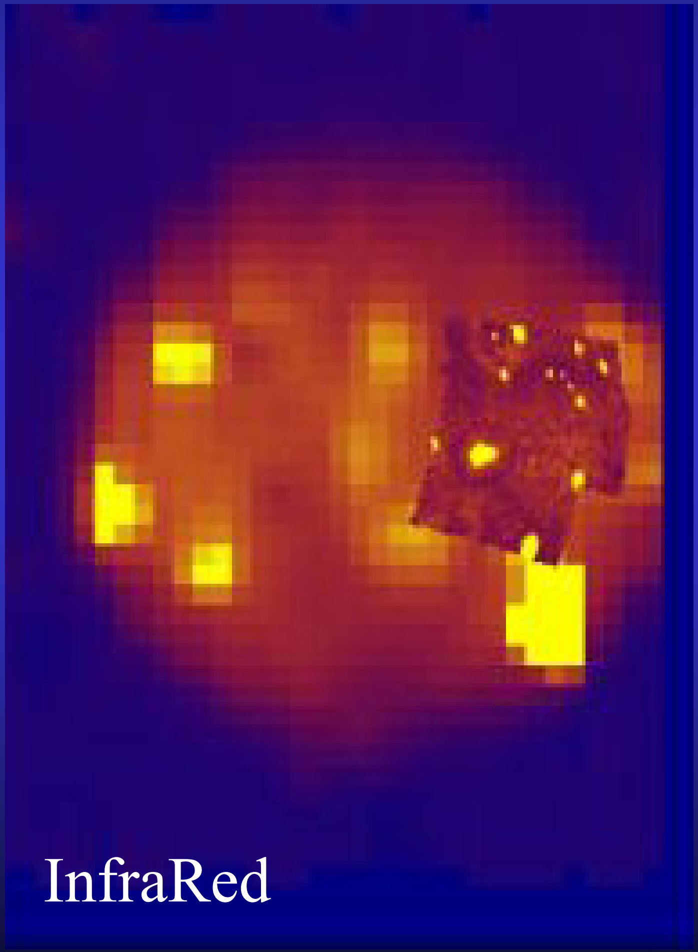

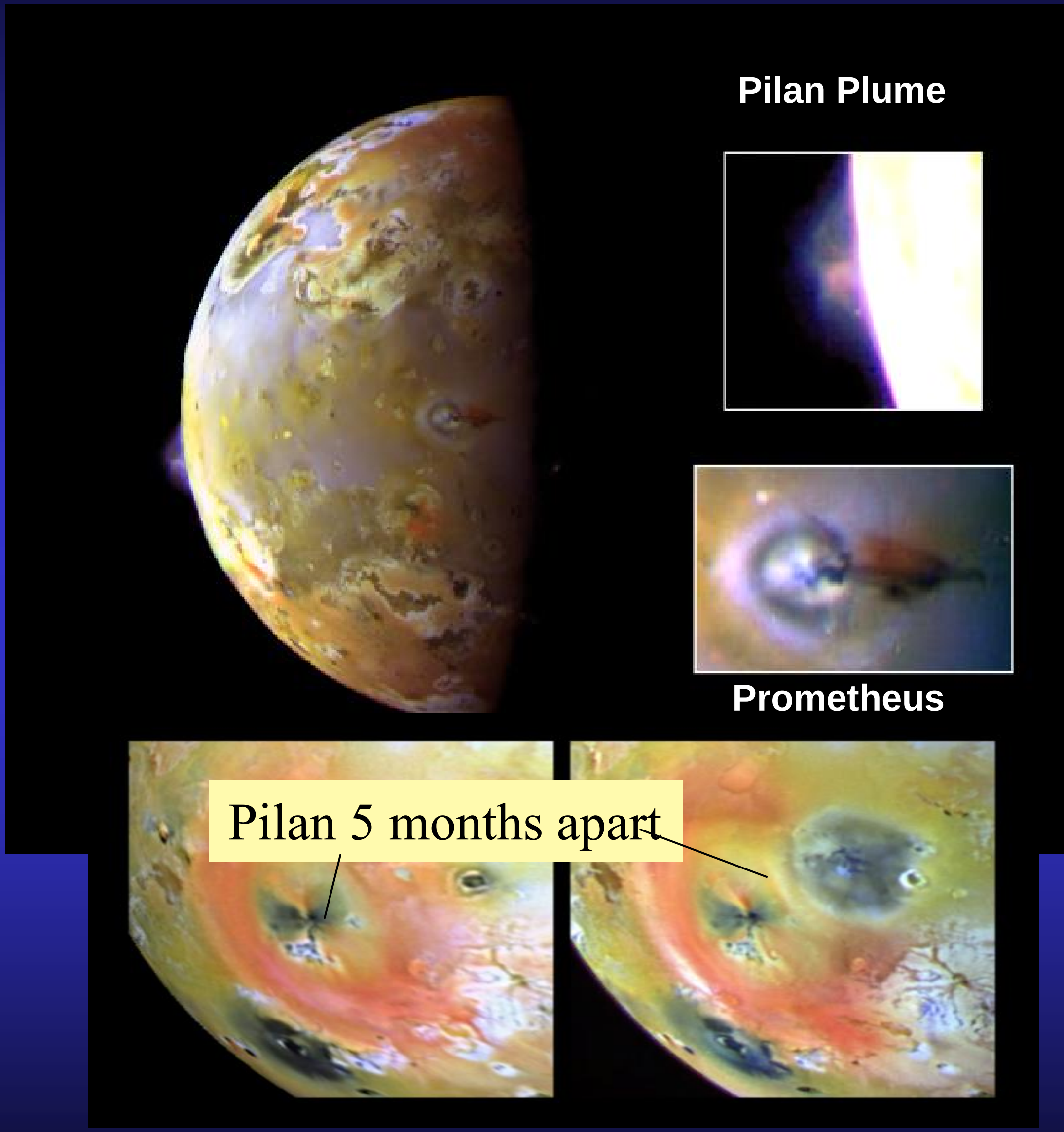

Io Plasma Torus (Schneider and Trauger)

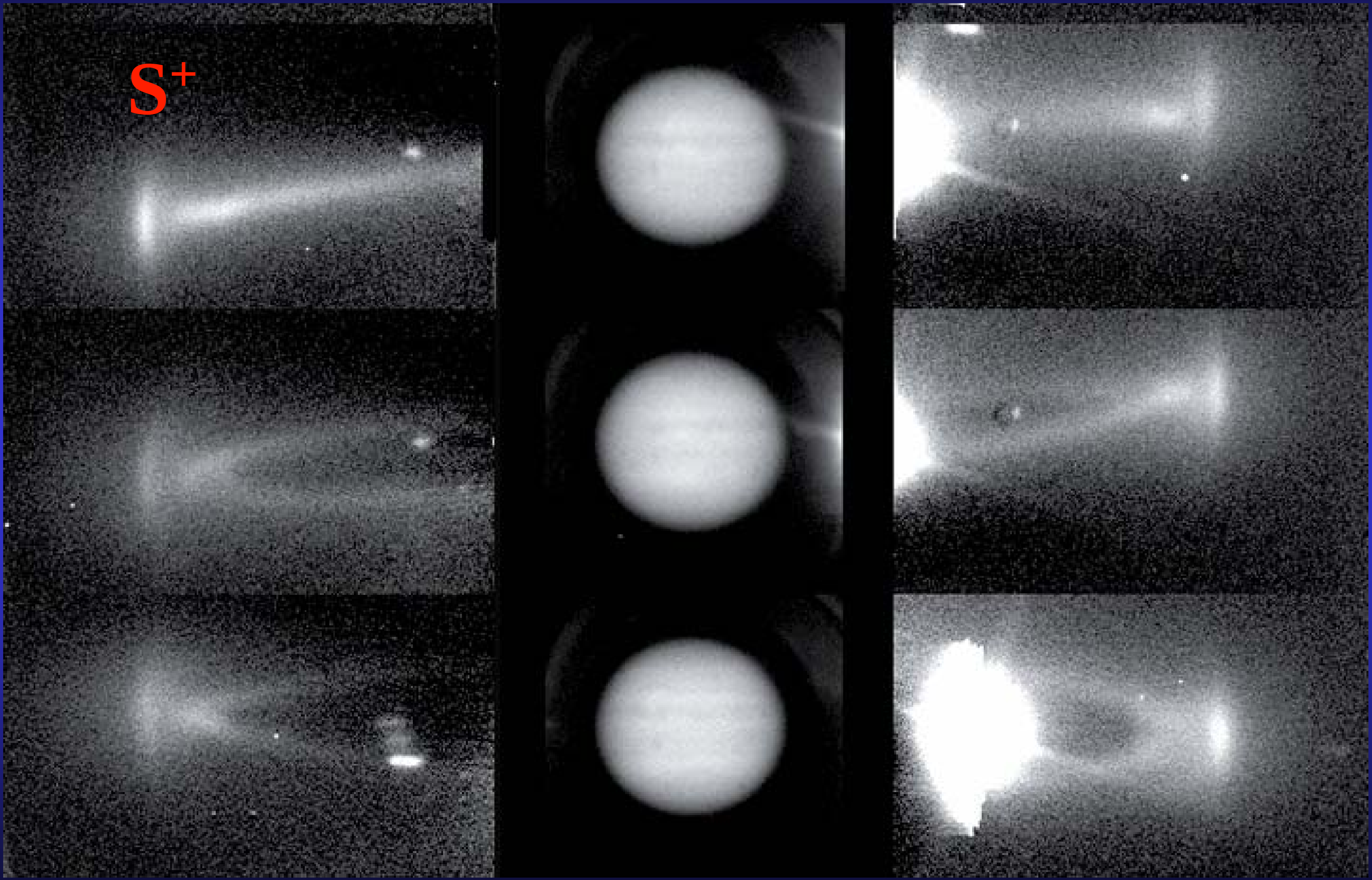

Jupiter's magnetosphere

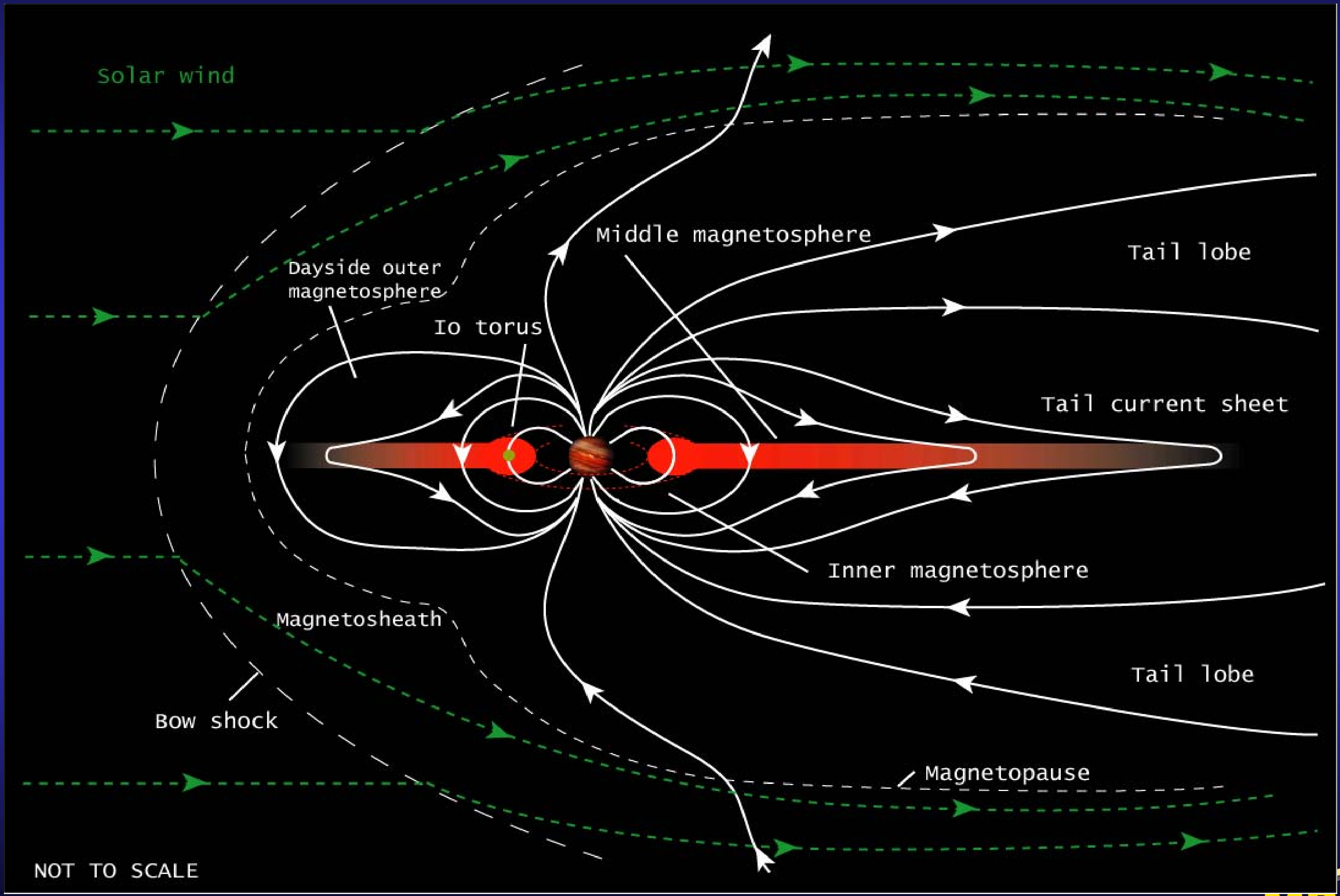

Regions in Jupiter's magnetosphere

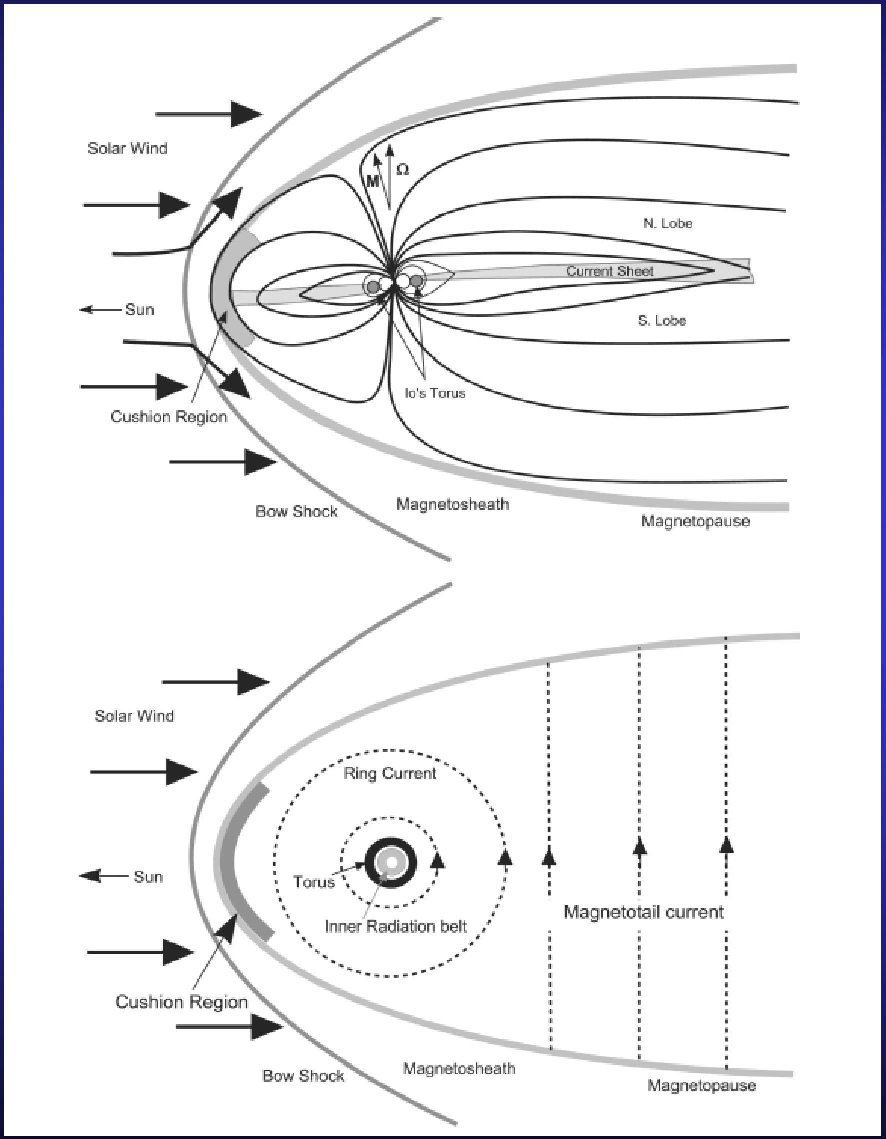

Particles inside 40 RJ

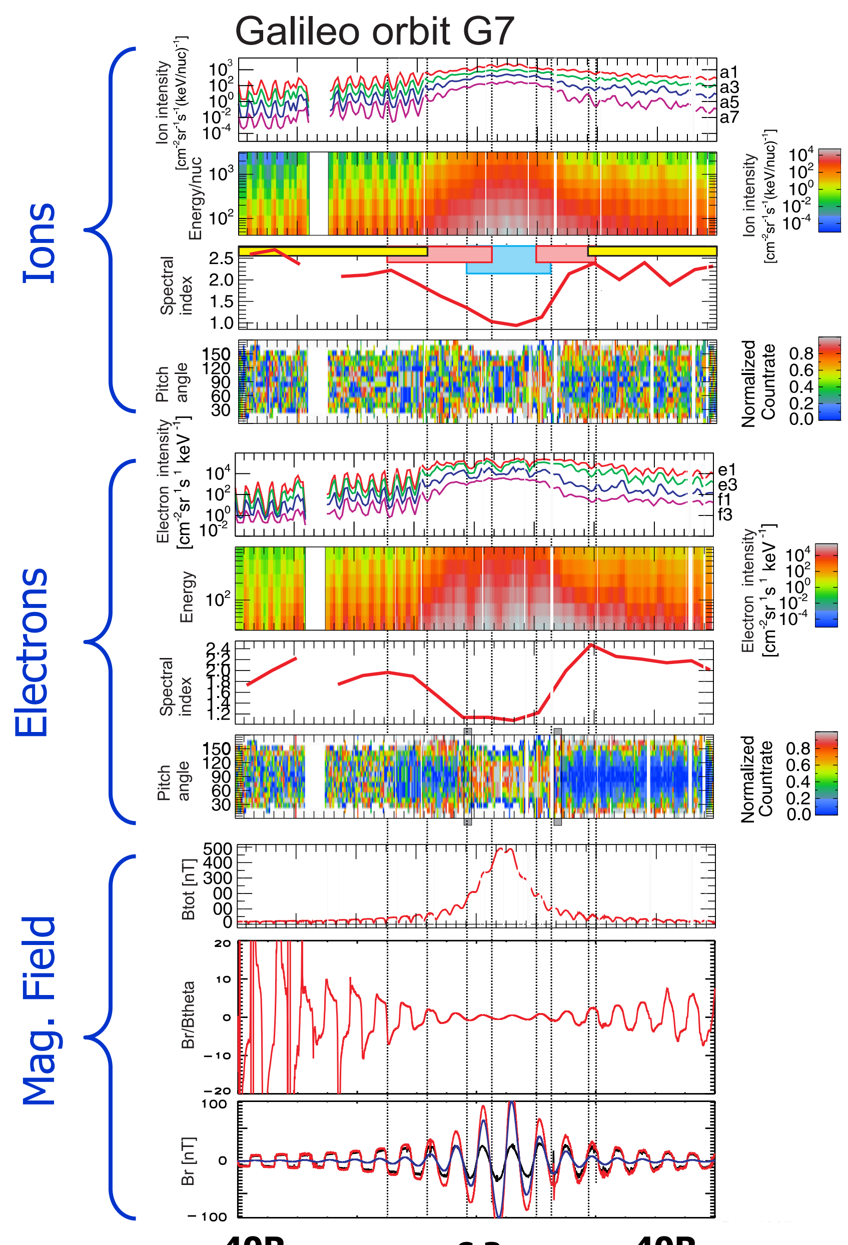

Tomás et al., 2004a

Periodic modulation of particle and field parameter

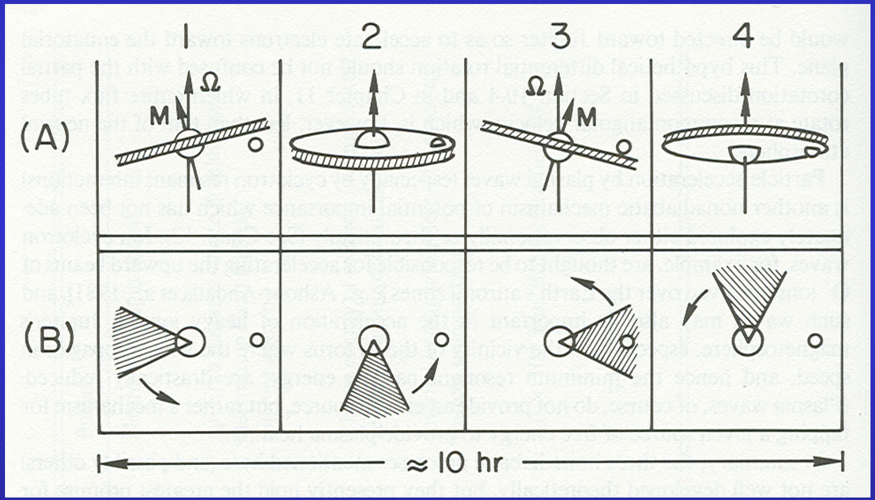

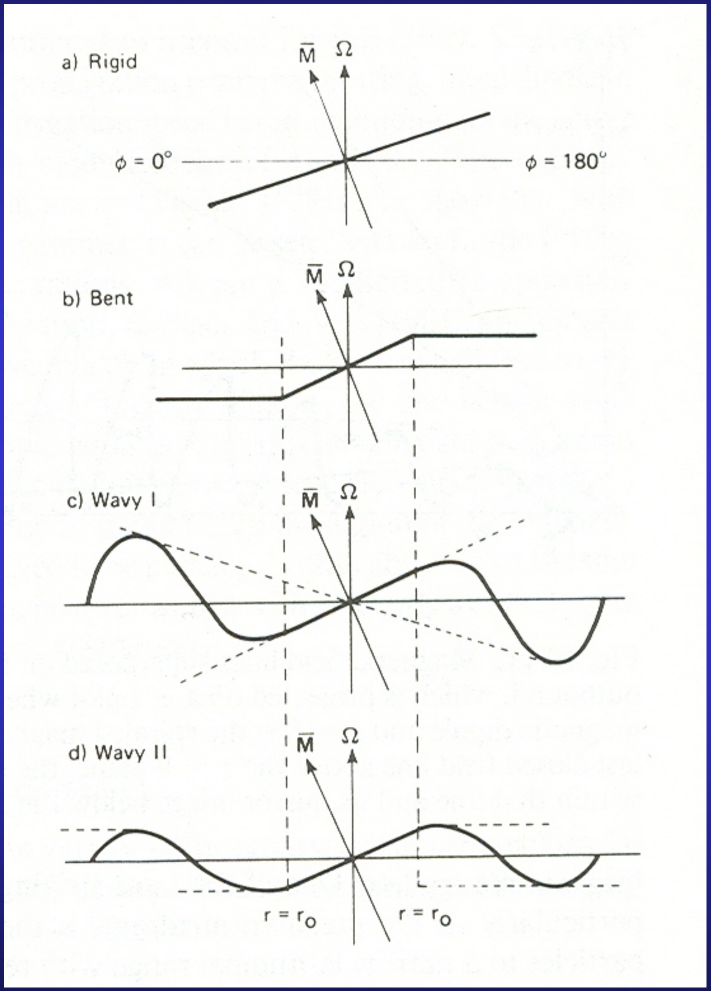

Jupiter

Structure and dynamics of the outer magnetosphere

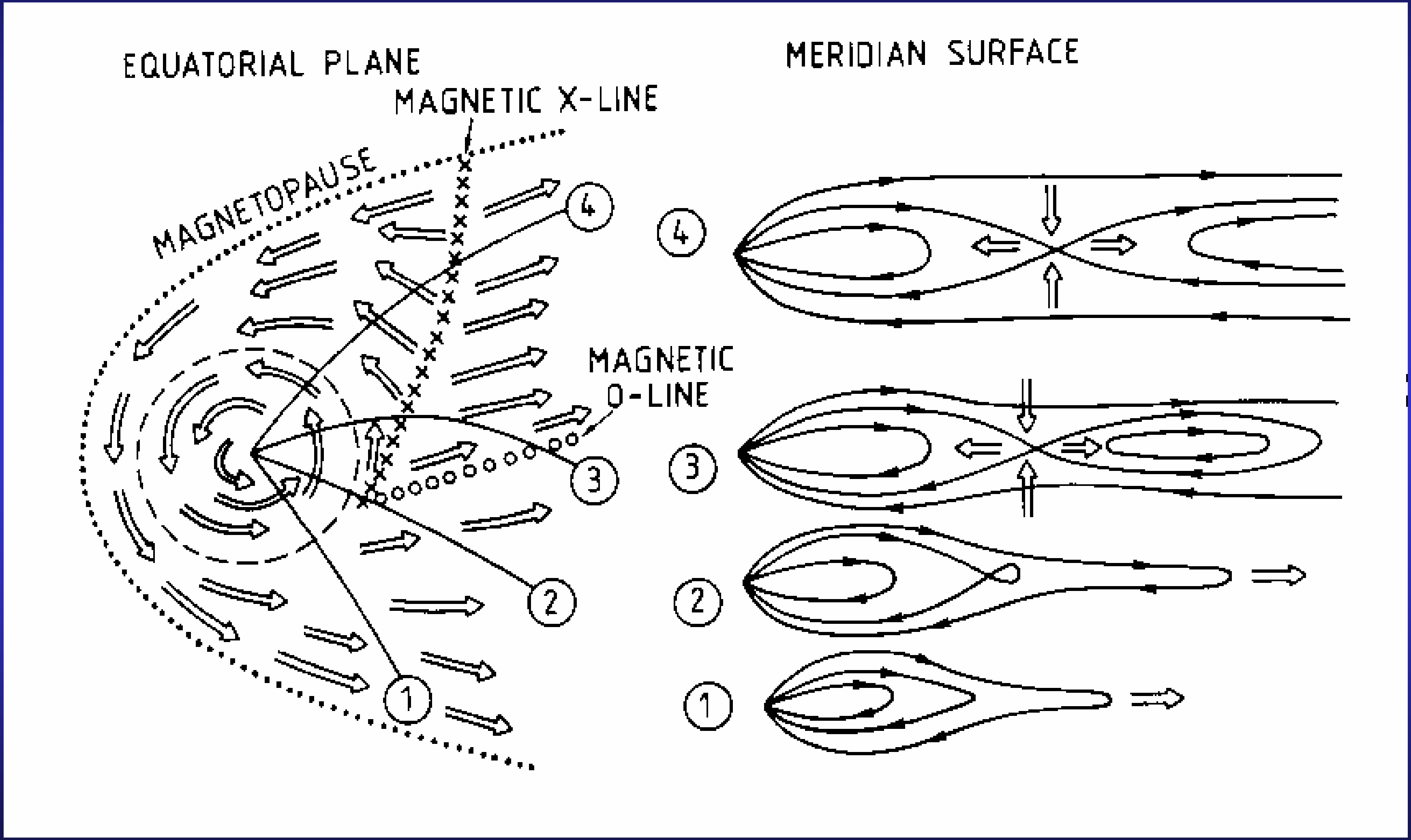

Vasyliunas 1983

Flow measurements in Jupiter's magnetosphere

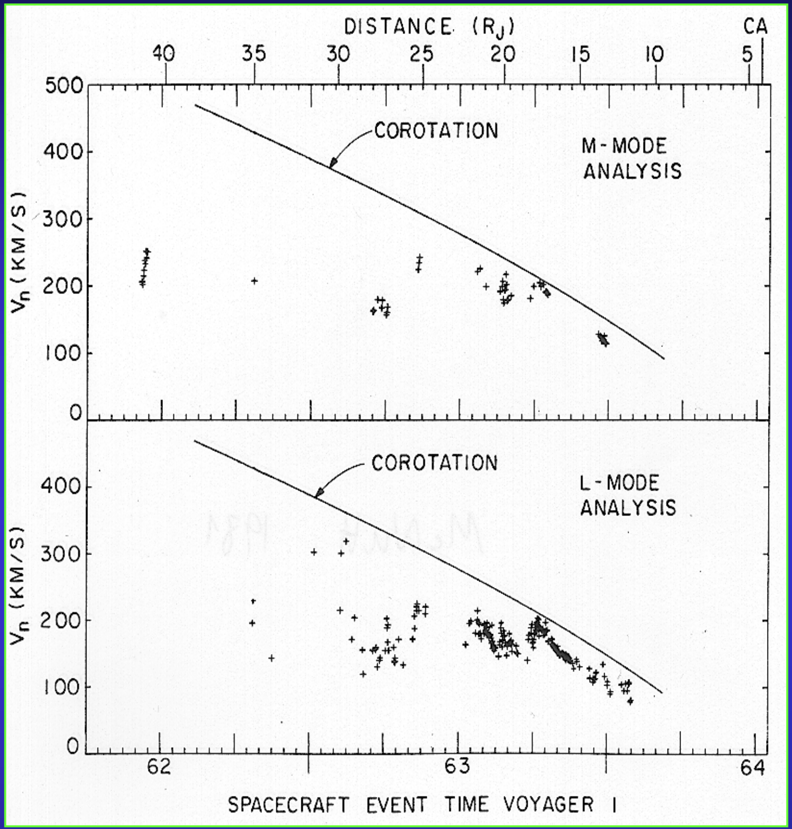

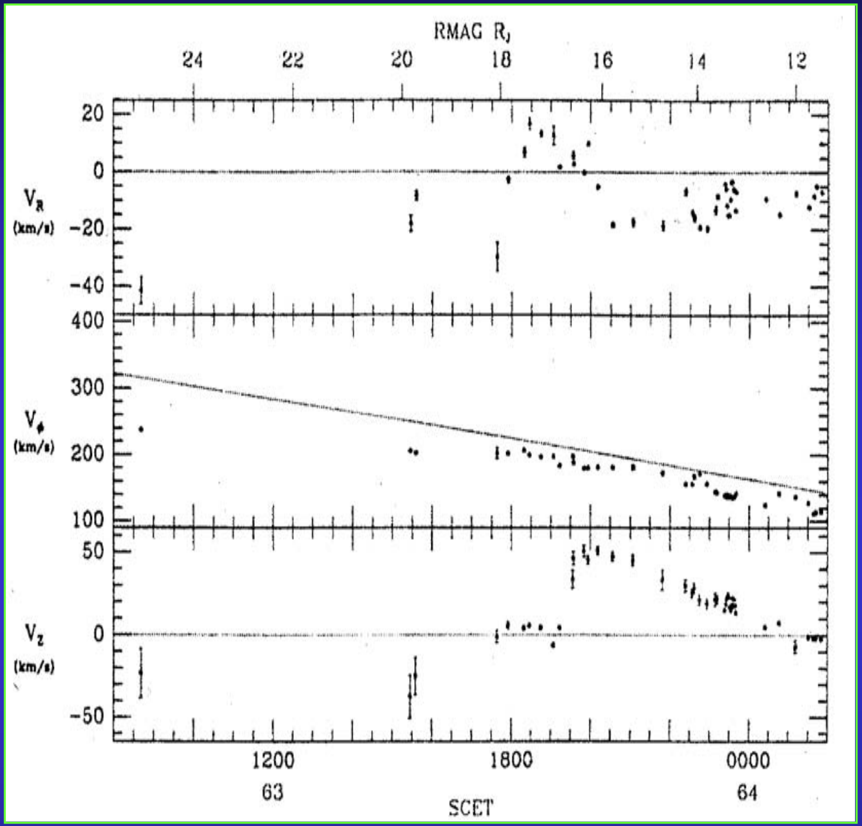

- **Voyager 1 PLS results**
  - **McNutt et al., JGR, 86, 8319, 1981**
  - **Sands and McNutt, JGR, 93, 8502, 1988**
- **Velocity lags rigid corotation trend to "constant" velocity outside 20 RJ**

Global Flow Pattern in Jupiter's equatorial plane

Galileo/EPD results

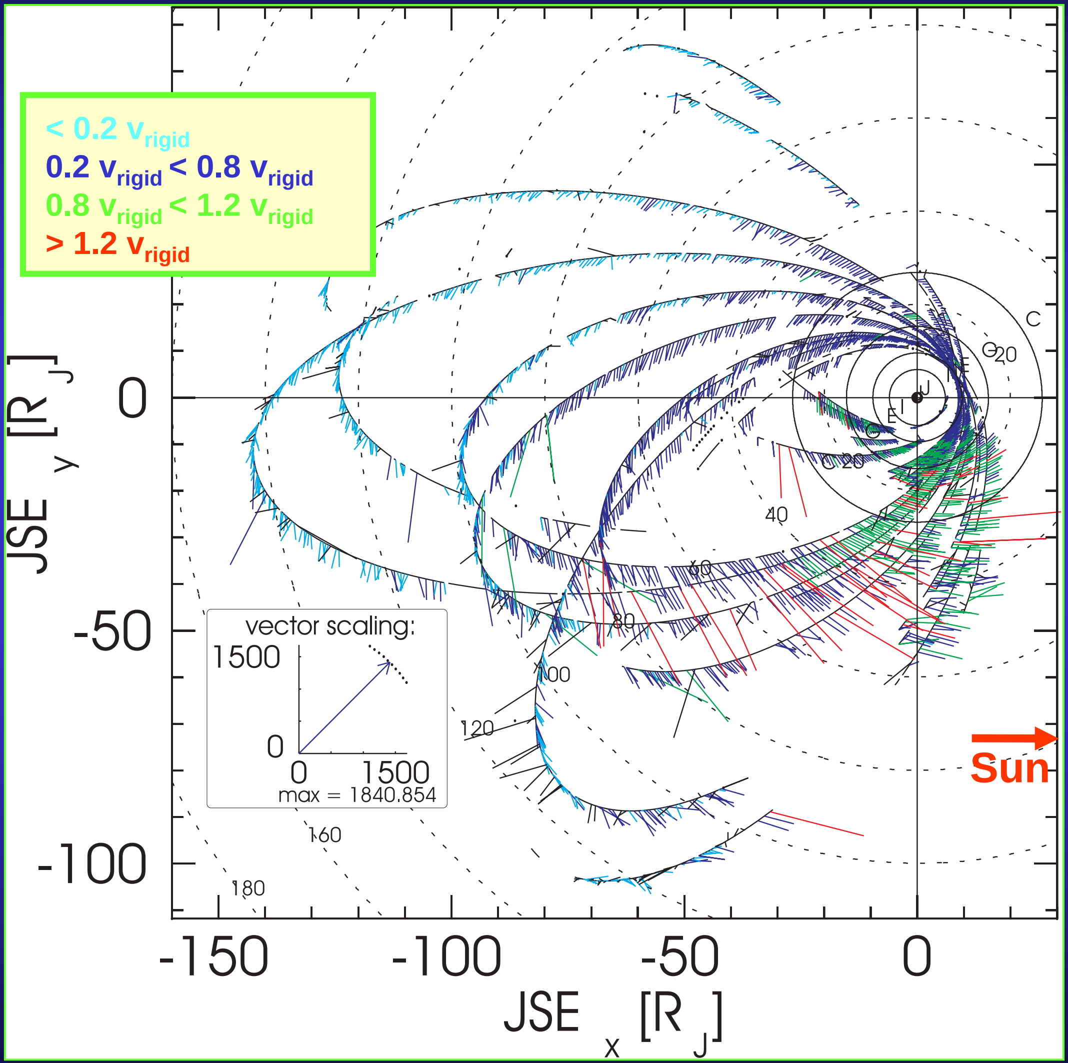

- flow is predominantly in corotation direction
- temporal stable in this averaged view
- flows in the deep magnetotail still in corotation direction, however substantially subrotational
- deviation from „normal“ state due to dynamic processes
- larger flows with radial outward components (100-200 km/s) at dawn compared to smaller flows with small radial inward components at dusk (50 km/s)

Krupp et al., 2001

Global Flow Pattern in Jupiter's equatorial plane

strong local time asymmetry between dawn and dusk

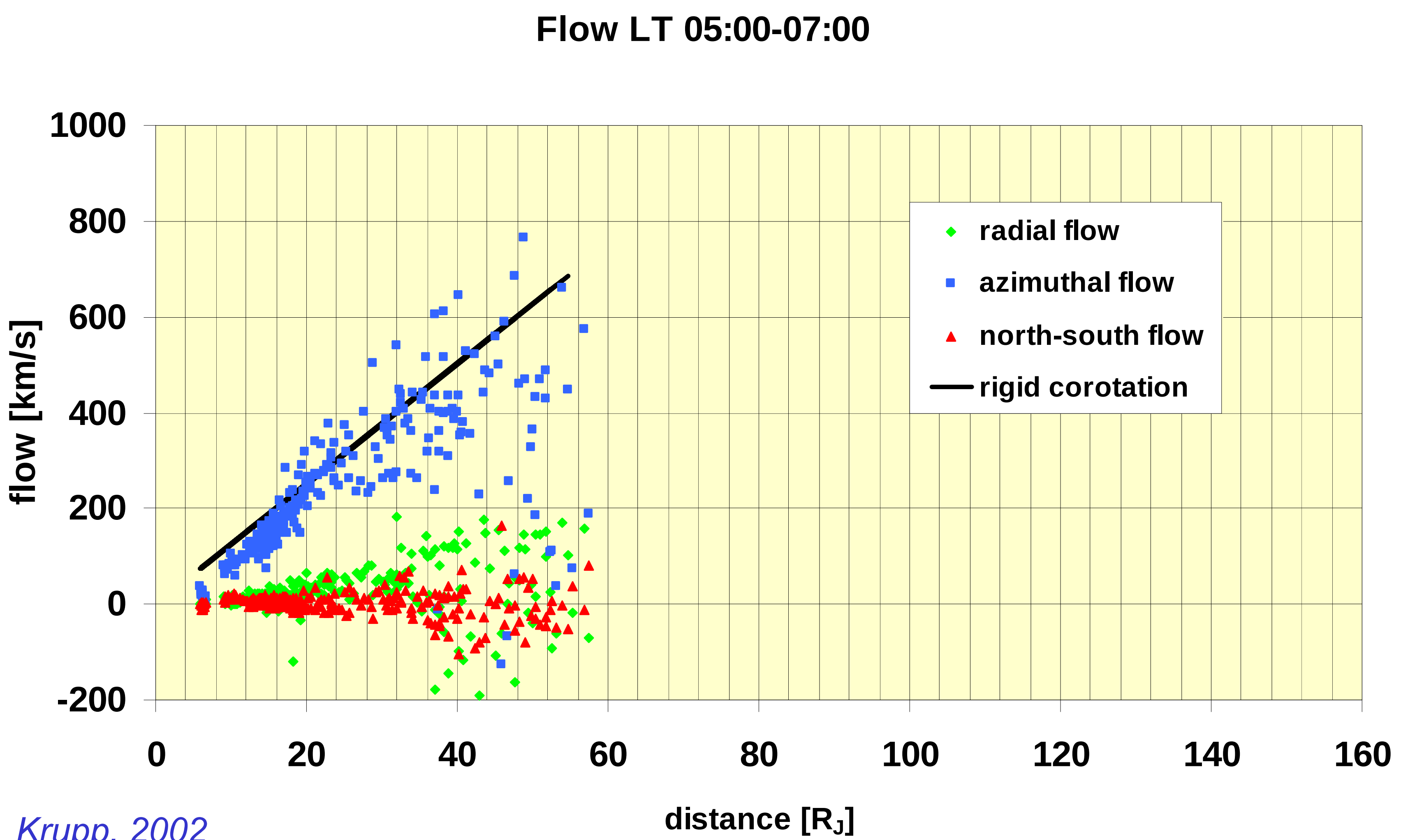

Krupp, 2002

Averaged flow pattern in the equatorial plane

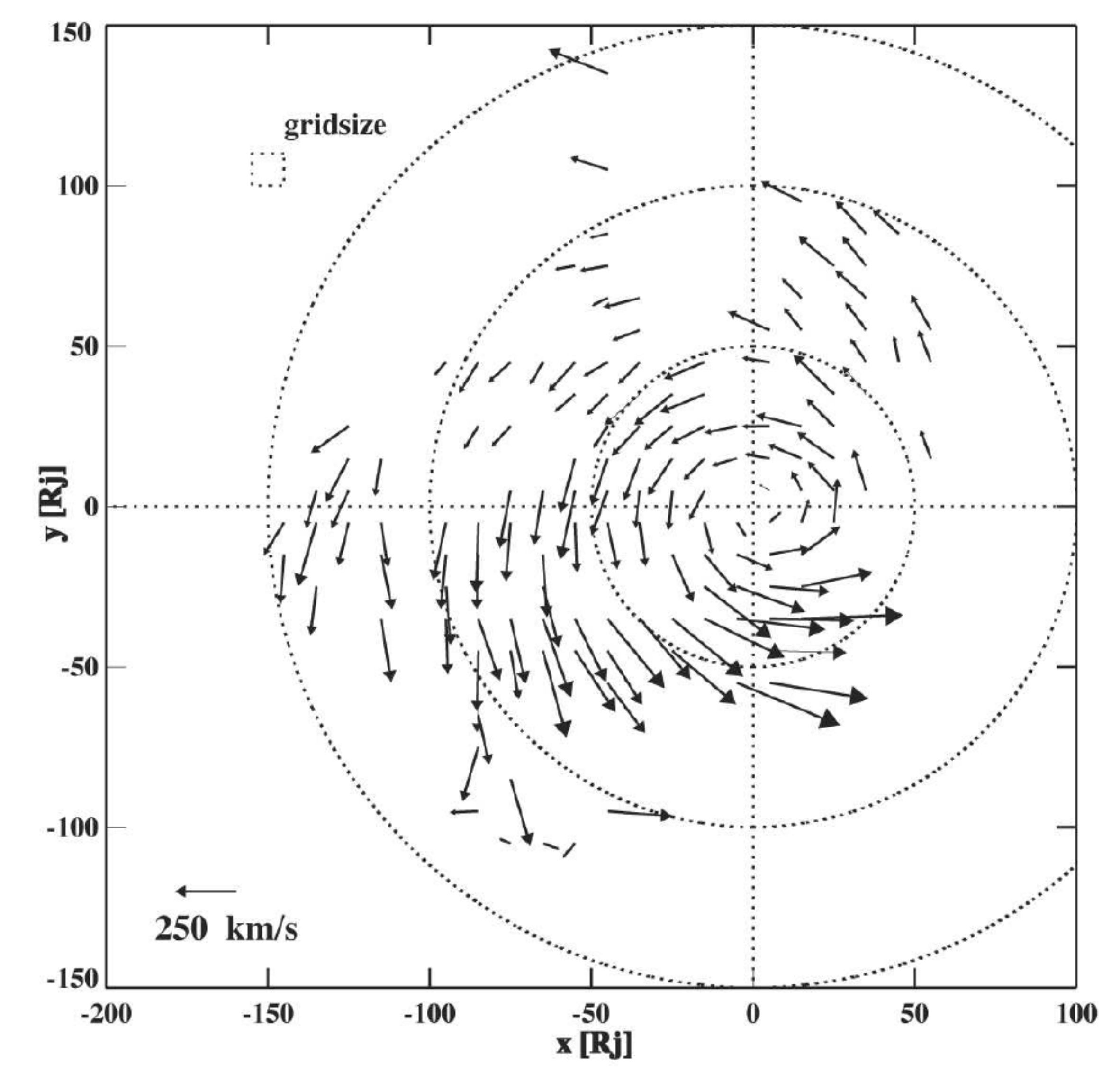

Configuration of magnetotail field lines and current sheet thickness

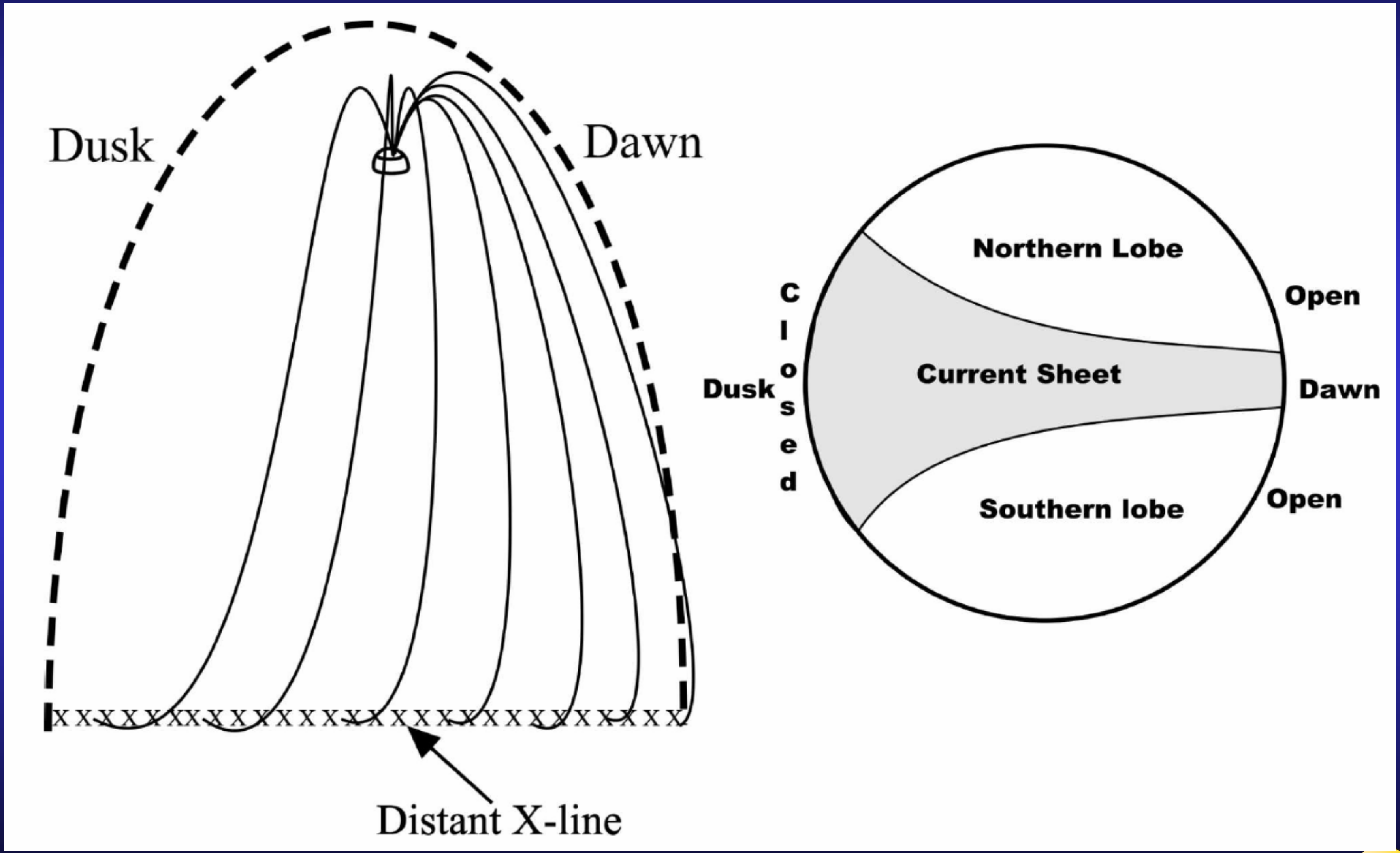

MHD simulations of the Jovian magnetosphere

IMF=0

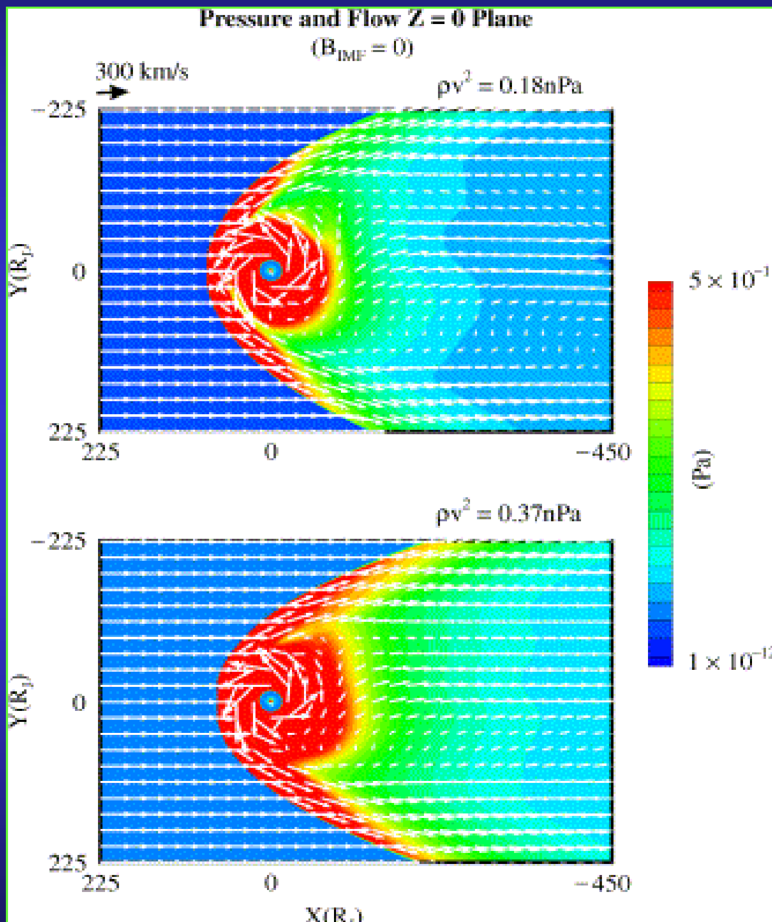

IMF=southward (top) and northward (bottom)

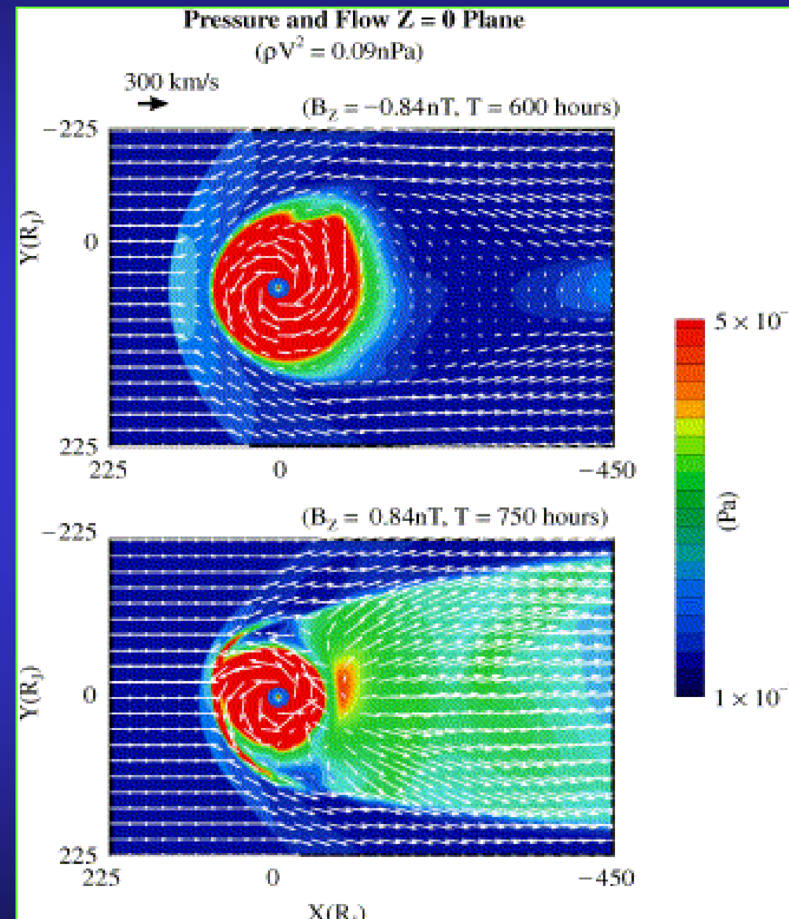

Walker, 2001

First global ion composition ratios of the Jovian magnetosphere

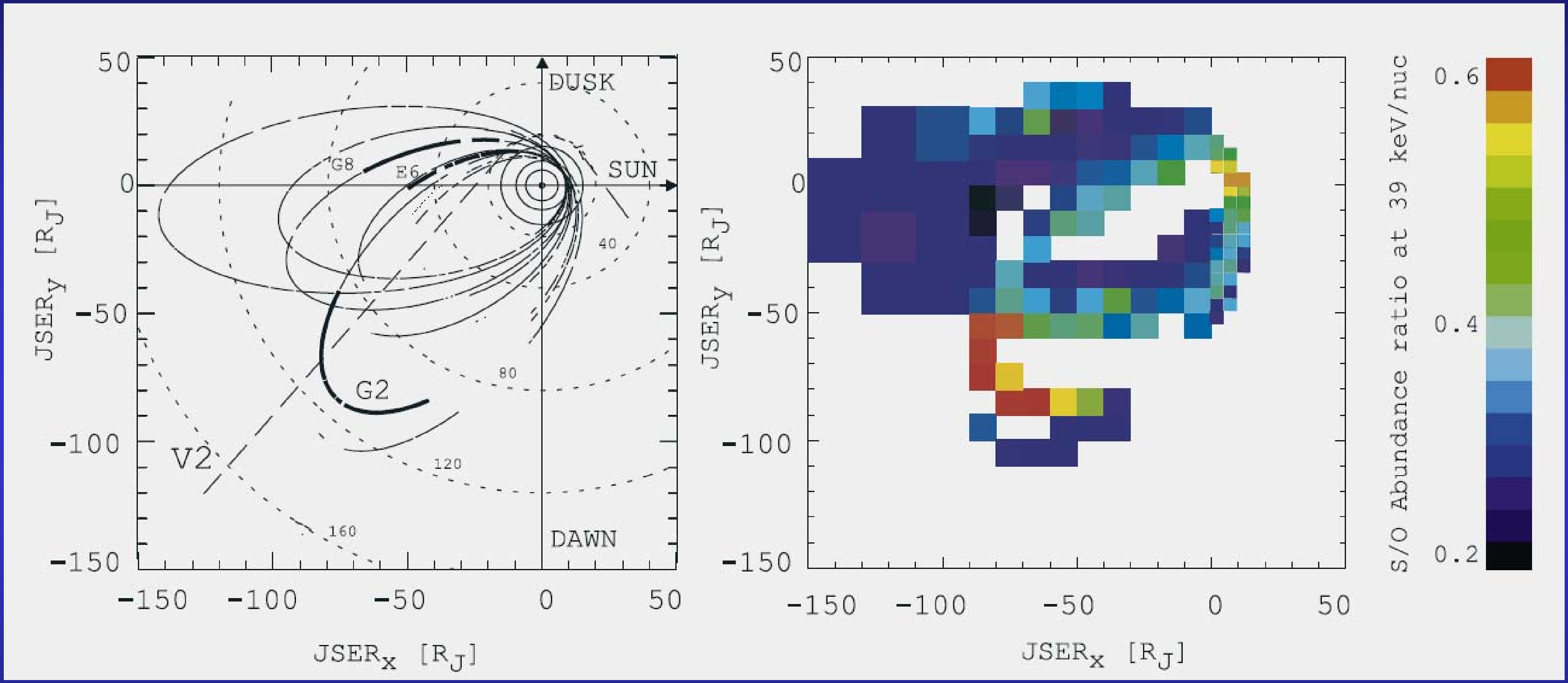

Radioti et al., 2005

First global ion composition ratios of the Jovian magnetosphere Galileo-Voyager comparison

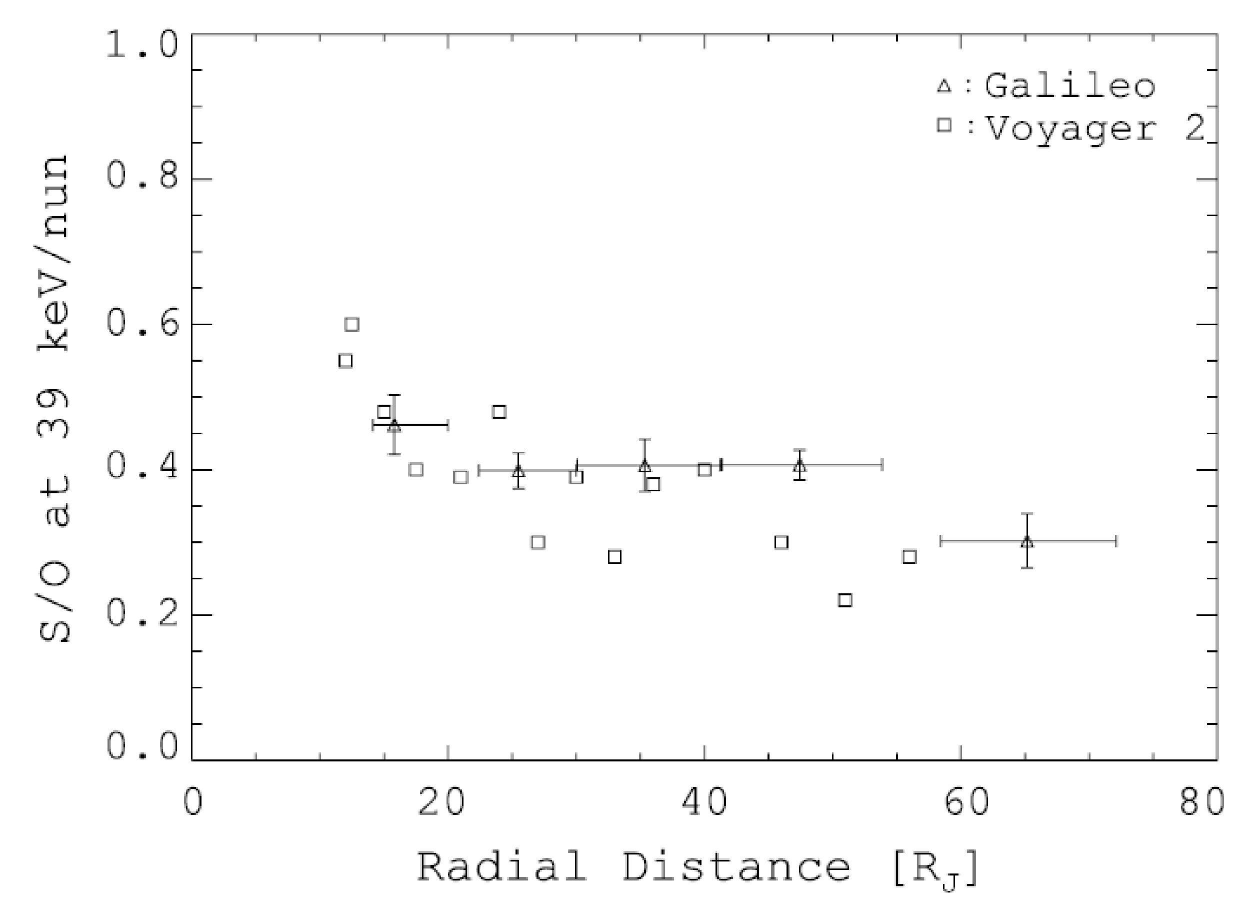

Radioti et al., 2005

Jupiter as a source of hot neutrals

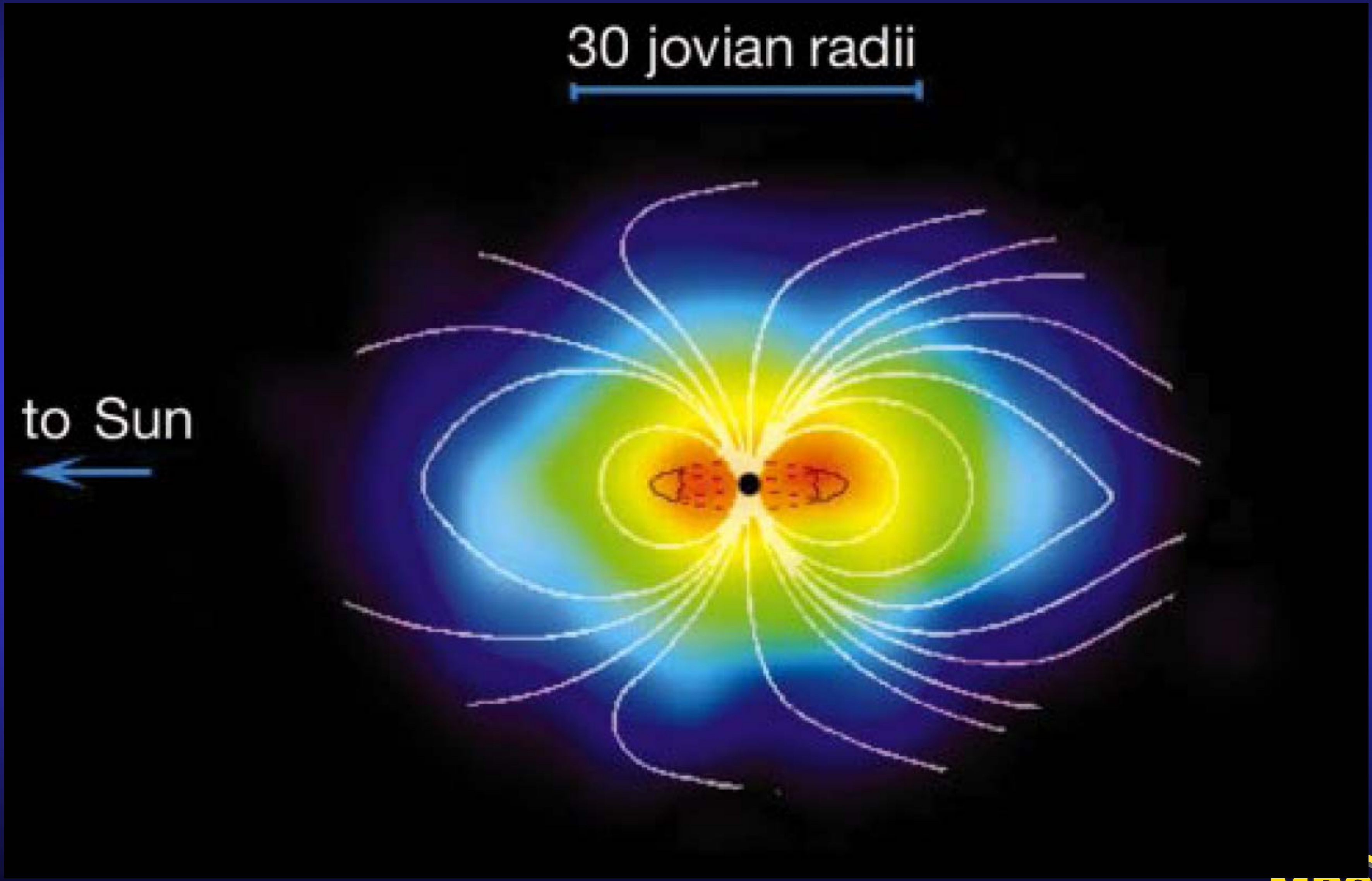

Jupiter as a source of hot neutrals

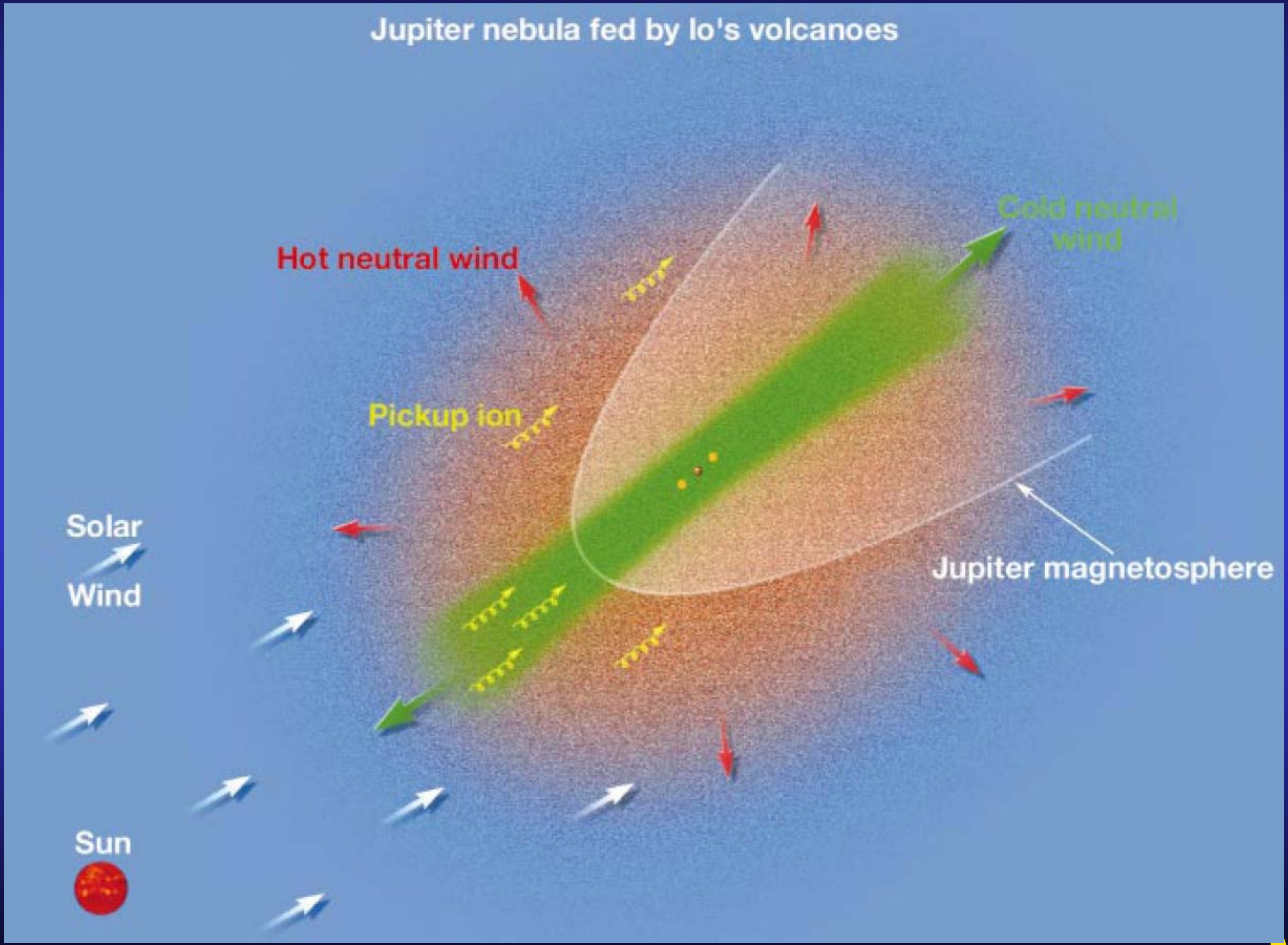

Energetic Neutral Atom (ENA) imaging

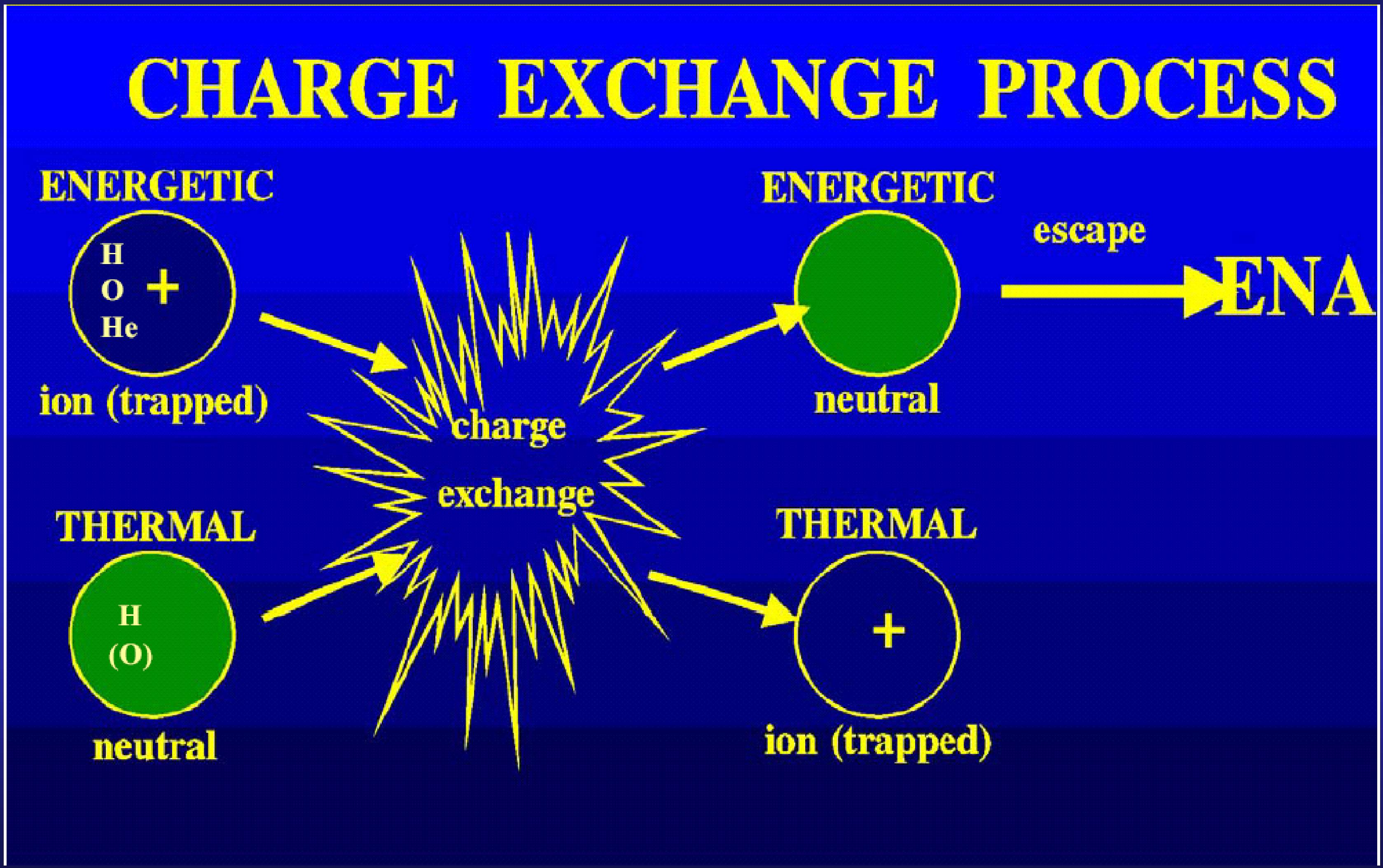

ENA principle

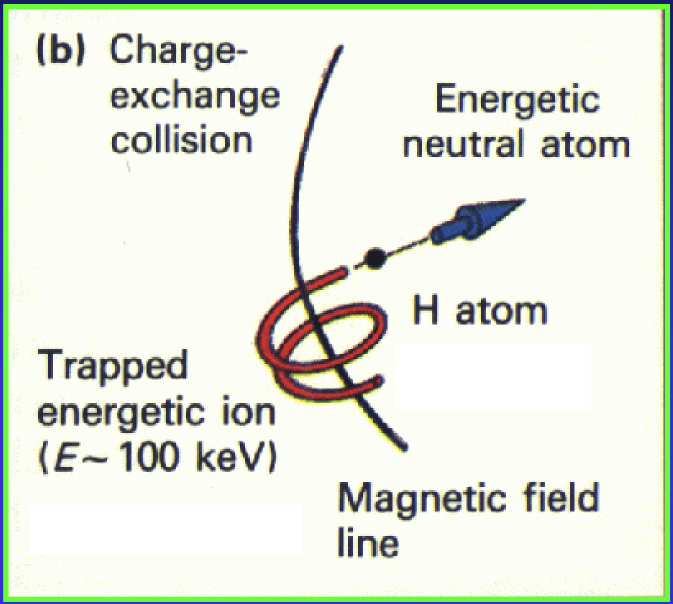

The co-existence of an energetic charged particle population (solar wind, magnetospheric plasma) and a planetary neutral gas leads to interaction, e.g., through charge-exchange:

$$A^{+}(\text{energetic}) + P(\text{cold}) \Rightarrow A(\text{energetic}) + P^{+}(\text{cold})$$

Little exchange of momentum → conserve velocity
ENA are not influenced by E- and B-fields; they travel on straight ballistic path like a photon
Directional detection of ENAs yields a global image of the interaction and allows to deduce properties of the source populations.

ENA production mechanism in space plasmas

Charge - exchange reaction with atmospheric / exospheric gases
Sputtering of planetary atmospheres
Backscattering from the planetary atmospheres (ENA albedo)
Sputtering from planetary surfaces
Ion neutralization / sputtering on dust particles
Recombination (CMI)

ENA principle

The directional ENA flux (J_{ena}) at a point in space represents an integral along the chosen line-of-sight of the product of the hot ion flux toward the observation point ($j_{ion}(\mathbf{r},\mathbf{v}, t)$), the cold neutral density ($n_{neutral}(\mathbf{r},t)$), and the charge exchange cross section. That is,

$$j_{ENA} \cong \int_0^\infty dr \times j_{Ion}(\vec{r},\vec{v},t) \times n_{Neutral}(\vec{r}) \times \sigma_{CE}(|\vec{v}|)$$

where

r is the location along the line-of-sight at which the charge exchange interaction occurs,

v is the ion vector velocity at the instant of the interaction

t time

Dynamics of the Jovian magnetosphere

radial transport
interchange motion
injections
plasma sheet dynamics
particle bursts
boundary phenomena
aurora

Jupiter - Particle motion in the magnetosphere

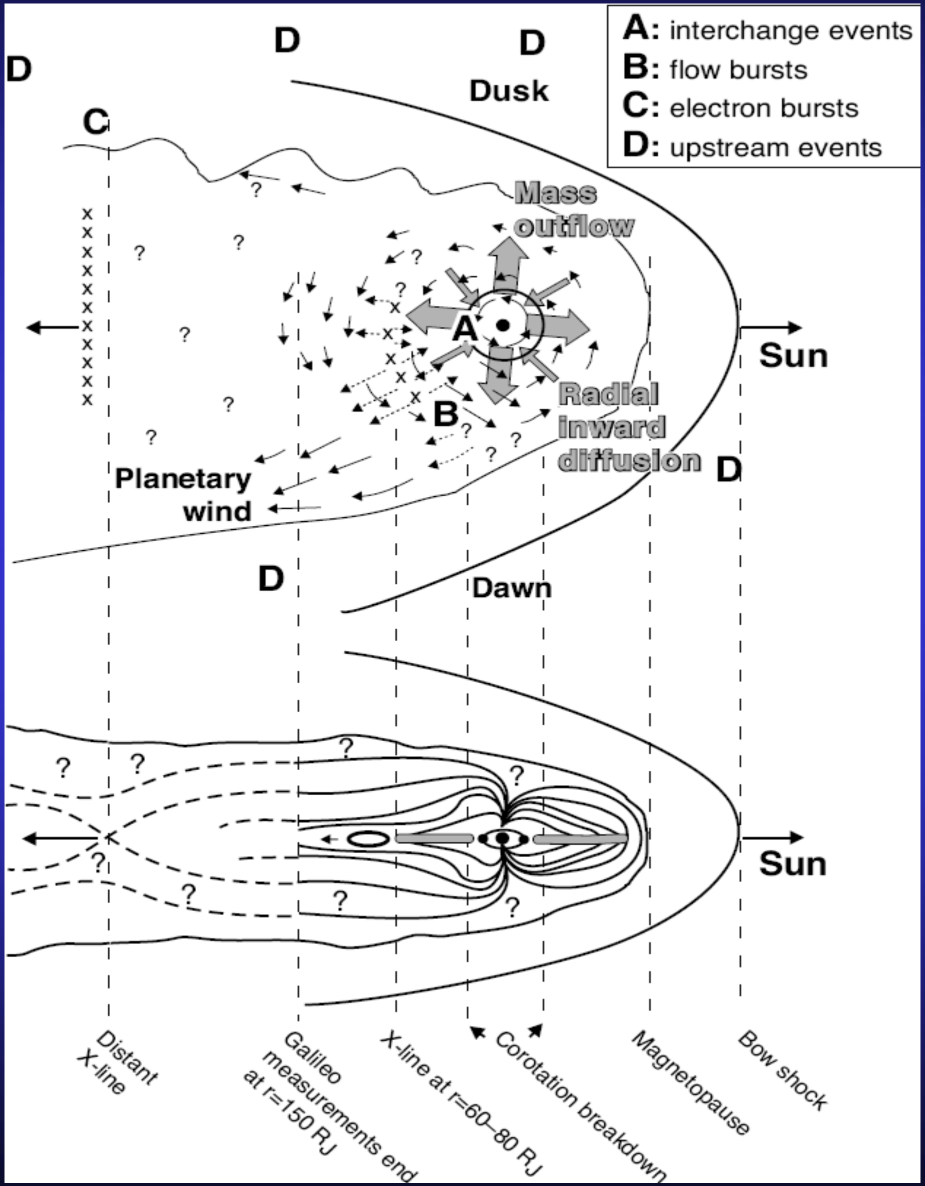

Interchange motion

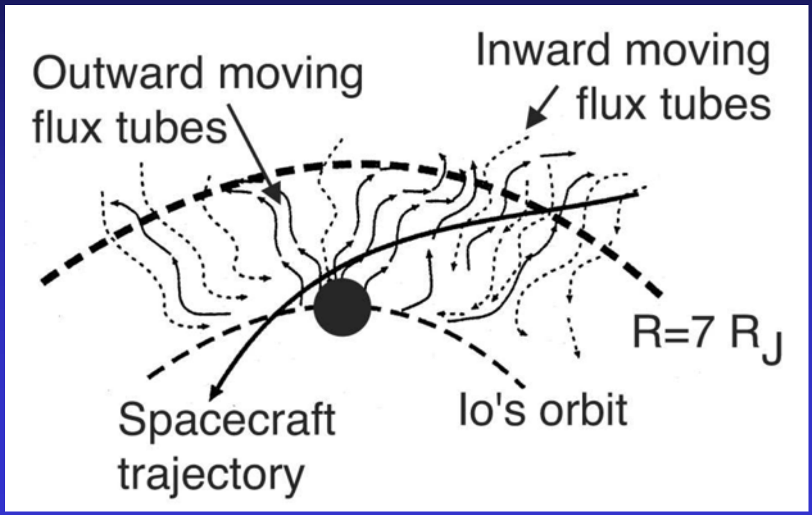

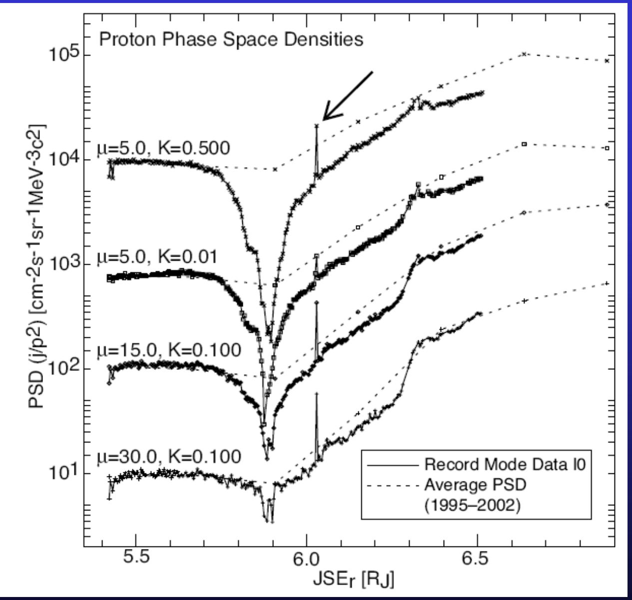

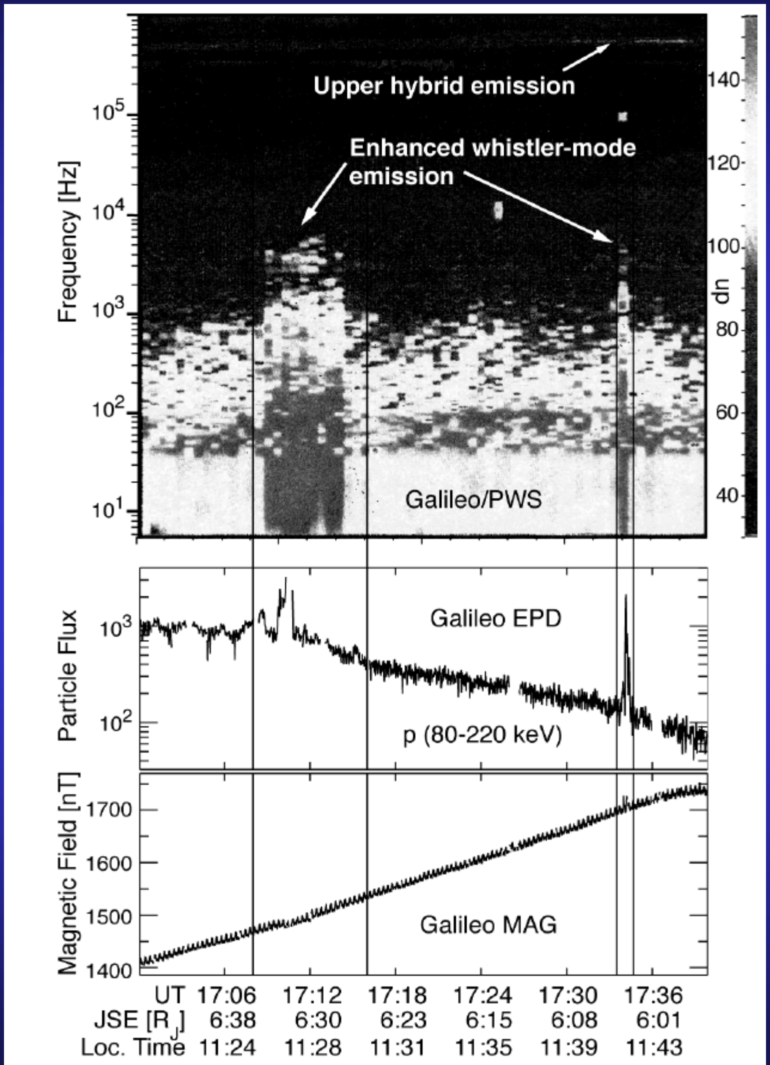

Jupiter's Aurora - The Movie

Fixed magnetic co-ordinates rotating with Jupiter

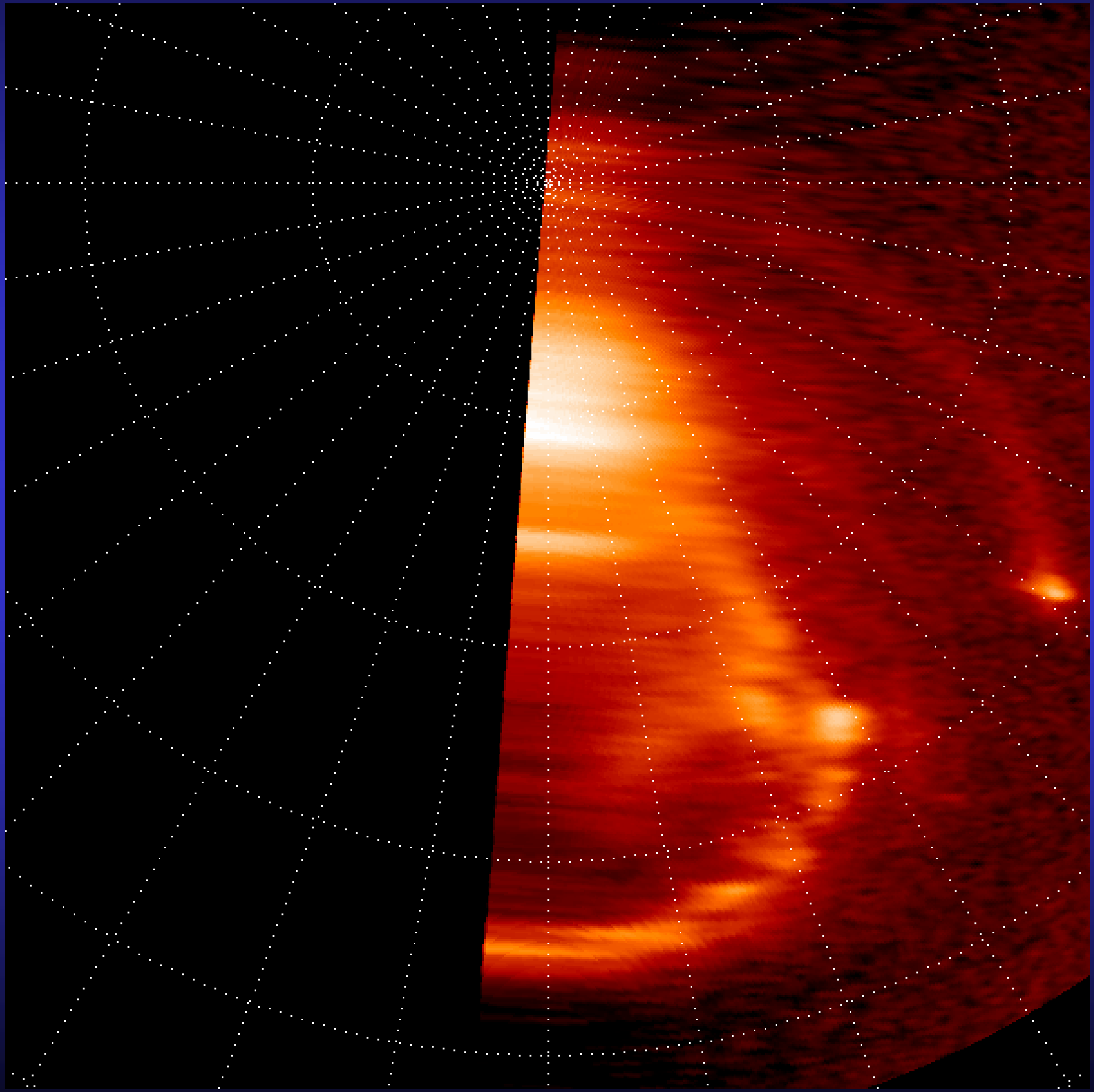

Clarke et al.
Grodent et al.
HST

Jupiter
Different types of aurora

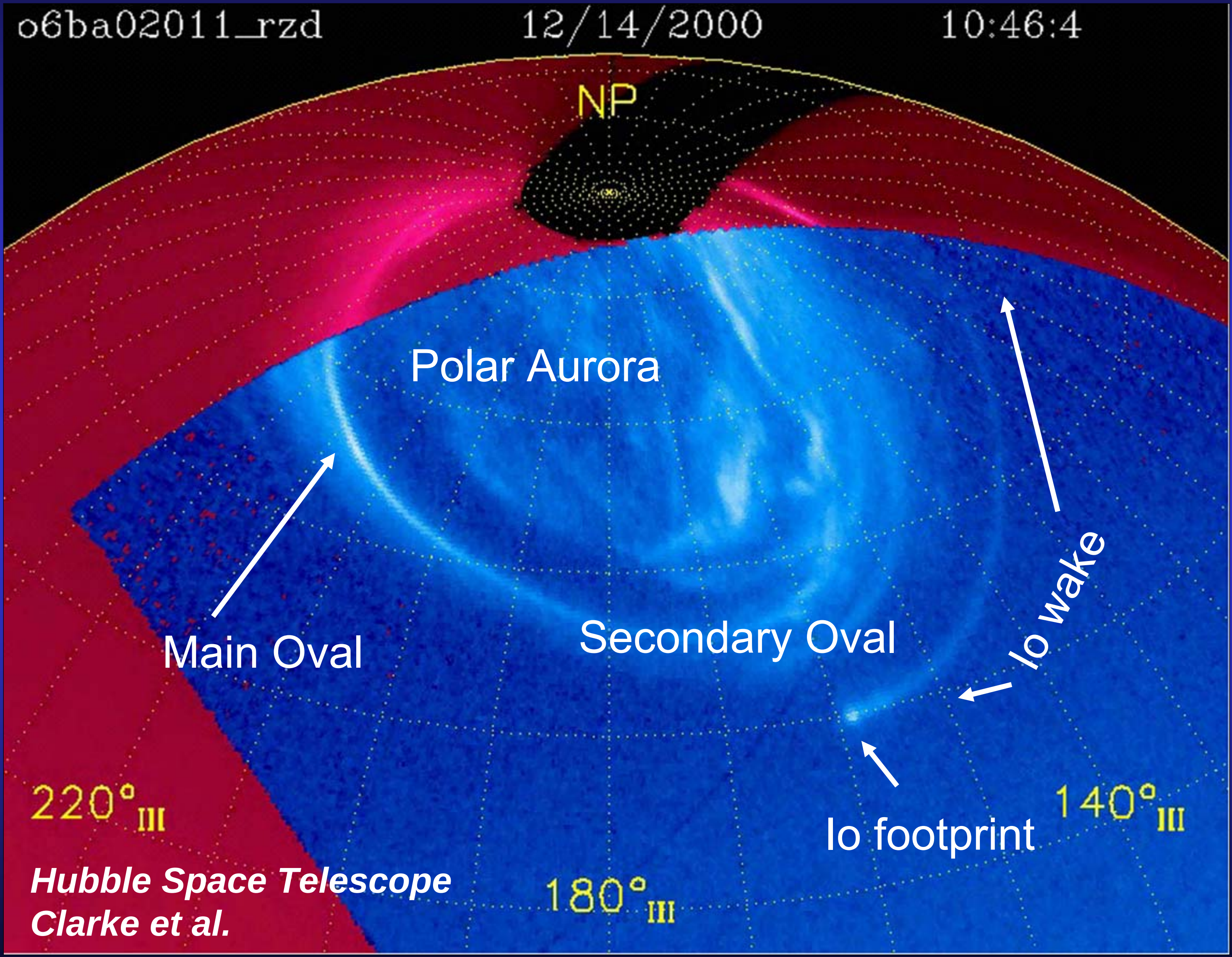

Hubble Space Telescope
Clarke et al.

Jupiter`s main aurora

- Shape constant, fixed in magnetic co-ordinates
- Magnetic anomaly in north
- Steady intensity
- ~1° Narrow

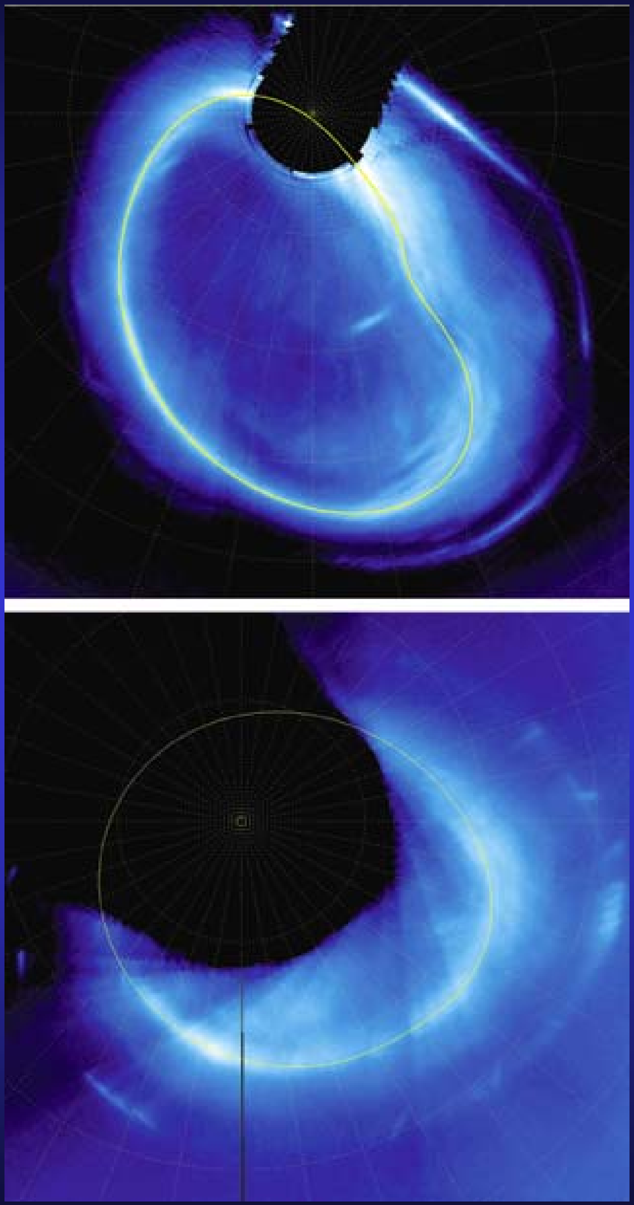

Clarke et al., Grodent et al. HST

Large-scale current system in the Jovian magnetosphere

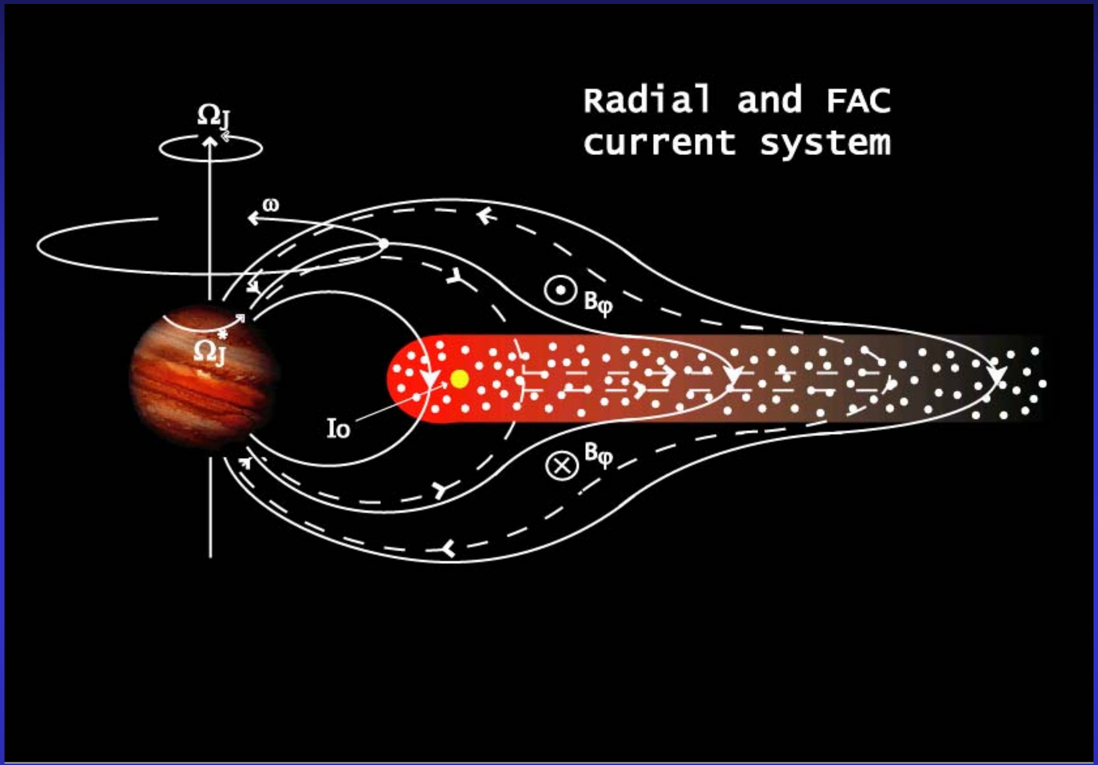

After Hill (1979)
and Vasyliunas (1983)

- Discovery of a local time asymmetry in the system of azimuthal currents which distend the field lines away from the planet (Bunce and Cowley, 2001a; Khurana, 2001)
- Investigations of field-aligned currents associated with magnetosphere-ionosphere coupling currents found to be ~1μAm-2 (Bunce and Cowley, 2001b; Khurana, 2001)

Origin of the Jovian main aurora

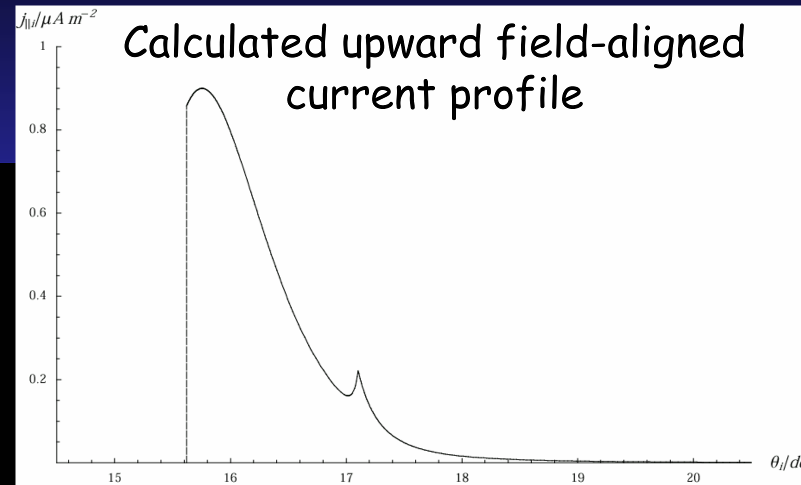

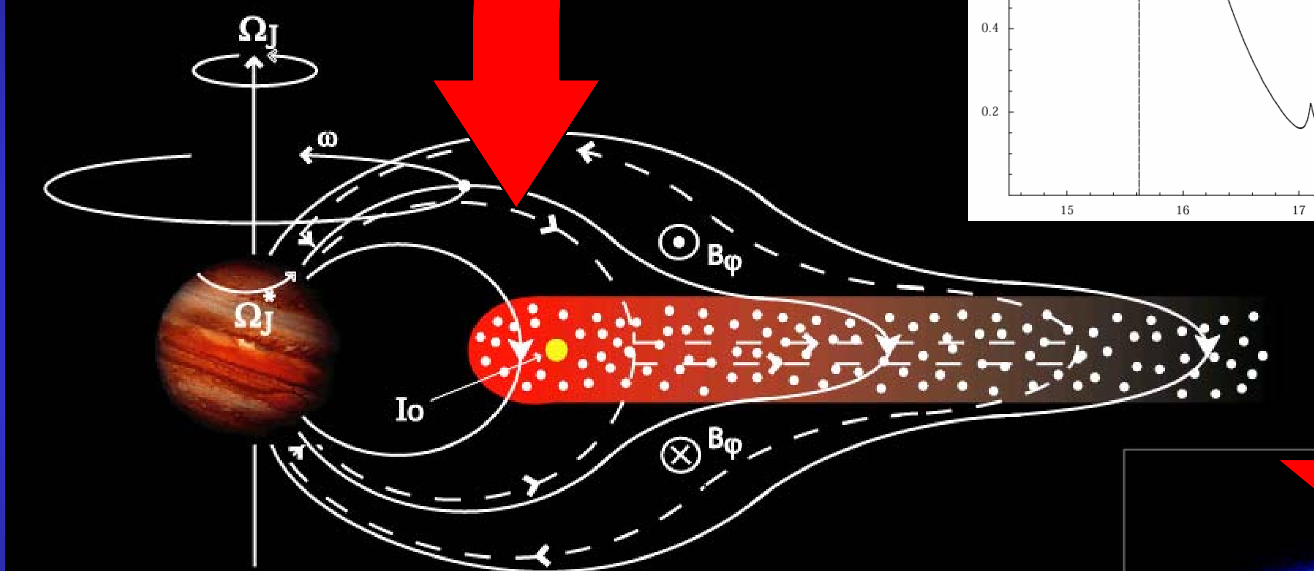

- Bunce and Cowley (2001b), Cowley and Bunce (2001), Hill (2001) and Southwood and Kivelson (2001) suggest the main auroral oval is due to the breakdown of corotation of the equatorial plasma
- Modulation of the oval in anti-correlation with solar wind dynamic pressure (C&B, 2001, 2003a&b; S&K, 2001)

Particle measurements at equator and correlation with secondary oval

- Most prominent and well defined boundary → **change in the electron pitch angle distributions located between 10 and 17 R_J.**

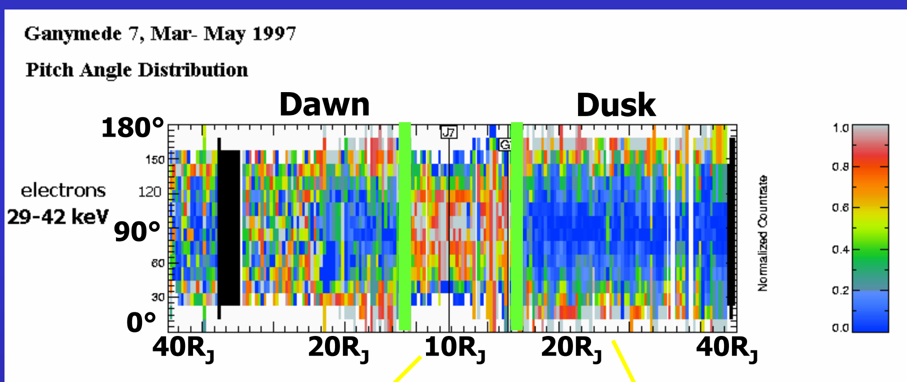

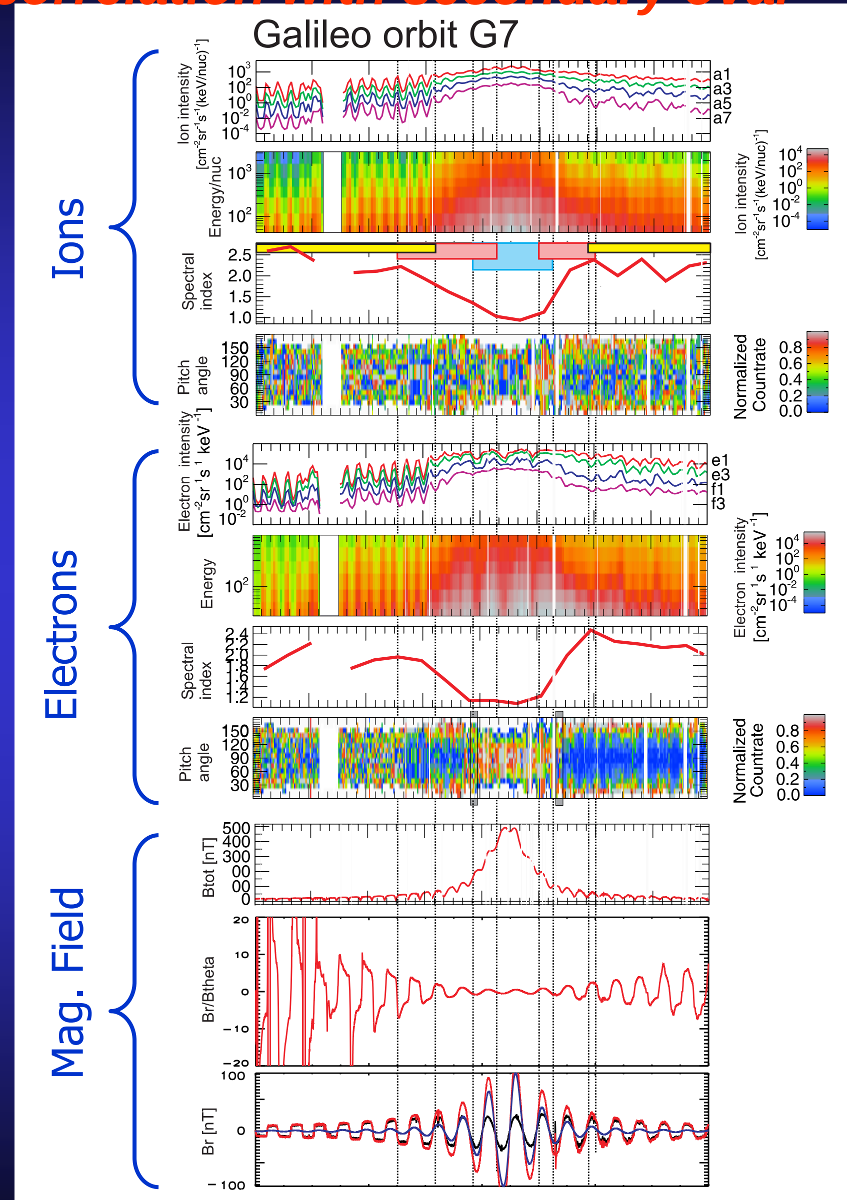

Tomás et al., 2004a

Inner Region

Pancake distribution with electrons maximum at 90^0

Outer Region

Field aligned

bi-directional electrons

Tomas, 2004, 2005

Galileo observations

- Local time dependence of the PAD boundary in the equatorial plane

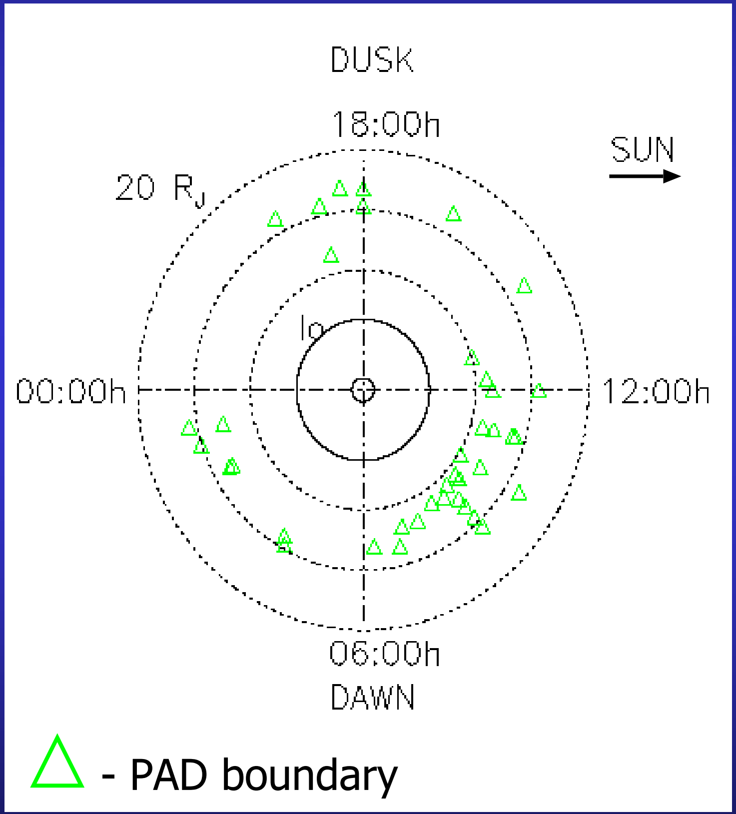

- Coverage of the Jovian magnetosphere in most of the local time sectors.

- No strong local time asymmetry between dawn and dusk.

Tracing the magnetic field lines

➢ Comparing the footprints of the PAD boundary (VIP4 model) with the HST observations

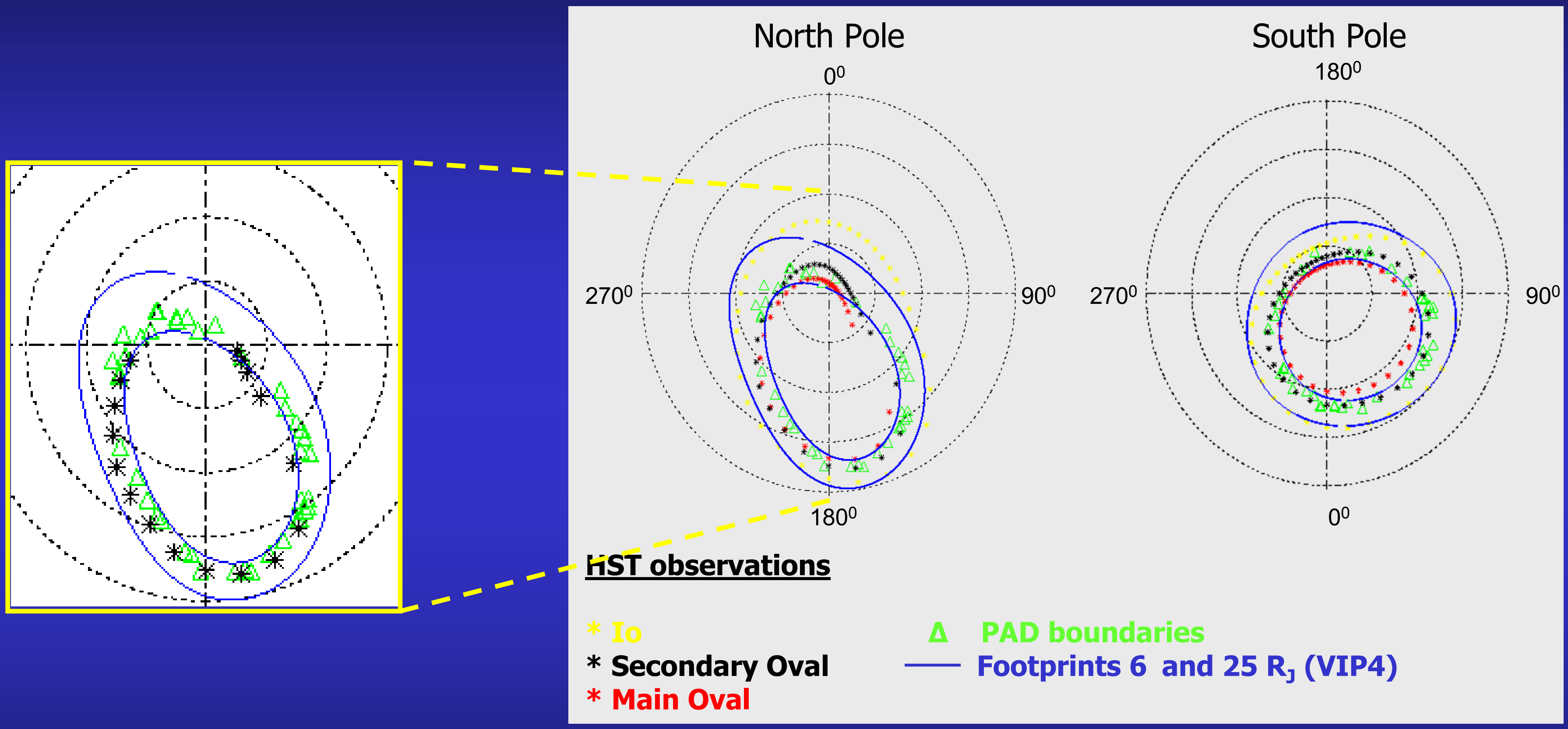

➢ Good conjugation between the PAD boundary and the secondary oval

Wave-particle interaction

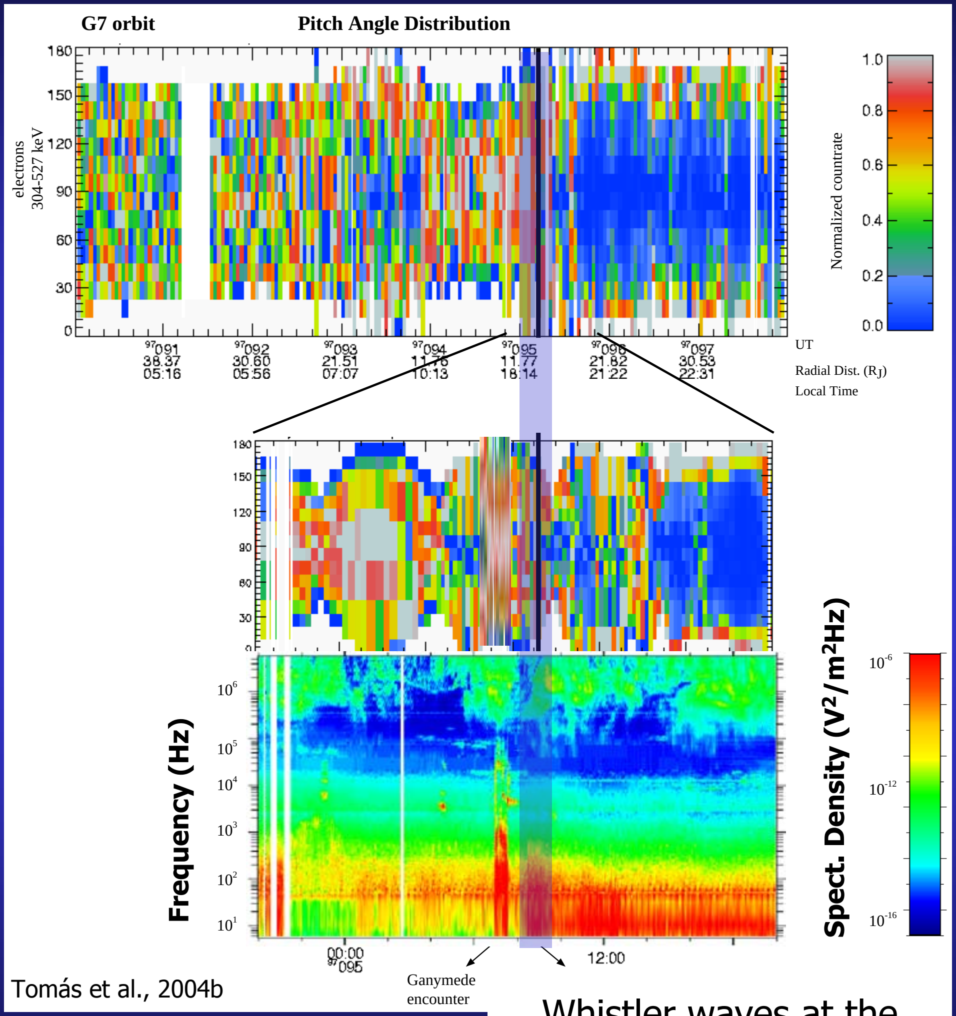

Tomás et al., 2004b

Whistler waves at the PAD boundary

- Pitch angle diffusion coefficient

$$D_{\alpha\alpha} = \frac{2\pi f_c}{\gamma}\left(\frac{B'}{B}\right)^2 \cdot \varepsilon$$

- Strong diffusion limit

$$D_{sd} = \left(\frac{v}{4R_J}\right)\frac{1}{L^4}$$

Considering:

L – [10, 17] R_J B – [350, 50] nT

f_c – [10^4, 10^3] Hz E′ – [1.0, 0.1] mV/m

$D_{\alpha\alpha} \sim 2\, D_{sd}$ → The conditions for strong pitch angle diffusion are satisfied.

Max-Planck-Institut für Sonnensystemforschung

Precipitation energy flux

- Considering:
- The precipitation energy flux given by **:**

$$\varepsilon = \int_{E_{min}}^{E_{max}} E \cdot j(E,\gamma) \cdot dE$$

- Measured electron's spectra at the PAD boundary.
- Strong pitch-angle scattering.

- Electron's energy : $E_1 \in [55, 304]$ keV.

  $E_2 \in [55, 188]$ keV.

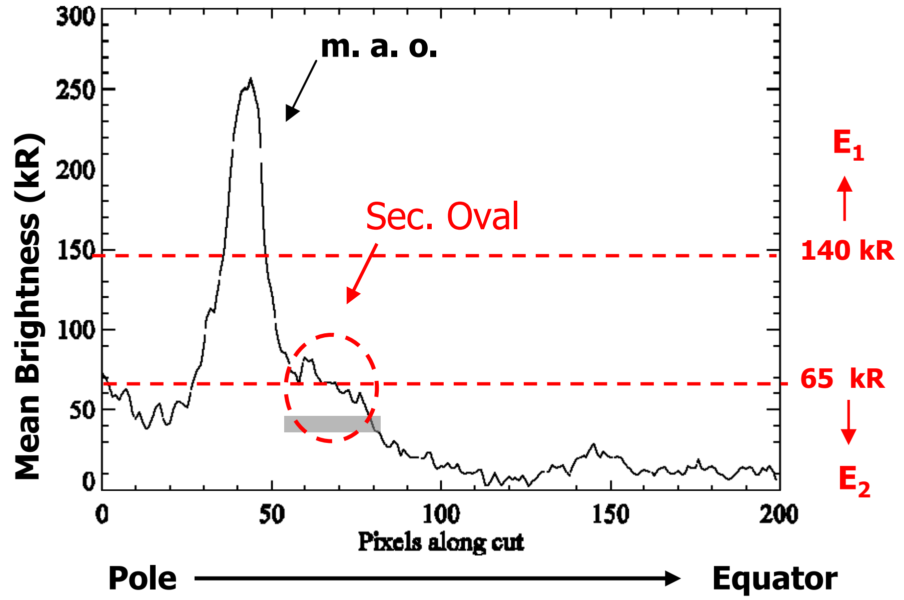

Courtesy of D. Grodent, Univ. Liège

Sufficient to directly produce the observed auroral emissions of the secondary oval without the need of a field aligned potential drop.

Max-Planck-Institut für Sonnensystemforschung

Cassini – Galileo Rendezvous at Jupiter

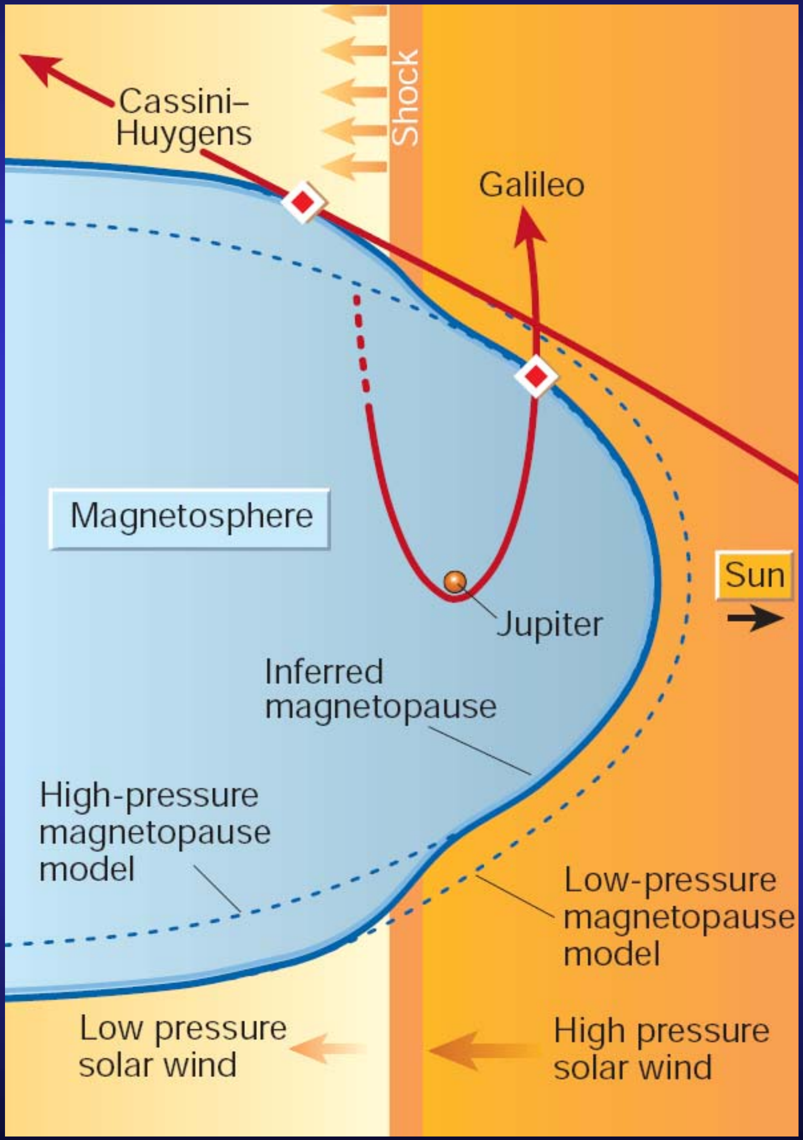

Dynamics in Jupiter's magnetosphere

Energetic Particle Injections & correlation to auroral emissions

24 hour Galileo Energetic Particle Spectrogram

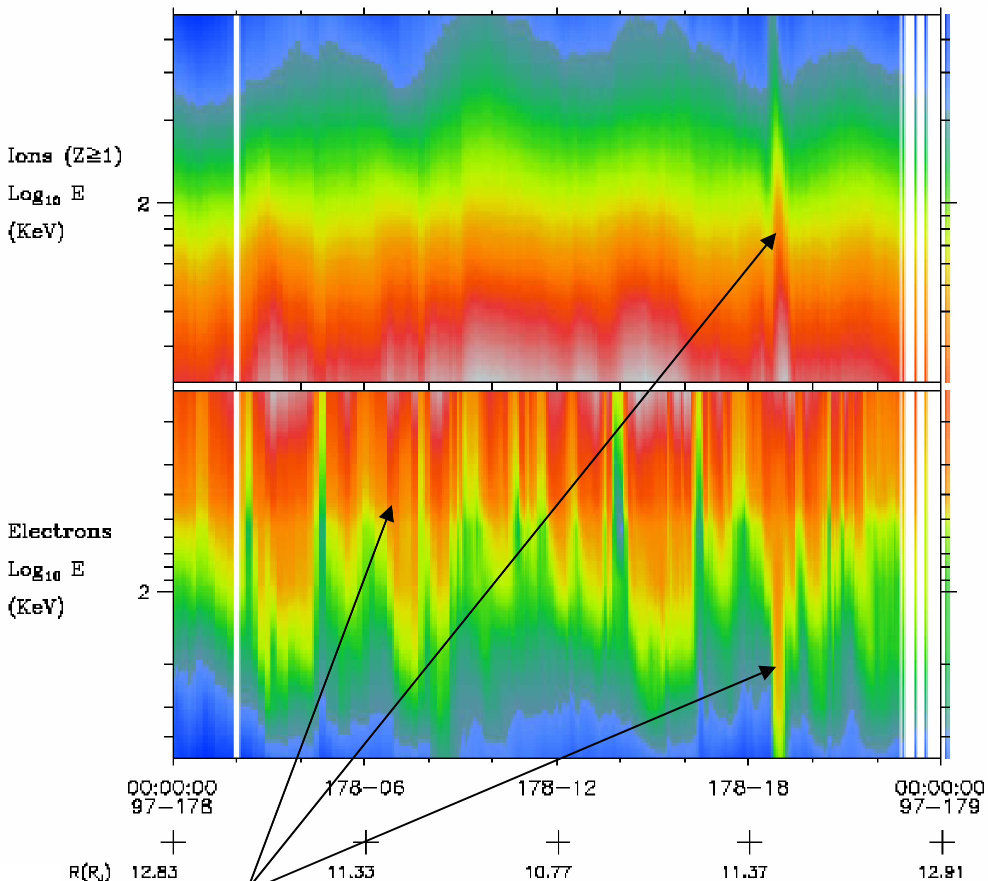

HST Image of Jupiter's UV aurora

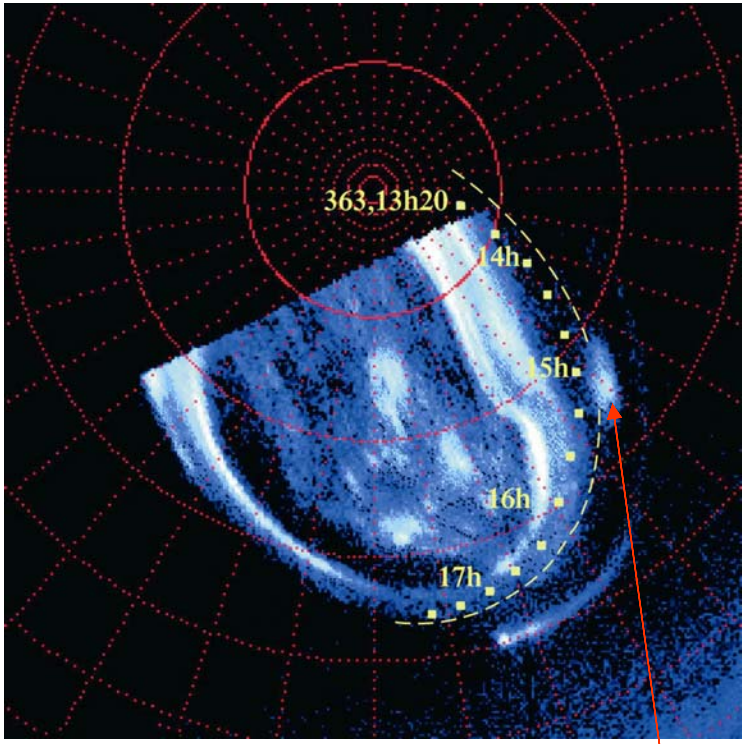

Mauk et al., 1997; 1999, 2000

Extreme "storm-time" dynamics observed in the vicinity of Europa's orbit

Auroral manifestation of near-Europa storm dynamics

Dynamics in Jupiter's magnetosphere

Particle injections

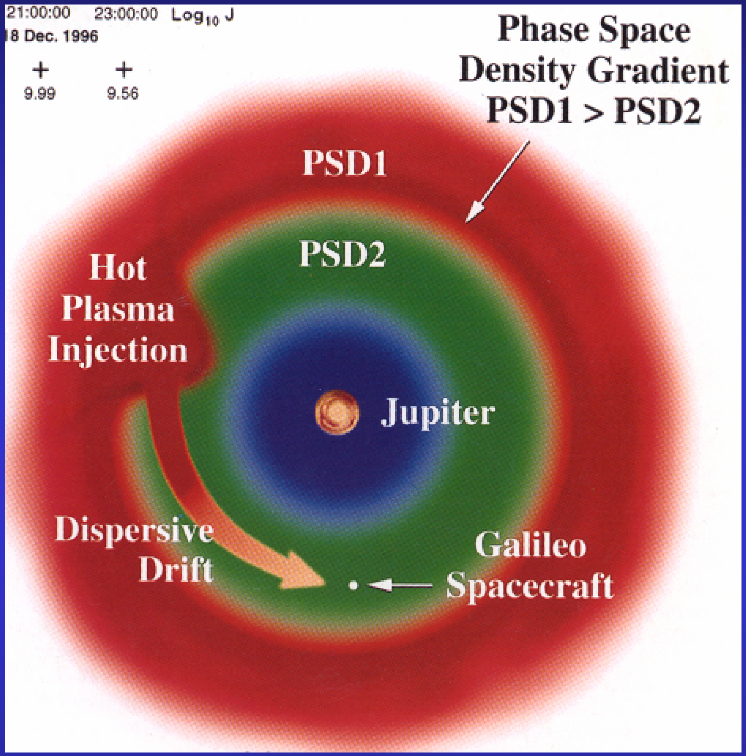

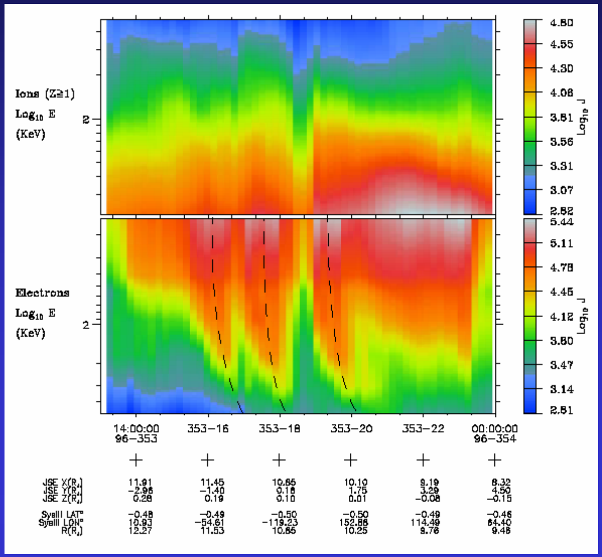

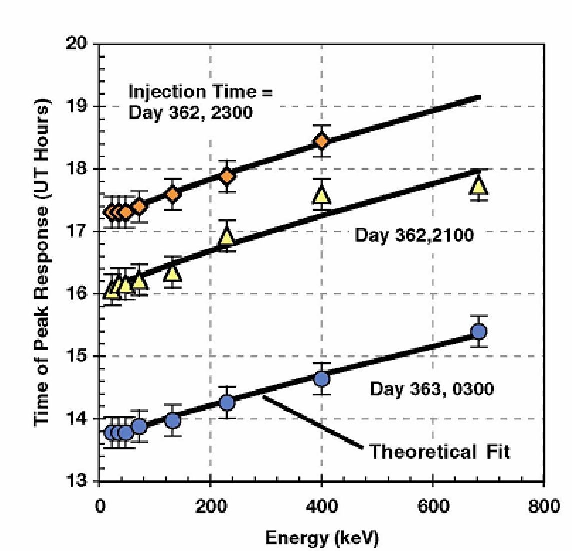

The behaviors of Jupiter magnetosphere injections were understood by invoking sudden radial injections over confined regions in azimuth followed by slow, dispersive, azimuthal drifts.

Dynamics of the Jovian magnetotail

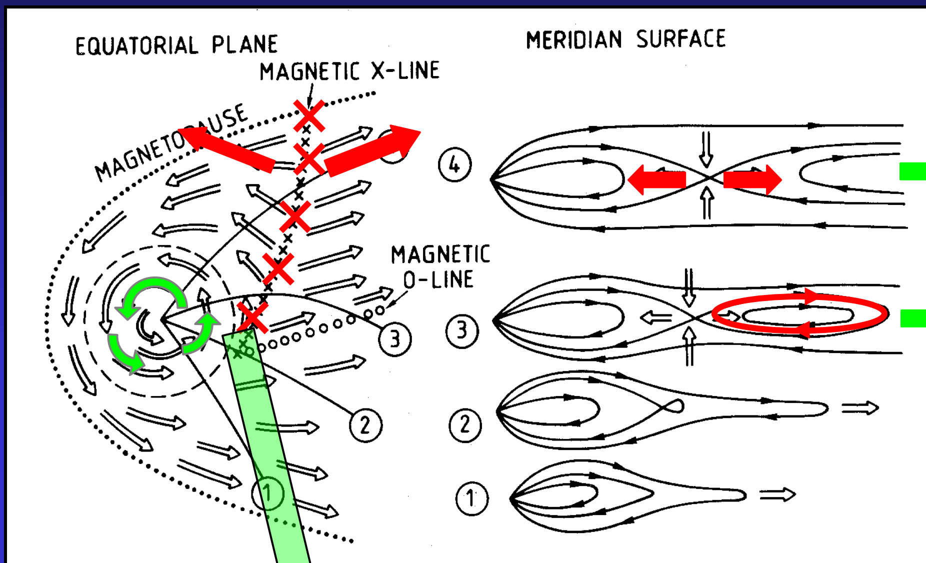

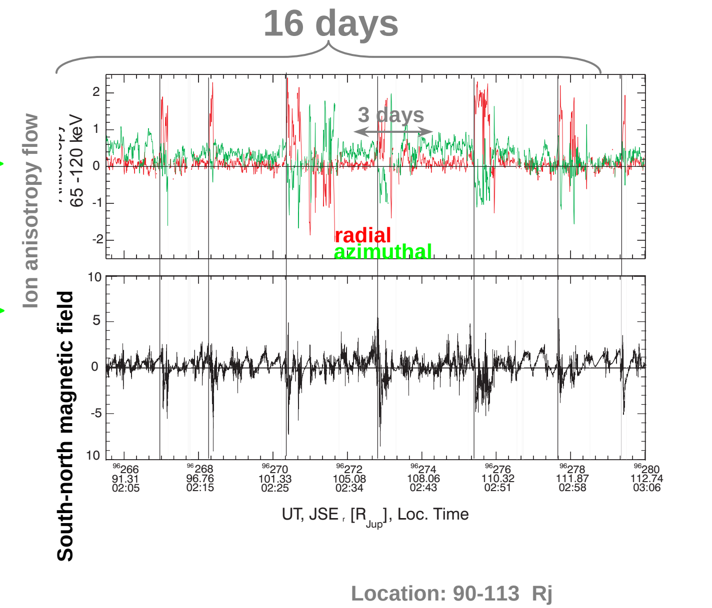

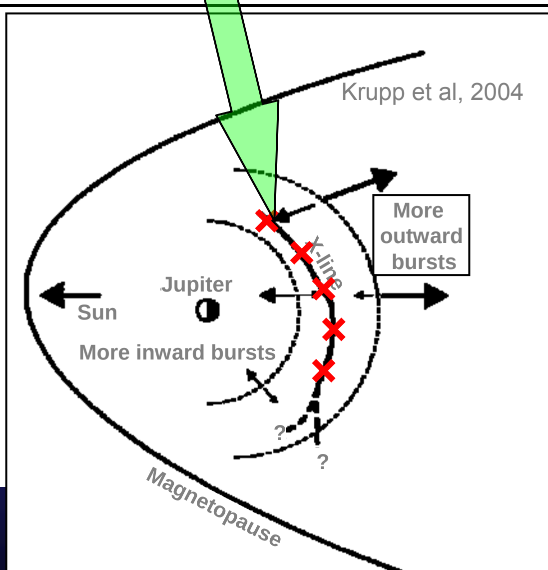

Transient *periodical disturbances*
with repetition period of several days
(the most characteristic 2-3 days)
are observed in the Jovian magnetotail!

Global nature of several days periodicities

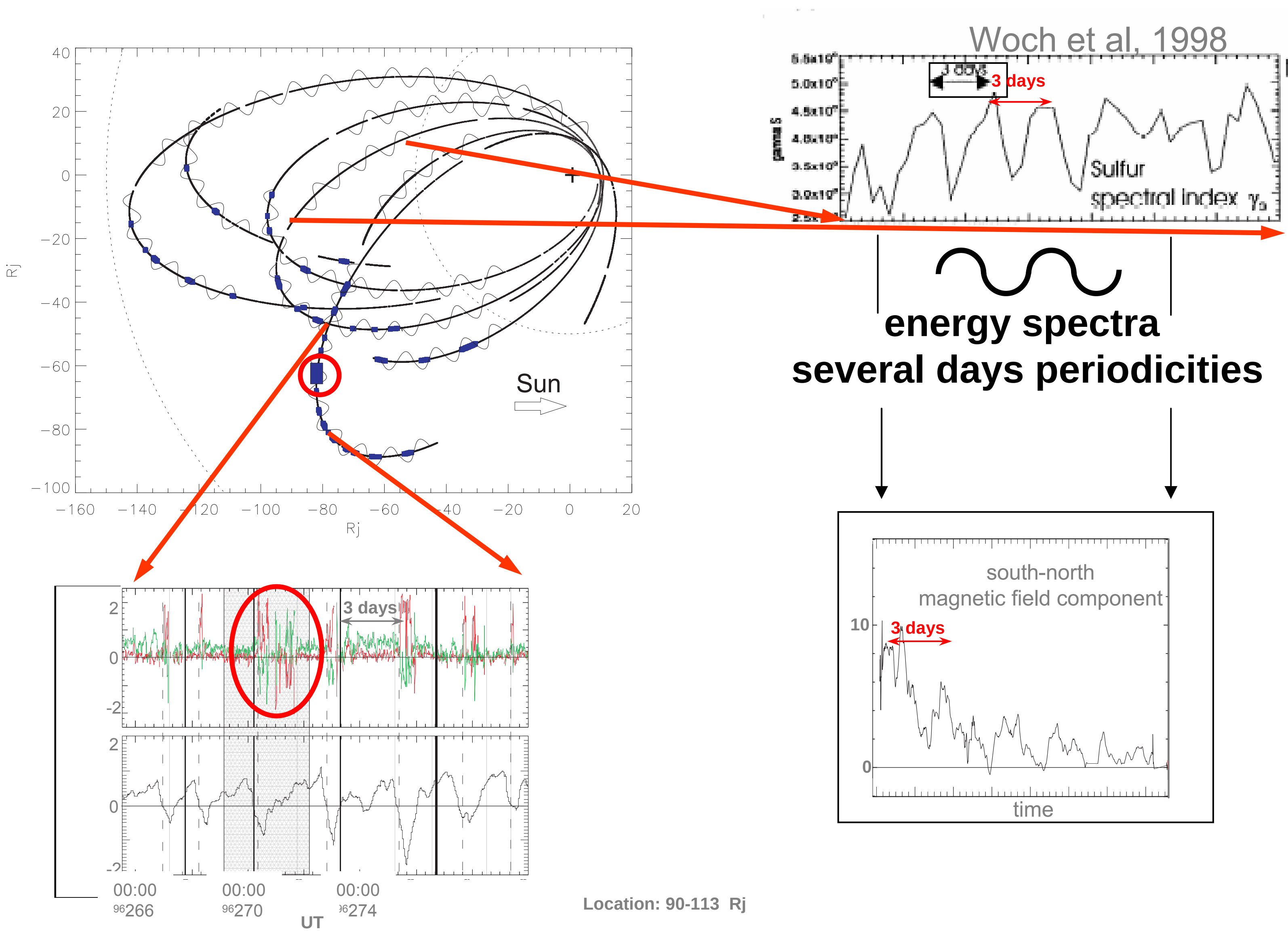

Location: 90-113 Rj

Interpretation of observations

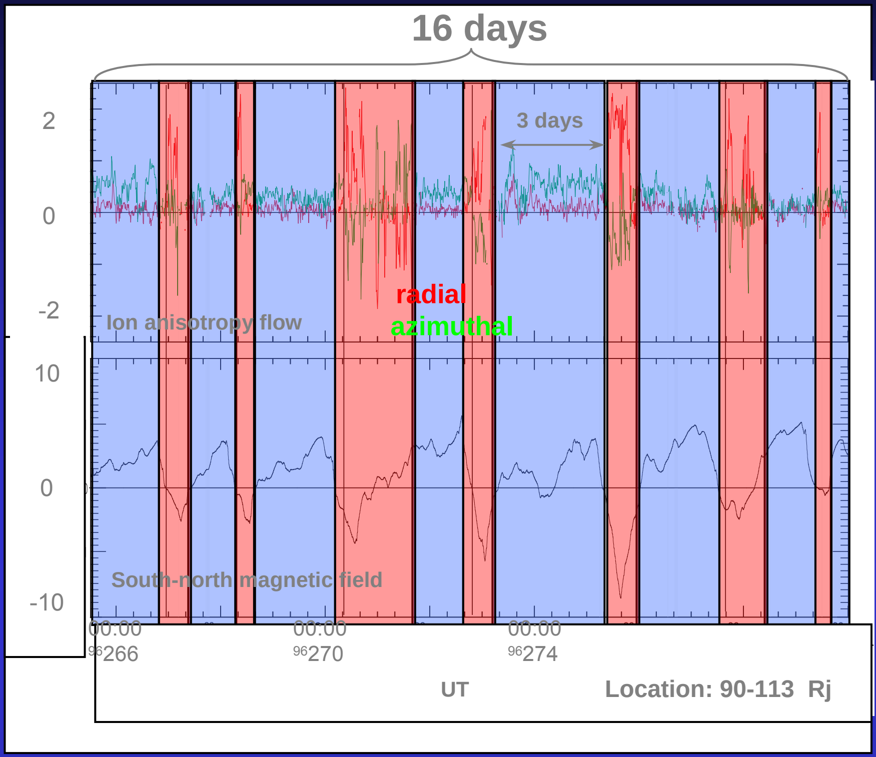

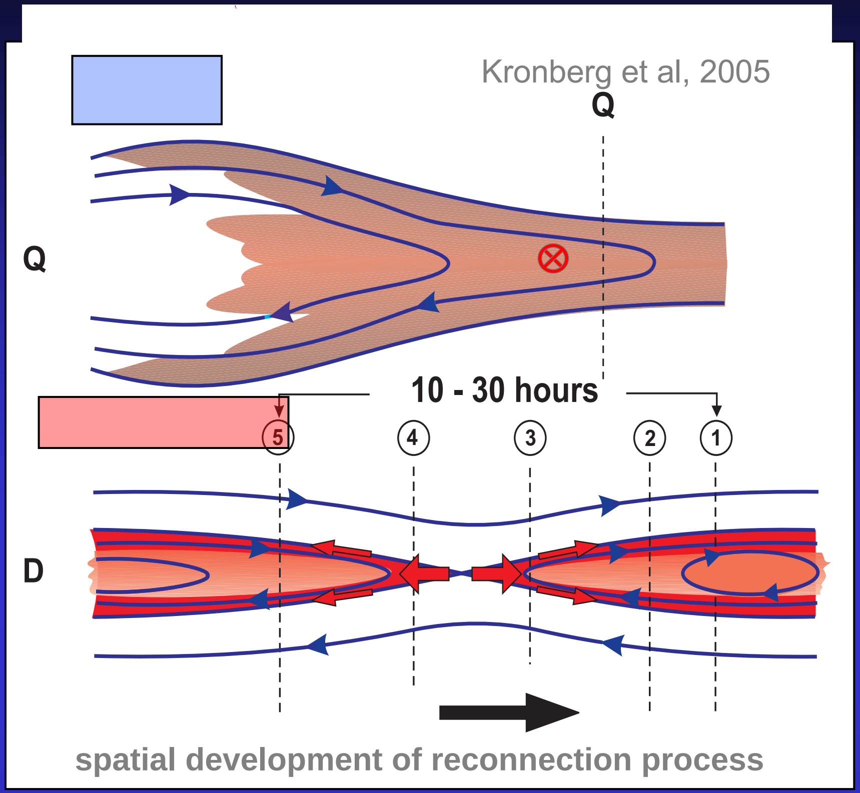

Quiet state

corotational plasma flow

+

stretching of the magnetotail

↓

mass-loading

Disturbed state

radial inward and outward flow bursts

+

thin plasma sheet

+

reconnection

↓

mass-release

MPS Max-Planck-Institut für Sonnensystemforschung

Internally driven magnetotail

Theory

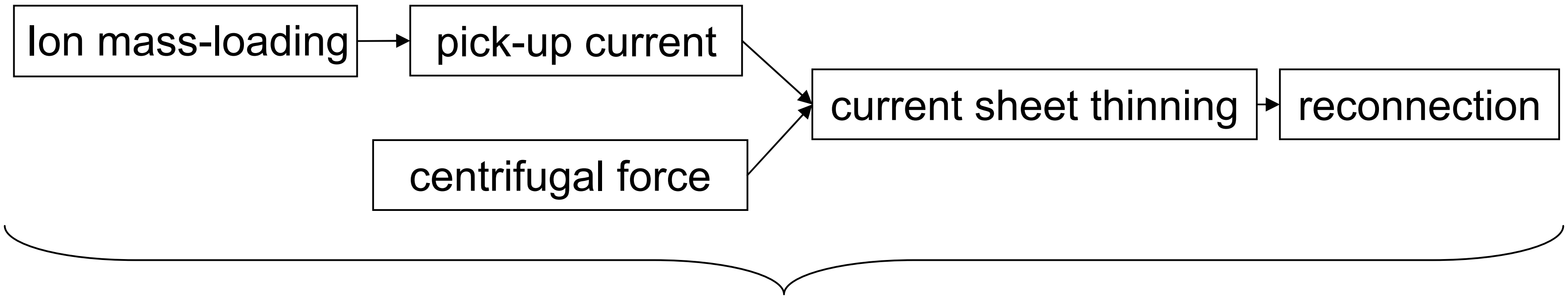

several days (as data show)

Local stress balance in the middle and outer magnetosphere is contained in the momentum equation for the plasma

$$\left[\rho\omega^2 r + \nabla P = \vec{j} \times \vec{B} \right]$$

centrifugal force density — pressure gradient — magnetic force density

Current system in the Jovian magnetosphere

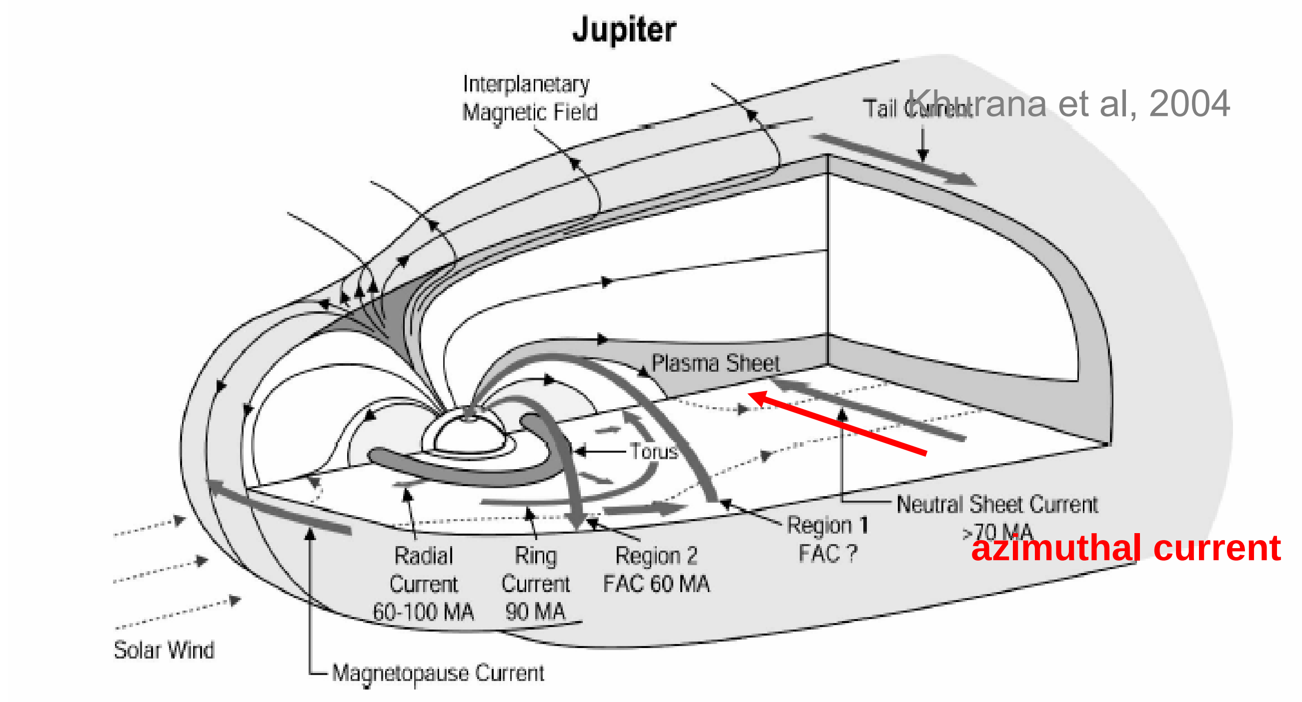

The currents at the equatorial plane of the magnetotail are

$$\left[\vec{j}_r + \vec{j}_\varphi = -\dot{\rho} r B_\theta \omega \vec{e}_r - \frac{\rho \omega^2 r}{B_\theta} \vec{e}_\varphi\right]$$

Time estimations

Ampere's law:

$$(\nabla \times \vec{B})_{\varphi} = \mu_0 j_{\varphi} \approx -\frac{B_r}{d}$$

$$\frac{\partial B_\theta}{\partial t} = \frac{\partial \rho}{\partial t} \frac{\mu_0 \omega^2 r d}{B_r}$$

$$\Delta t = \frac{\Delta B_\theta B_r}{\dot{\rho} \mu_0 \omega^2 r d}$$

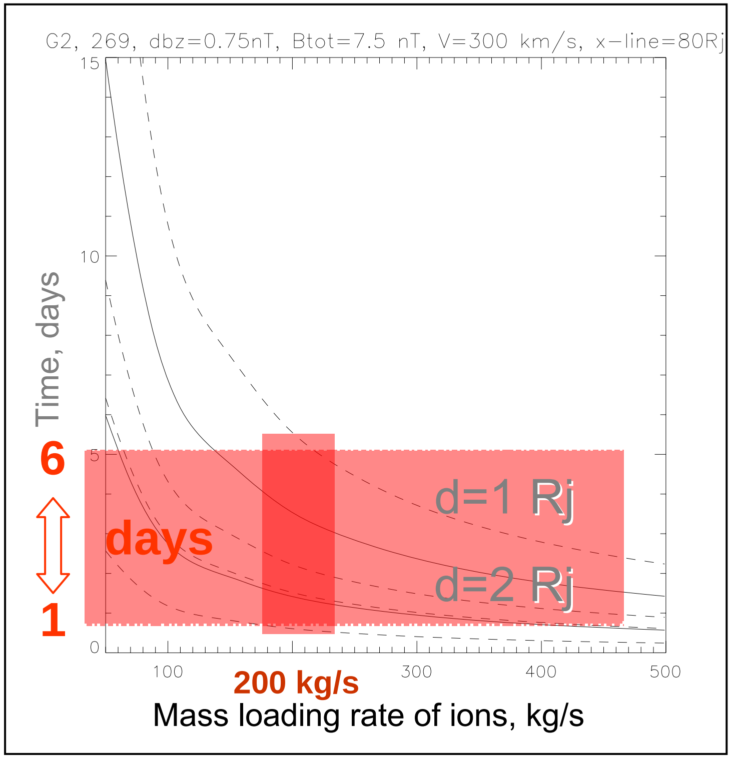

Input parameters:

$\Delta B_\theta \approx 0.1 B_r$	0.75 nT
$\omega = V / R$	$3 \cdot 10^5 (m/s)/R$
Distance to x-line	80 Rj
The most probable mass loading rate	200 kg/s

Radio emissions at Jupiter from various regions

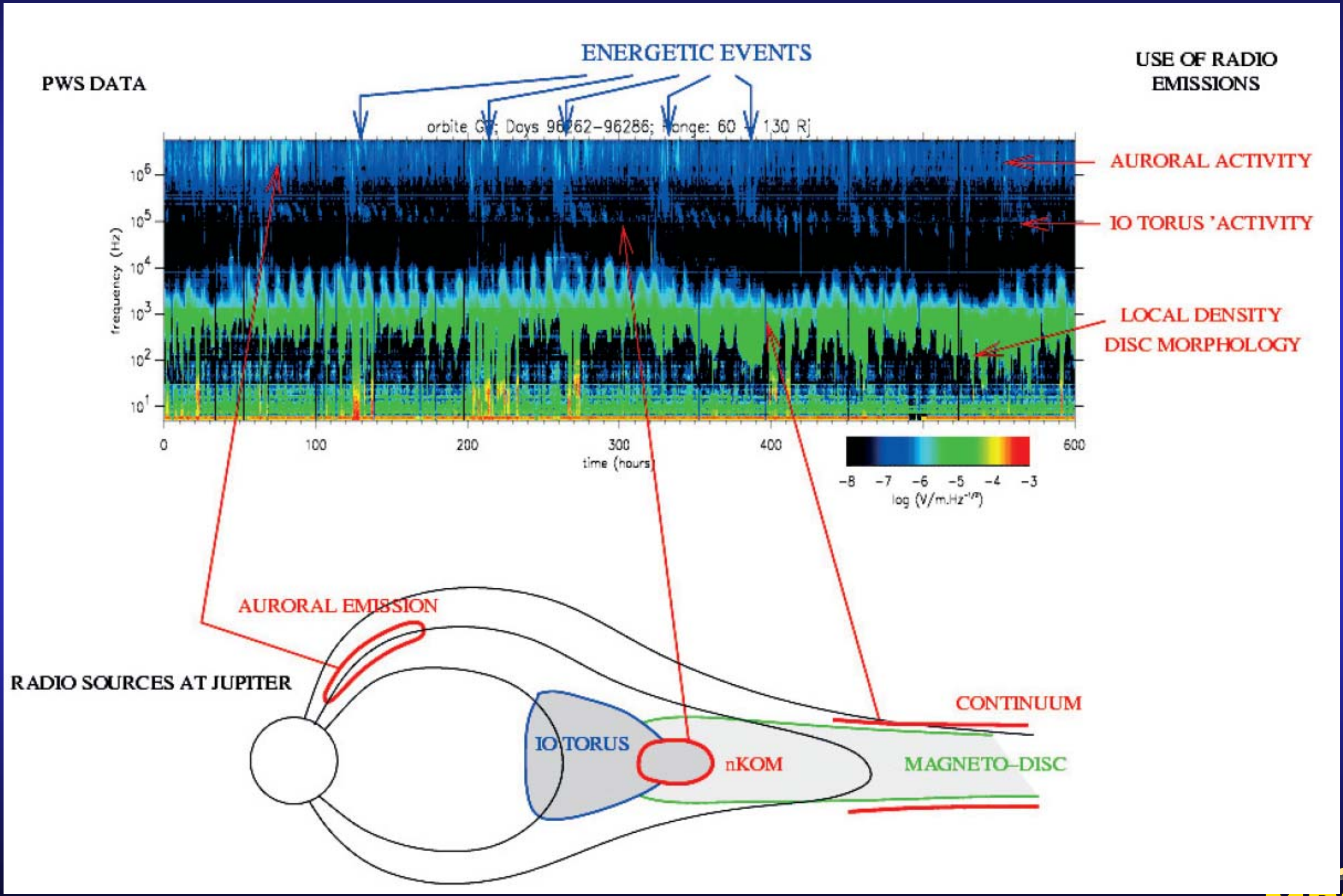

Jupiter

Aurora and tail disruptive events (Grodent et al., 2004)

	In Situ* Russell et al., Woch et al., Krupp et al.	Auroral Spots
Distance	70-120 Rj	>100 Rj
Local Time	postmidnight	premidnight
Size	~25 Rj	5-50 Rj
Duration	Mins-hours	5 min-1hour
Recurrence	4 hours-3days	1-2 days

Jupiter

Tail disruption events - numbers

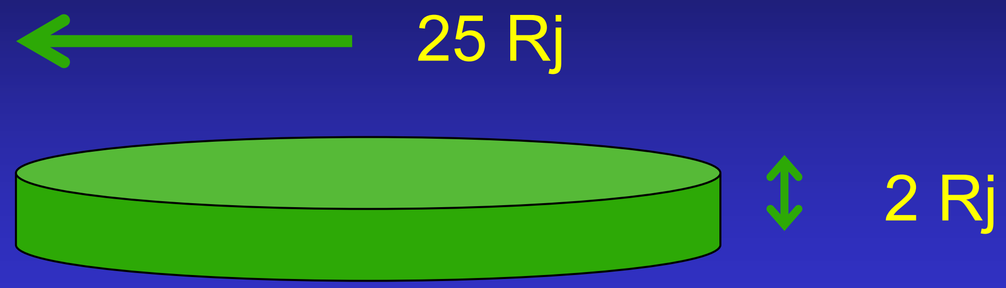

~8000 Rj x 0.01 ions/cc

= 500 tons per plasmoid

1 per day = 0.006 ton/s

1 per hour = 0.15 ton/s

Dynamics in the Jovian magnetosphere

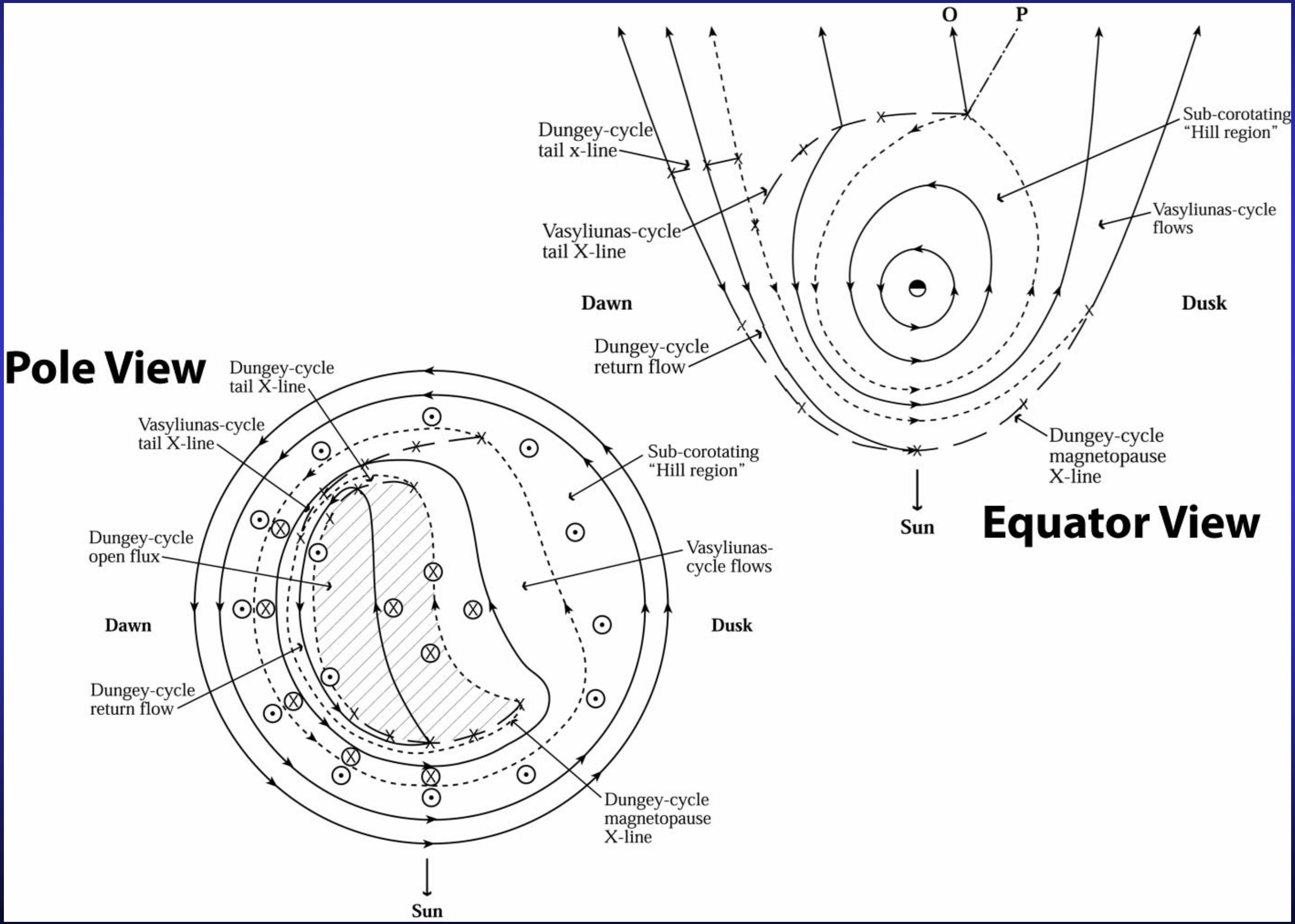

Configuration of the Jovian magnetosphere

Polar View

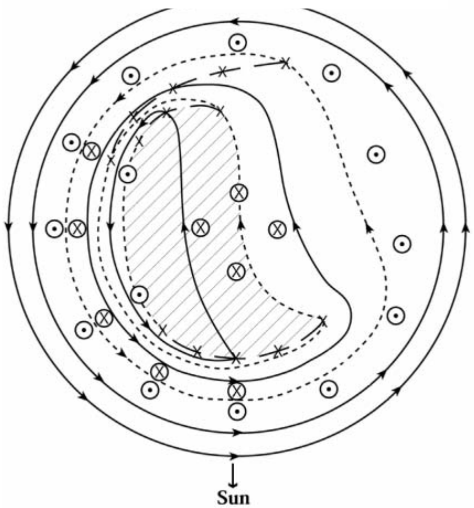

Equatorial View

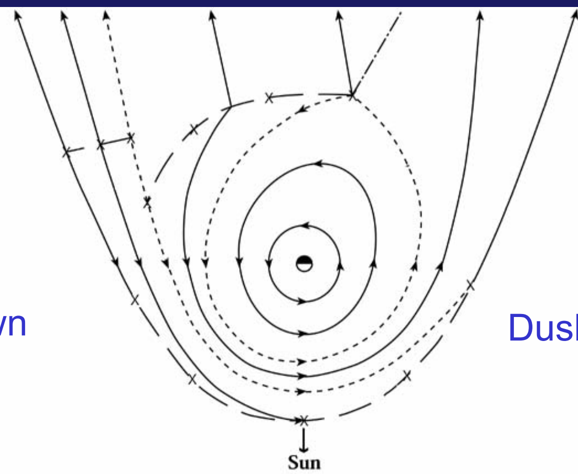

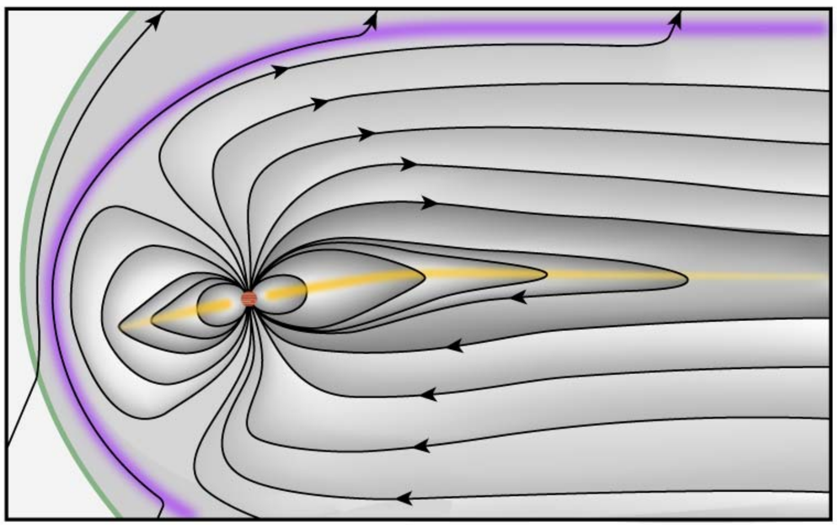

Side View

Cowley et al. 2003

Dynamics in the Jovian magnetosphere
Jupiter aurora

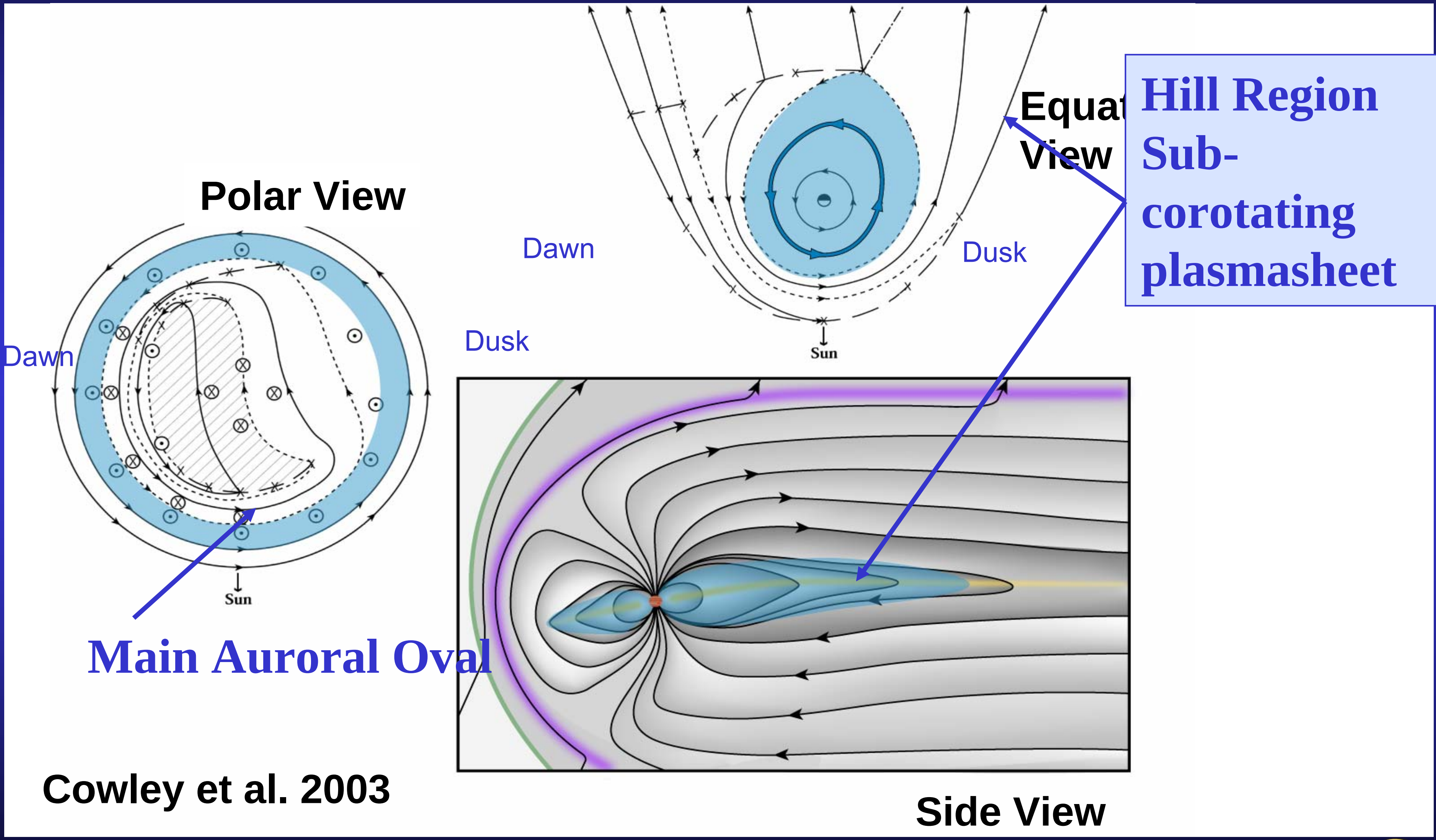

Cowley et al. 2003

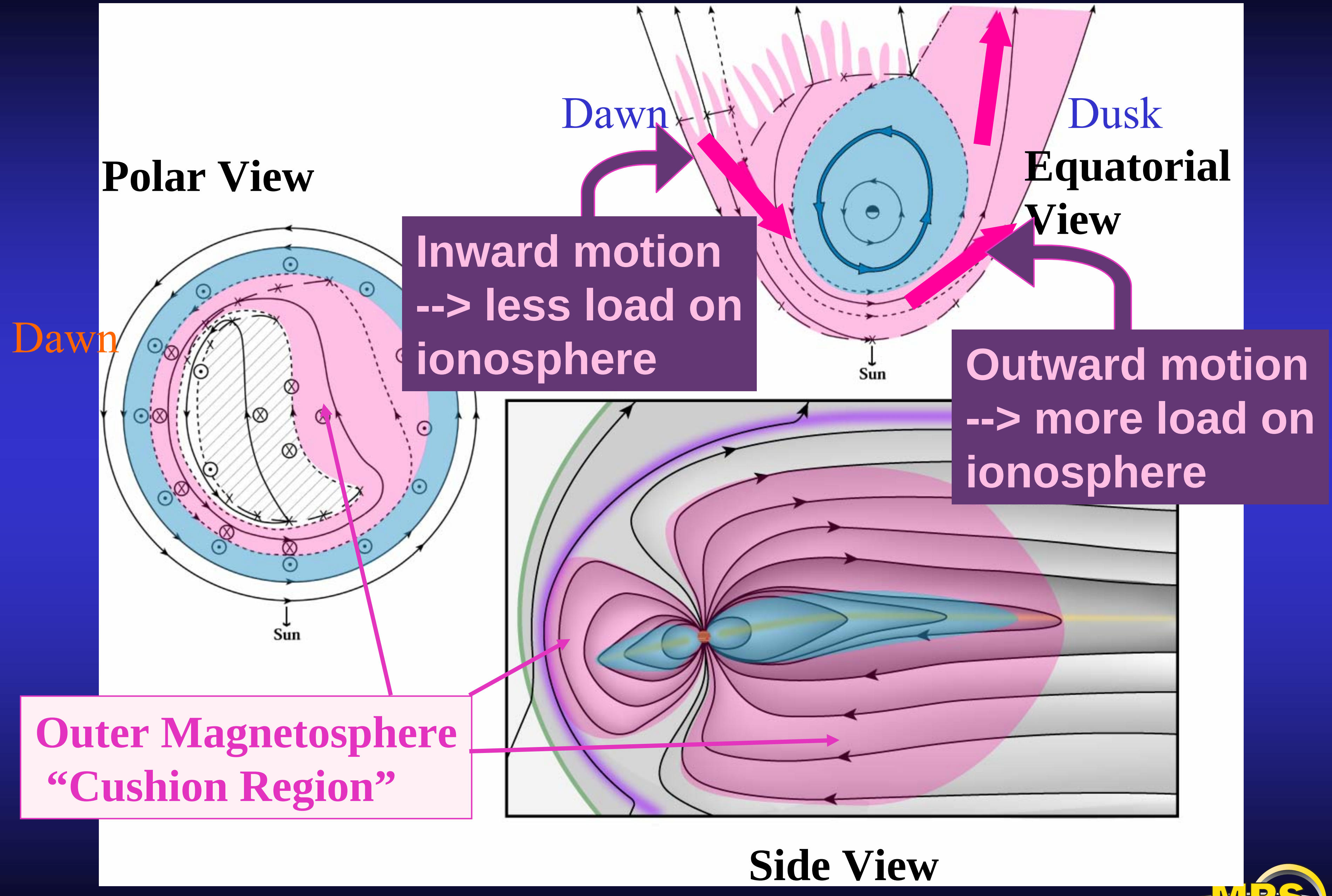
Polar View
Dawn
Sun
Dawn
Dusk
Equatorial View
Sun
Inward motion --> less load on ionosphere
Outward motion --> more load on ionosphere
Outer Magnetosphere "Cushion Region"
Side View

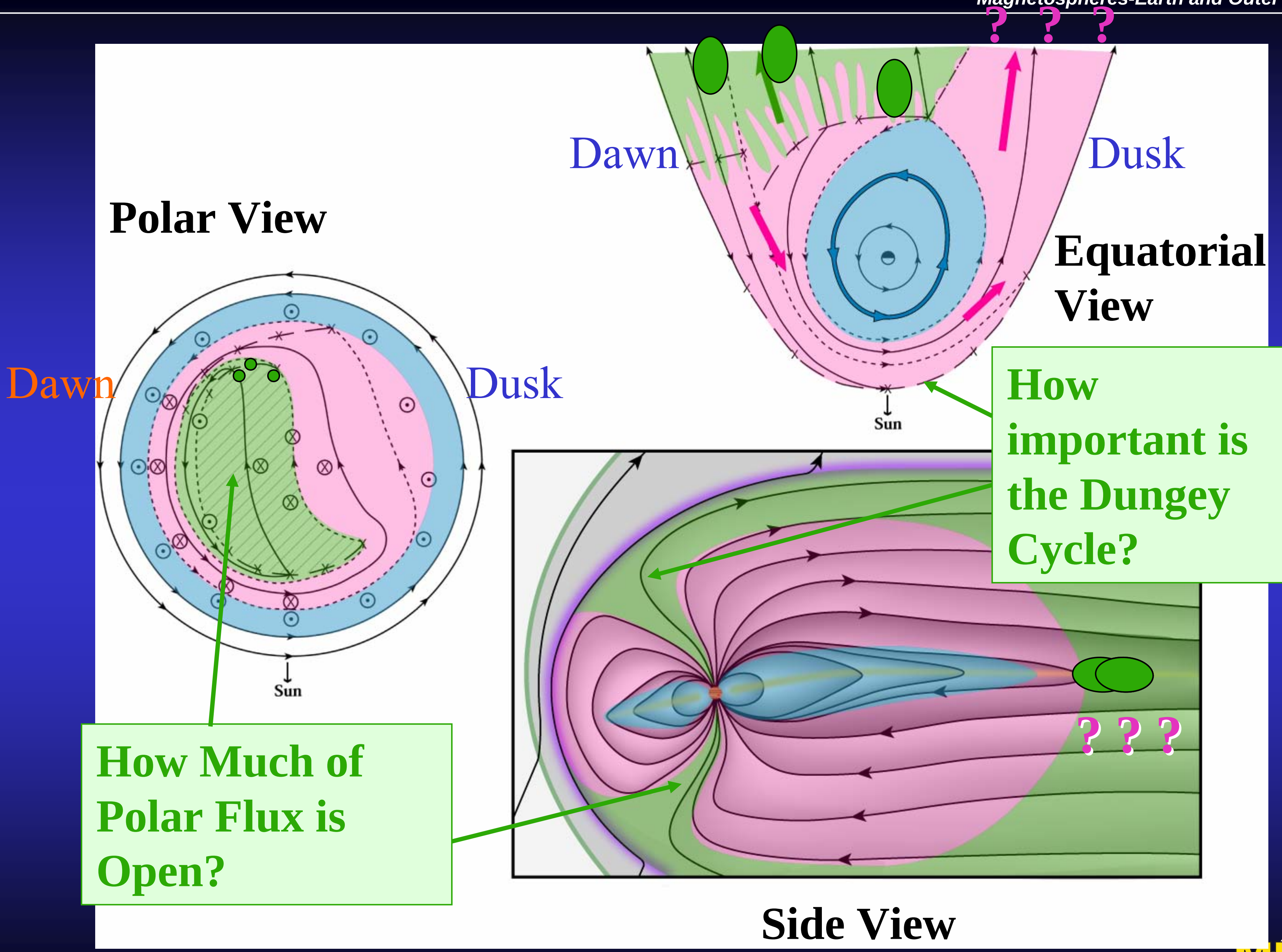
? ? ?
Dawn
Dusk
Equatorial View
Sun
Polar View
Dawn
Dusk
Sun
How important is the Dungey Cycle?
? ? ?
How Much of Polar Flux is Open?
Side View

Dynamics in the Jovian magnetosphere

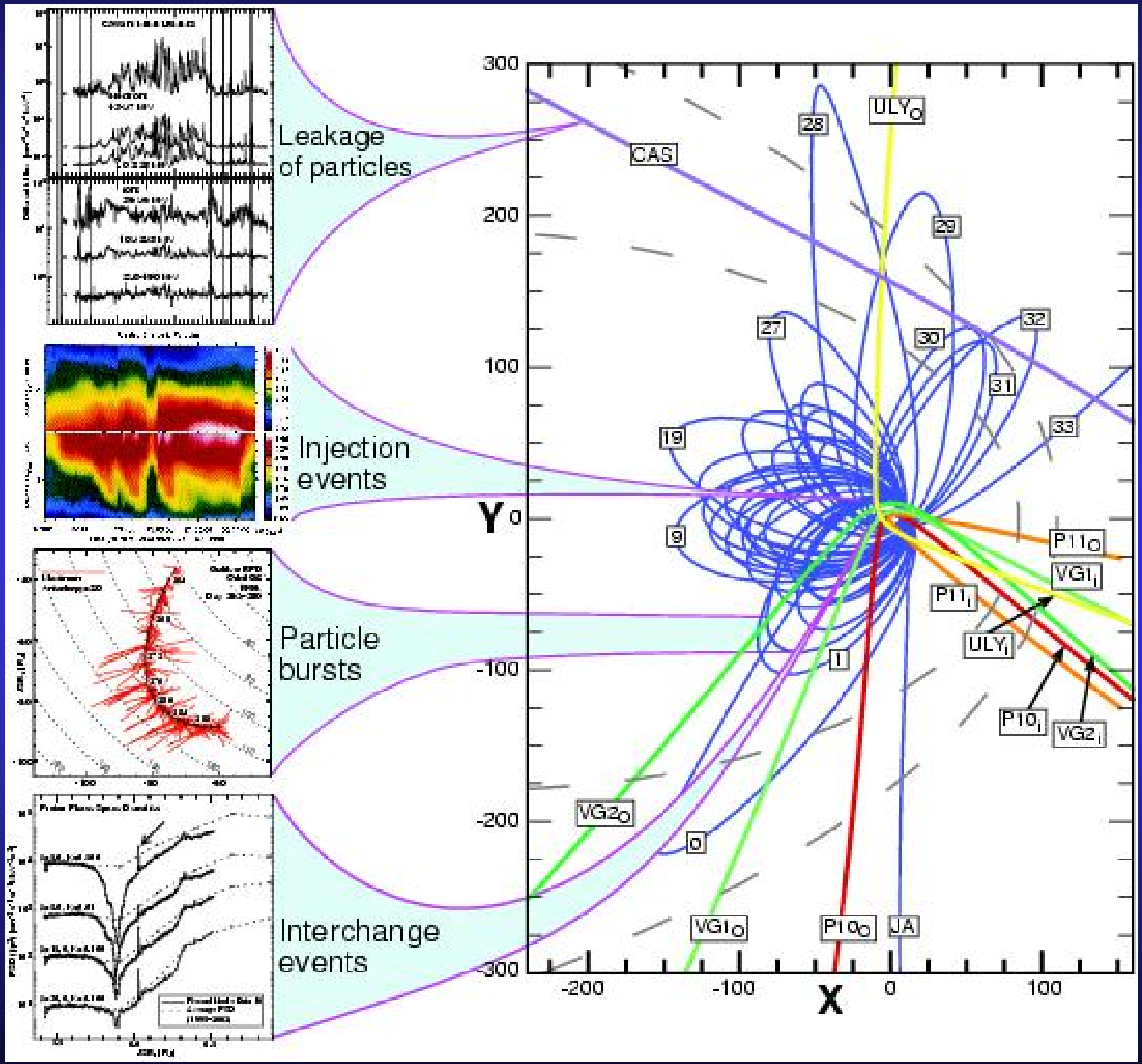

Max-Planck-Institut für Sonnensystemforschung

Ganymede magnetosphere

A magnetosphere within a magnetosphere

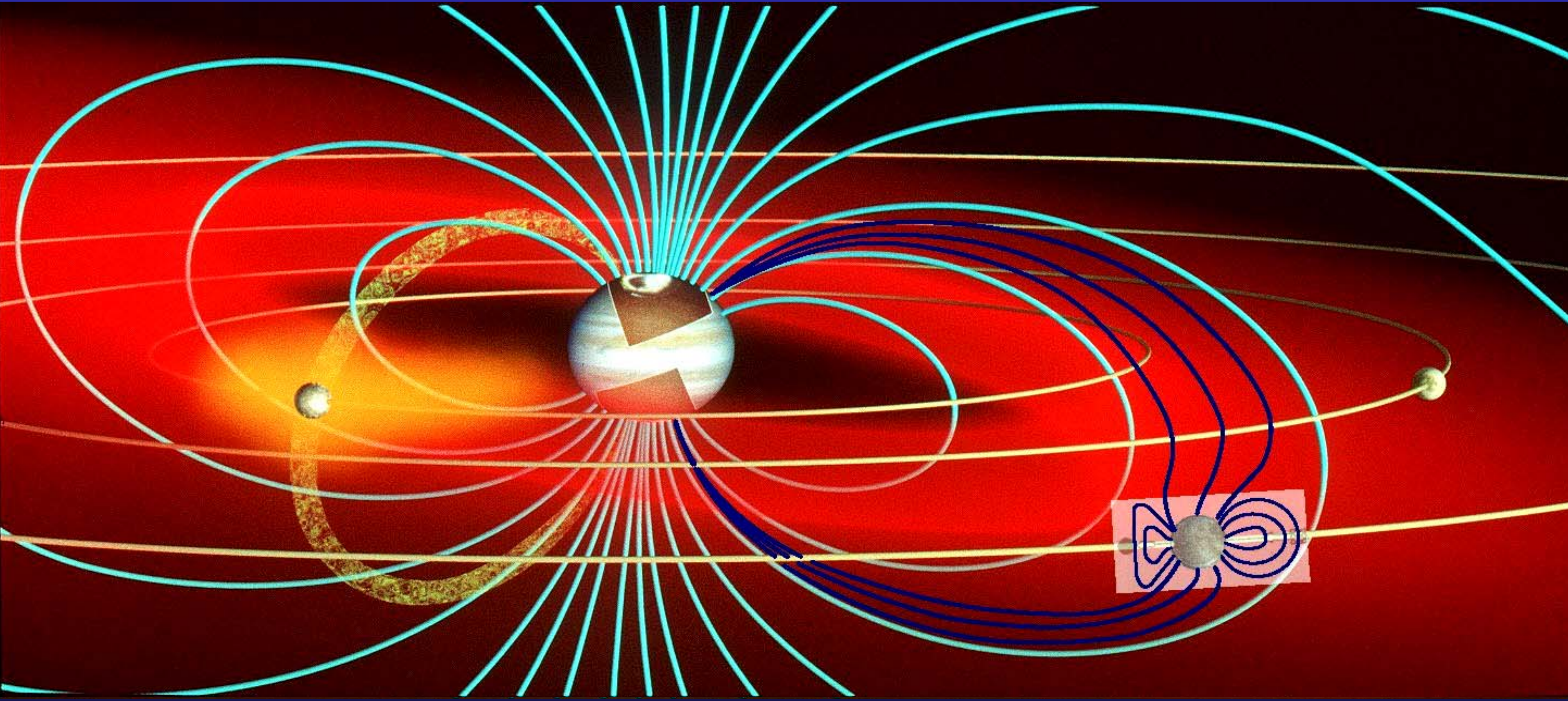

Ganymede:
Electron beams in Ganymede‘s magnetosphere

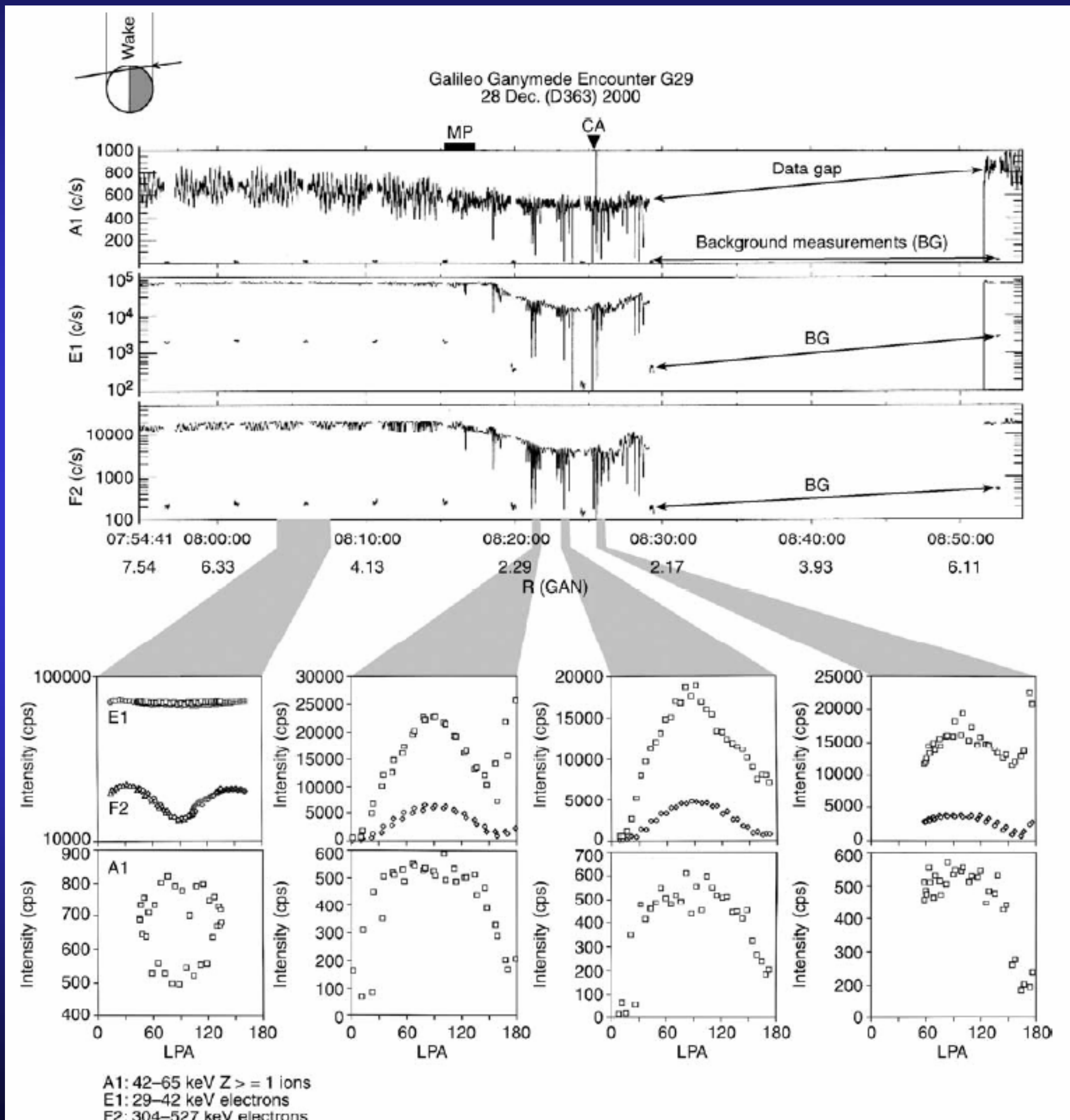

Williams, JGR, 2004

EPD results from Galileo‘s orbit 29

- ***Ganymede‘s magnetosphere more complex***
- ***Electron beams may be formed by the entry and subsequent quasi-chaotic drift of ambient Jovian electrons***

Ganymede:
Electron beams in Ganymede's magnetosphere

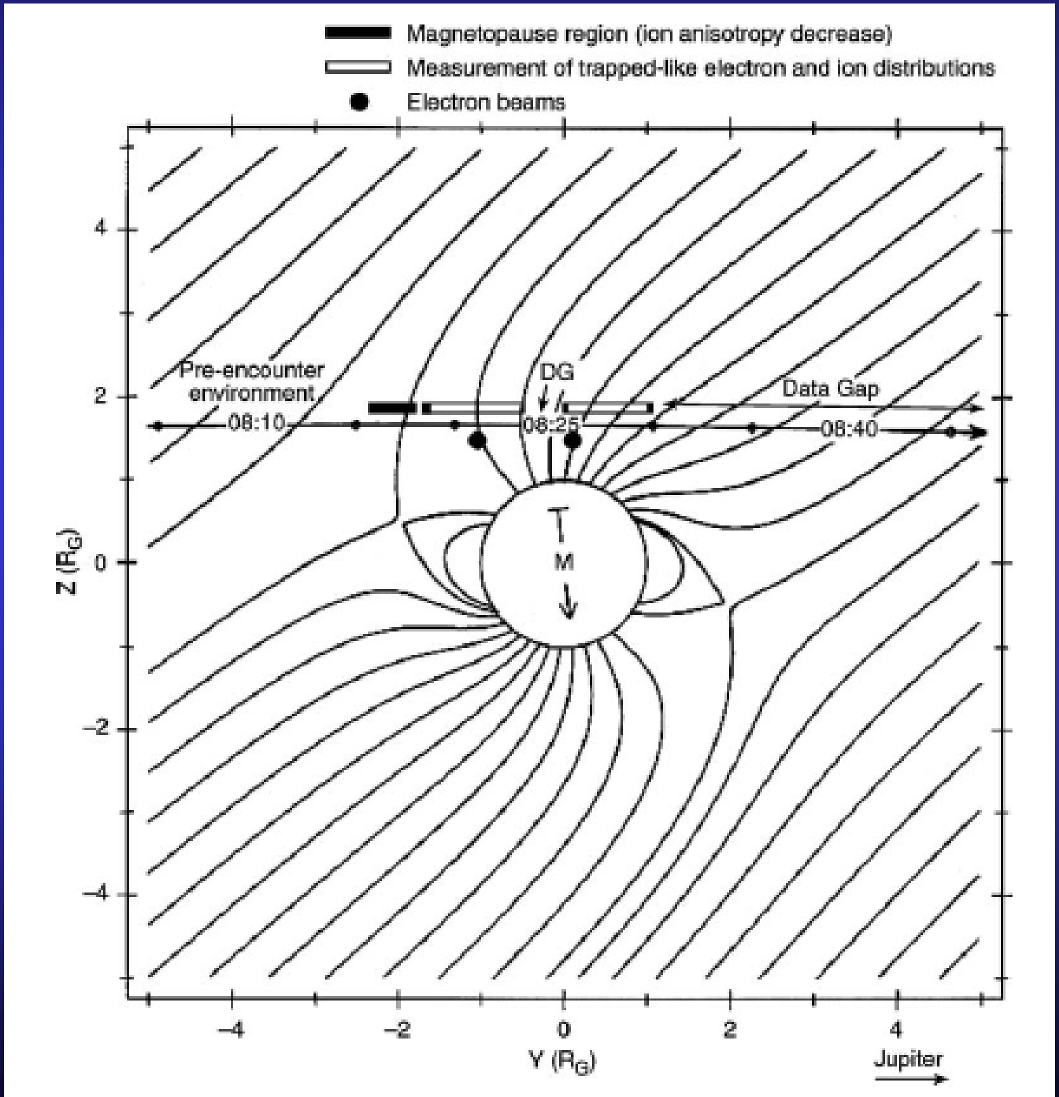

Williams, JGR, 2004

EPD results from Galileo's orbit 29

- *Ganymede's magnetosphere more complex*
- *Electron beams may be formed by the entry and subsequent quasi-chaotic drift of ambient Jovian electrons*

Ganymede:

Multi-Fluid simulations in Ganymede's magnetosphere

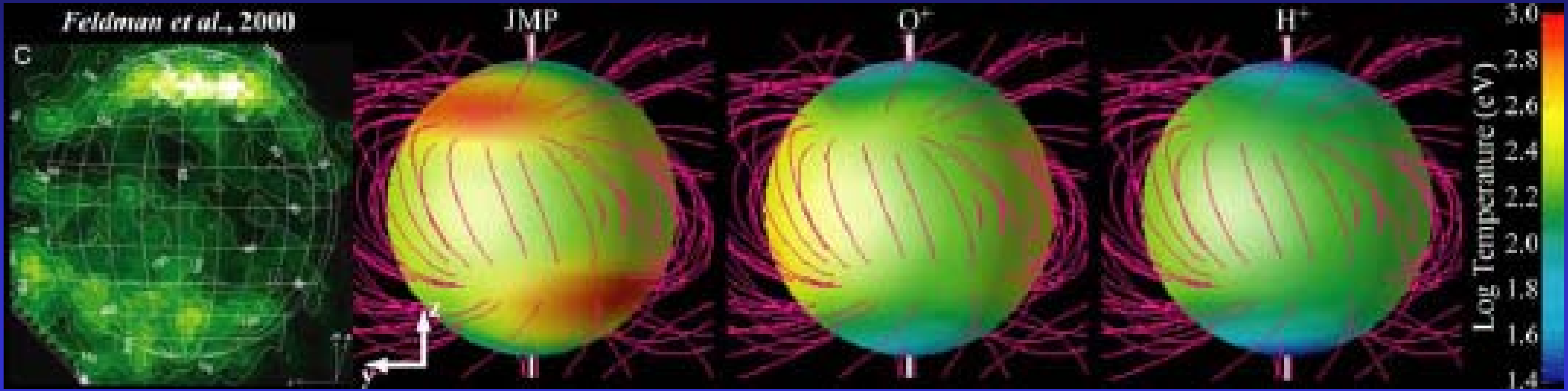

Paty and Winglee, GRL, 2004:

Simulation results compared to Galileo magnetometer measurements and Hubble observations of Ganymede's UV aurora

→ good agreement of precipitation in the cusp

→ ionospheric outflow rates determined (10^26 ions/s)

plasma-moon interactions

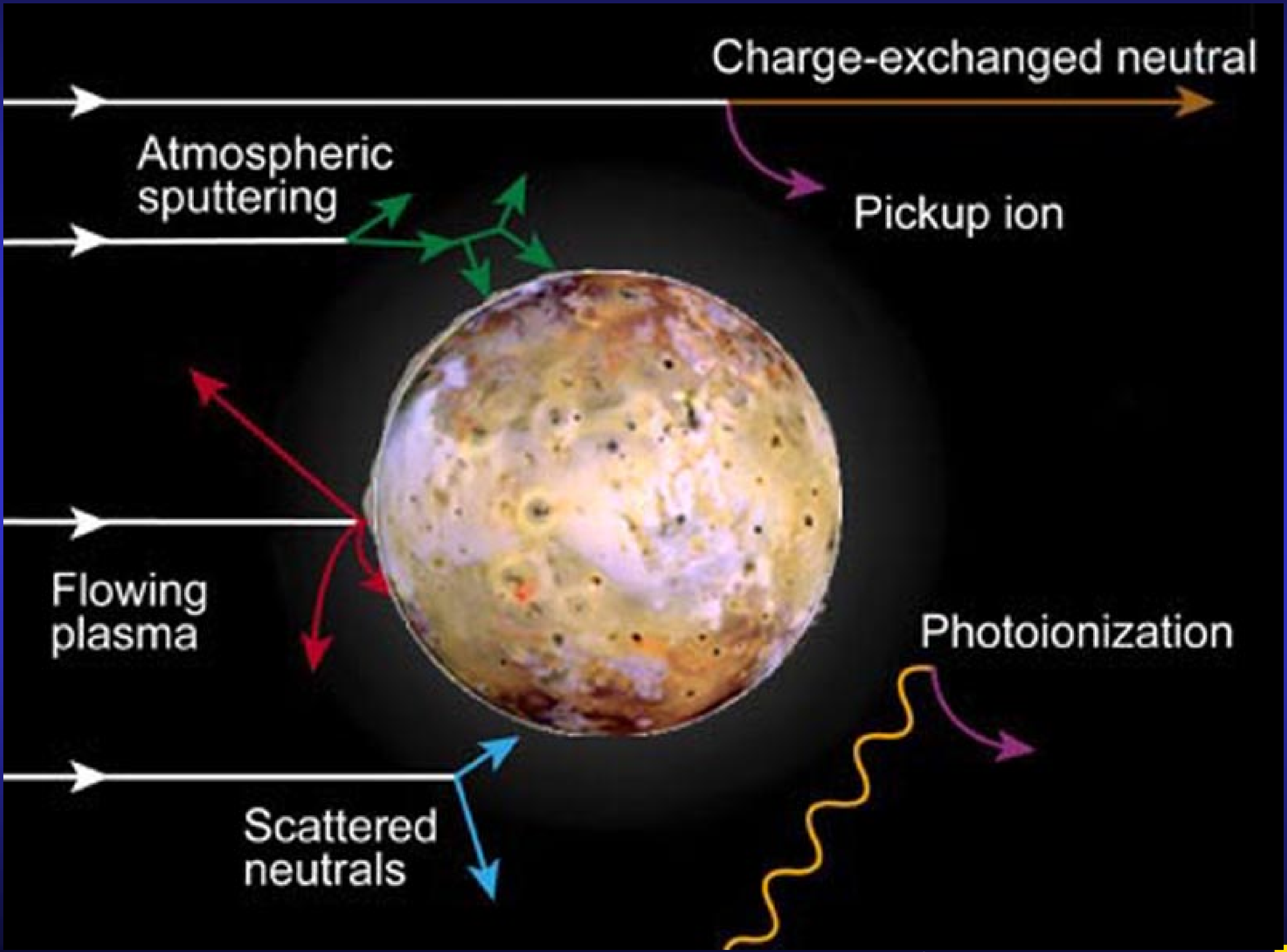

After Spencer & Schneider 1996

Interaction between magnetospheric plasma and Io-Torus

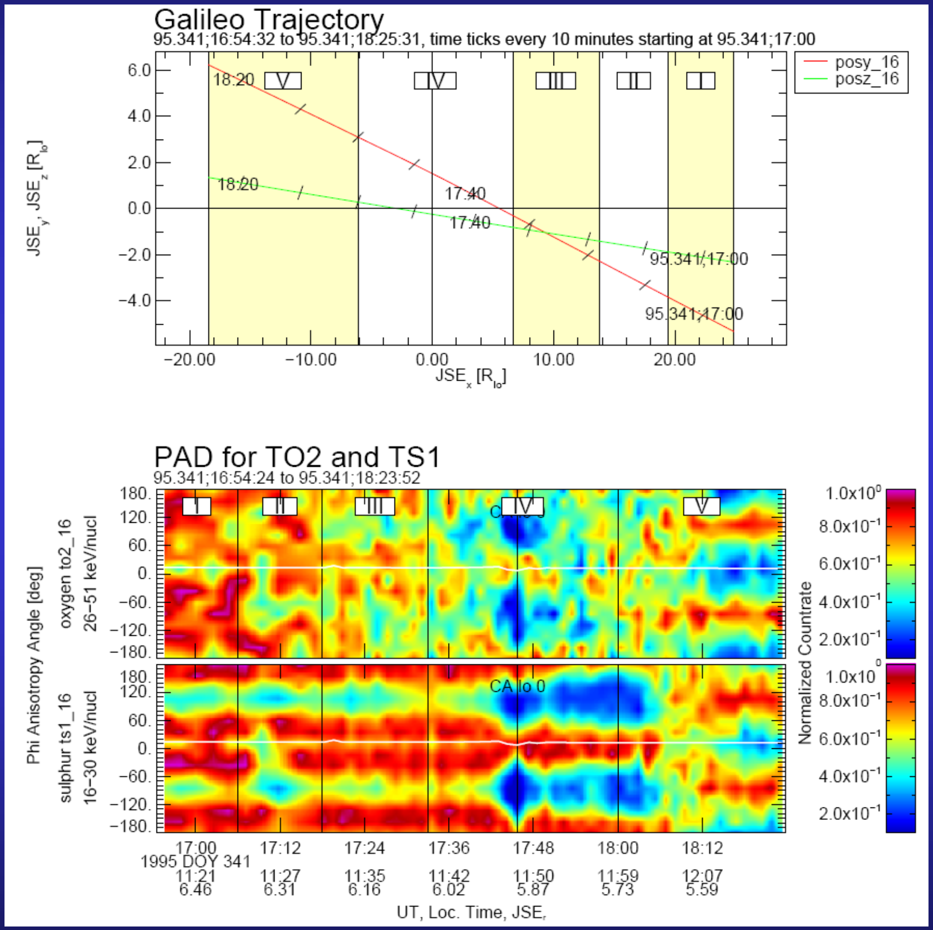

Lagg et al., 1998

Particle Observations:

- *bounce loss cone* (0° and 180° PA) for protons, oxygen and sulphur
- additional loss cone at 90° PA for sulphur

Possible loss mechanisms:

- *bounce loss cone:* scattering processes near Jupiter
  → depletion at 0° (and 180°) pitch angle
- scattering processes in Io-torus region
  → depletion at 90° pitch angle

Interaction between magnetospheric plasma and Io-Torus

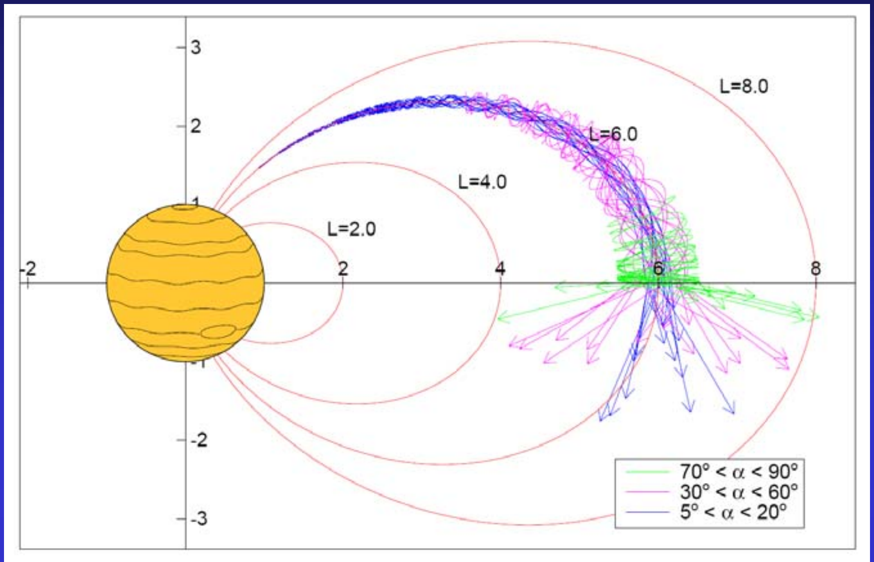

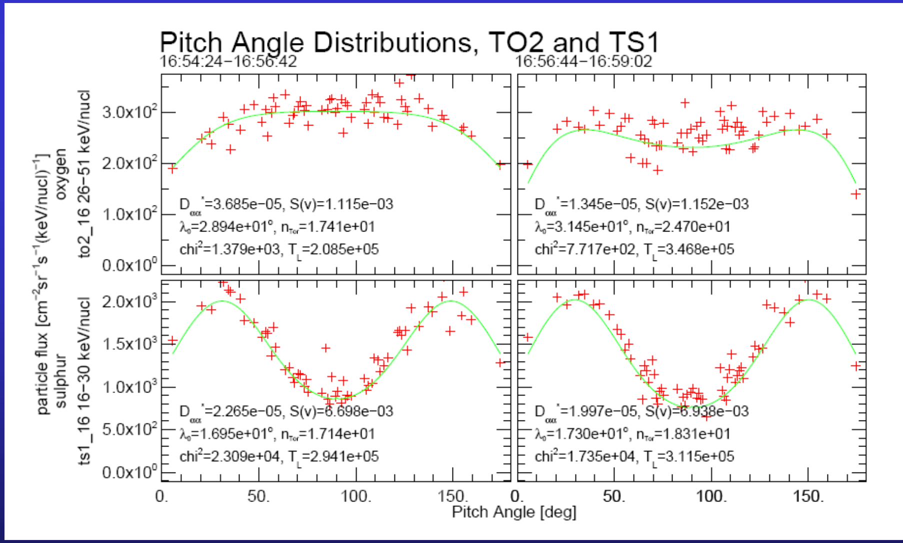

Possible loss mechanisms for 90 deg PA:

- bounce resonant waves
- satellite sweeping
- shell splitting
- particle-particle interactions in Io-torus

Lagg et al., 1998

particle-particle interaction in the Io-Torus

- Coulomb scattering → small cross section
- charge exchange ion-ion → not observable with EPD
- charge exchange ion-neutral:

estimating average neutral number density n and lifetime тau_*cx* [*Ip*, 1981]:

$$\bar{n}(\lambda_m) = \int_{\lambda=0}^{\lambda_m} \frac{n_{Torus}(\lambda)}{v_{\|}(\lambda)} ds \Big/ \int_{\lambda=0}^{\lambda_m} \frac{1}{v_{\|}(\lambda)} ds \quad , \quad \tau_{cx} = \frac{1}{\bar{n}\sigma_{cx} v}$$

assume Gaussian distribution for neutral torus density:

$$n_{Torus}(r,\lambda) = n_0 \exp^{-\left(\frac{\lambda}{\lambda_0}\right)^2} \exp^{-\left(\frac{r-R_{Torus}}{r_0}\right)^2} \approx n_0 \exp^{-\left(\frac{\lambda}{\lambda_0}\right)^2}$$

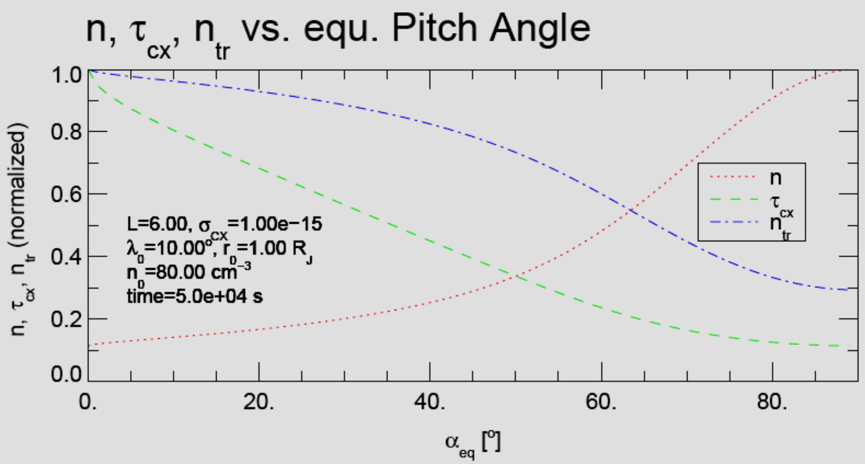

Lagg et al., 1998

neutral density in the Io-Torus from energetic particle measurements

channel	energy [keV/nucl]	reaction	σ_{cx} [cm^2]	$D_{\alpha\alpha}$ [cm^{2}s^{-1}]	T_L [s]	λ_0 [°]	n_0 [cm^{-3}]
sulphur							
TS1	16 - 30	$S^+ + X$	$2.36 \cdot 10^{-15}$	$2.1 \cdot 10^{-5}$	$3.0 \cdot 10^5$	17	18
TS2	30 - 62		$2.02 \cdot 10^{-15}$	$4.4 \cdot 10^{-5}$	$1.9 \cdot 10^5$	23	25
TS3	62 - 310		$9.00 \cdot 10^{-16}$	$4.9 \cdot 10^{-5}$	$1.4 \cdot 10^5$	23	34
oxygen							
TO1	12 - 26	$O^+ + X$	$1.51 \cdot 10^{-15}$	$6.9 \cdot 10^{-5}$	$2.3 \cdot 10^5$	31	11
TO2	26 - 51		$1.09 \cdot 10^{-15}$	$2.8 \cdot 10^{-5}$	$2.3 \cdot 10^5$	30	23

modell/observation of	density OI [cm^{-3}]	density SI [cm^{-3}]
Brown [1981]	30	
Smith and Strobel [1985]	30	6
Skinner and Durrance [1986]	$>29\pm16$	$>6\pm3$
this work	$\approx$25	

Lagg et al., 1998

Europa torus from chargedand neutral particle measurements

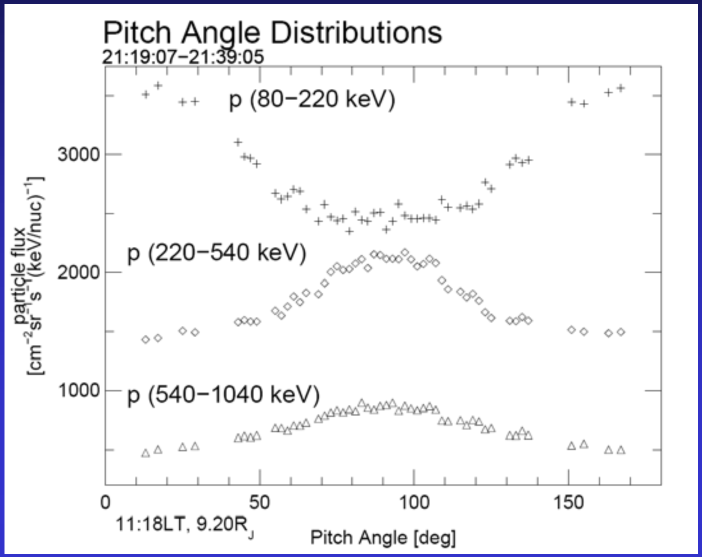

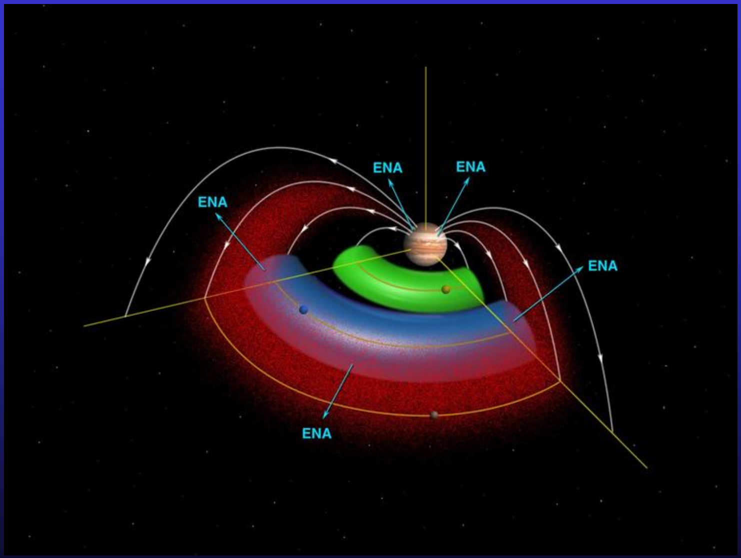

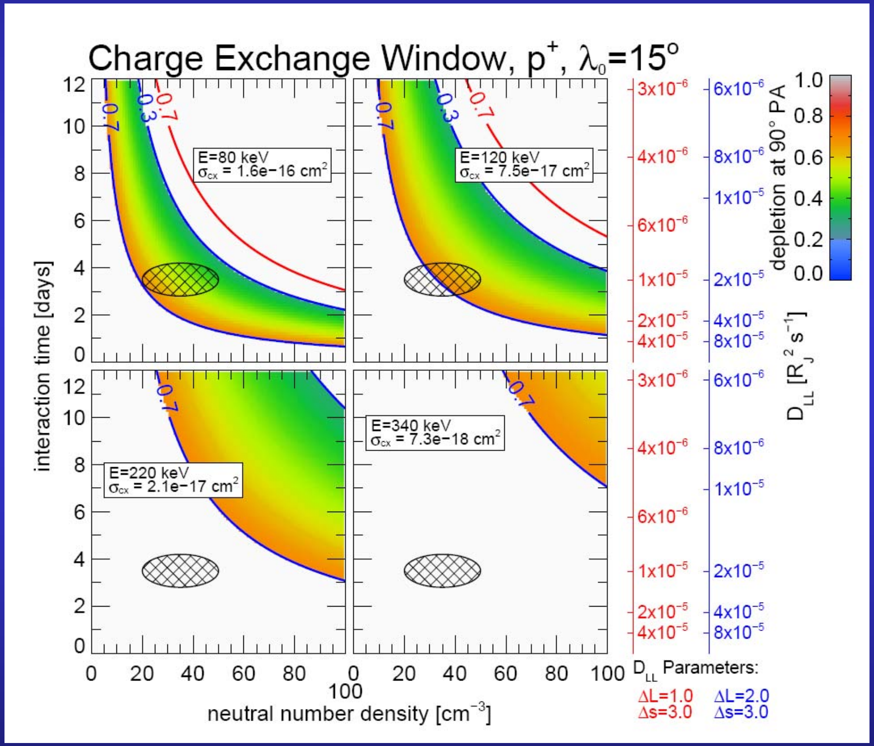

Lagg et al., 2001